EFFECTS OF TIME ON IMPURITY DIFFUSION AND CONCENTRATION-DEPENDENT INTERDIFFUSION COEFFICIENTS IN Cu-Ni SYSTEM

BY

SAMUEL IBUKUN AFOLABI

A thesis submitted to the Faculty of Graduate Studies of The University of Manitoba

in Partial Fulfilment of the Requirement for The Degree of

MASTER OF SCIENCE

Department of Mechanical Engineering, University of Manitoba

Winnipeg. Canada.

ABSTRACT

Considerable focus has been directed toward investigating the interdiffusion coefficients in binary systems, primarily due to their pivotal role in metallurgical processes and material performance assessments. An essential parameter in this context is the isothermal concentration-dependent interdiffusion coefficient. While interdiffusion coefficients are widely recognized as being influenced by temperature and concentration, the element of time can exert substantial influence due to the presence of diffusion-induced stress (DIS) within the system.

The present research experimentally investigates the effect of time on concentration-dependent interdiffusion and impurity diffusion coefficients in Cu-Ni binary systems and their alloy compositions. The investigation delves into the effect of solute source concentration and anomalous behaviors of temperature as the attributable indications of DIS at play.

To implement the research work, a newly devised numerical diffusion model by Olaye and Ojo [20] is integrated with a forward simulation approach in this study. This model incorporates different atomic diffusion coefficients and ensures solute conservation. The model also merges fully explicit finite difference analyses with the Leapfrog/Dufort-Frankel scheme, thus enabling the determination of concentration-dependent interdiffusion coefficients. This approach overcomes the limitations associated with traditional techniques like the Boltzmann-Matano, Hall, Wagner and Sauer-Freise methods. By applying this method, both the interdiffusion and impurity diffusion coefficients are investigated at various diffusion times. The results reveal that the interdiffusion and impurity diffusion coefficients show time variations as a result of DIS in the system. This phenomenon contrasts the widely accepted notion of the interdiffusion coefficient being solely dependent on concentration and temperature without considering time. Overlooking this critical aspect could have substantial implications in the analysis of diffusion data and an

accurate understanding of microstructural transformations initiated by diffusion-controlled phase changes in metallic systems.

ACKNOWLEDGEMENTS

With utmost respect and profound appreciation, I extend my heartfelt gratitude and deep sense of indebtedness to my esteemed advisor, Prof. Olanrewaju A. Ojo. His introduction to the current research focus and unwavering guidance have been truly inspiring. I am deeply thankful for his constant support, valuable suggestions, constructive assessments, provision of materials and financial assistance throughout the entire duration of this research endeavor.

I sincerely acknowledge the efforts of Dr. Lina Zhang and Mr. Mike Boskwick for their invaluable technical support. My gratitude extends to the Graduate Enhancement of Tri-agency Stipends (GETS program) and Fellowship for Education Purposes for the generous financial aid provided.

My sincere appreciation goes to Dr. Osamudiamen Olaye, Dr. Oluwadara Afolabi, Paul Fase, Amir Safaei, Rasool Mokhtari, Lulu Guo, Emmanuel Adejumo, and Oluwadoyin Hasstrup for their timely support.

Heartfelt thanks to my parents, Mr. and Mrs. Afolabi, and my siblings for their encouragement throughout my academic journey. Special gratitude is reserved for the Deeper Life Campus fellowship at the University of Manitoba for their prayers and moral support.

To my beloved wife, Patience Afolabi, I am profoundly grateful for her unwavering support, love, and care for our family throughout the entire duration of this program. Lastly, a big thank you to my son, Daniel, for his patience and endurance.

DEDICATION

I hereby present this thesis as a dedication to God Almighty.

TABLE OF CONTENTS

Page

LIST OF FIGURES

Page

LIST OF TABLES

LIST OF ABBREVIATIONS

BM – Boltzmann-Matano

SF – Sauer-Freise

SEM – Scanning electron microscope

DIS – Diffusion-induced stress.

FSM – Forward simulation method

HM – Hall method

EHM – Extended Hall method

EDM – Electron discharge machining

SE – Secondary electrode

BE – Backscattered electrode

EDS – Energy dispersive x-ray spectroscopy

LIST OF SYMBOLS

D(C): Concentration-dependent interdiffusion coefficient

D_{ave} : Average interdiffusivity

C : Concentration

T : Temperature

$\frac{dC}{dx}$: Concentration gradient

J: Flux

SiC: Silicon carbide

Ni: Nickel

Cu: Copper

Na_2CO_3: Sodium carbonate

NaOH: Sodium hydroxide

H_2SO_4: Sulfuric acid

HCl: Hydrochloric acid

$Cu_{90}Ni_{10}$: Copper-based alloy with 90 at % copper and 10 at % nickel

$Cu_{10}Ni_{90}$: Nickel-based alloy with 90 at % nickel and 10 at % copper

t: Diffusion time

x_m : Matano initial contact plane

x : Diffusion distance

CHAPTER ONE

1.1 Introduction

The phenomenon of atomic diffusion, which is responsible for mass transport, plays an important role in the study of phase changes in metals and semiconductors. The changes in atomic arrangements, known as phase transformations, have a profound impact on material properties. The practical implication is that microstructures can be changed through phase transformations, thereby enabling customization of material characteristics.

Industries such as the energy, aerospace, biomedical, and automobiles have used the principles of diffusion in solids to predict engineering material properties. Studying the microstructure of materials after phase transformation has been done for the past 150 years, with applications across variety of different sectors. The focus of physical metallurgists revolves around understanding the correlation between phase changes and changes in metal properties. The materials processing industries have been incorporating phase transformation techniques like coating, diffusion bonding, sintering, and heat treatments. These facilitate the processing of engineering material properties to improve overall performance standards.

Currently, diffusion plays a pivotal role in a number of metallurgical processes. For instance, carburization is used to enhance the surface hardness of steels. During the process, a carbon source like graphite powder or a carbon-containing gaseous phase diffuses into the steel components. Another application is dopant diffusion in semiconductor devices, a technique used to create *p-n junctions* to facilitate the controlled diffusion of dopant atoms into precisely defined regions of silicon wafers. Diffusion also contributes to the electrical conductivity of many conductive

ceramics, thus yielding ionically conductive materials. Such materials are utilized in different products including oxygen sensors in automobiles, touchscreen displays, fuel cells, and batteries. Additionally, diffusion is integral to the oxidation of aluminum, where a protective oxide layer formed prevents the further diffusion of oxygen and subsequent oxidation of the underlying aluminum. Notably, diffusion is used for thermal barrier coatings in aircraft engines, further illustrating its indispensable role in contemporary metallurgical practices [1].

The process of heat transfer through conduction, as well as the process of diffusion, both originated from the random migration of molecules. Adolf Fick recognized an analogy between these two processes in 1855 [2,3]. He established a quantitative basis for diffusion by using a mathematical equation for heat conduction that Joseph Fourier formulated in 1822. The mathematical model of diffusion in isotropic substances is based on the hypothesis that the rate of the transfer of a substance by diffusion through a unit area of a section is directly proportional to the concentration gradient measured normal to the section [2]. Fick's first law of diffusion expresses the relationship between diffusion the flux (J_i) of the species i and the concentration gradient (∇C_i) and given as:

$$J_i = -D\nabla C_i \tag{1.1}$$

where D is the diffusion coefficient.

For planar diffusion along the x direction, equation (1.1) is further simplified to:

$$J_i = -D\frac{\partial C_i}{\partial x} \tag{1.2}$$

At any given point in the system, the diffusion determines the concentration gradient of the species i and the rate of change of its concentration. Fick's second law gives this relationship as:

$$\frac{\partial C_i}{\partial t} = \frac{\partial}{\partial x}\left[D\left(\frac{\partial C_i}{\partial x}\right)\right] \tag{1.3}$$

When D is independent of the position, Fick's second law takes the form:

$$\frac{\partial C_i}{\partial t} = D\left(\frac{\partial^2 C_i}{\partial x^2}\right) \quad (1.4)$$

In reality, the process of diffusion in materials takes place under non-steady state conditions. As a result, the concentration gradient and flux at a particular position in the diffusing zone vary with time. This unsteady behavior can result in either the complete accumulation or total depletion of the diffusing species.

Moreover, both Fick's first and second laws of diffusion require a pivotal parameter known as the diffusion coefficient. The diffusion coefficient is a critical element in diffusion equations and analysis for predicting diffusion-related processes.

Another aspect which has received less attention in the literature, is the *impurity diffusion coefficient*, which is defined as the diffusion rate of a solute with an extremely low concentration in a solvent. This phenomenon has significant relevance in both practical and theoretical contexts. Conventionally, radioactive isotope tracers have been used to estimate impurity diffusion coefficients. However, owing to the high cost involved, conducting diffusion experiments with radioactive isotopes might be less prevalent, especially when dealing with noble metals [4] or circumstances without suitable radioactive tracer isotopes. As a result, a novel computational technique known as the forward simulation method (FSM) has emerged, which will be discussed in this research study. The reliability of this method has been demonstrated to accurately estimate impurity diffusion coefficients and interdiffusion coefficients.

Consequently, the accuracy of analyses that involve diffusion-controlled processes, which directly impact the anticipated performance of the materials, hinges on a concentration-dependent diffusion coefficient (D(C)) [5].

Furthermore, it is widely acknowledged that the diffusion coefficient is dependent on concentration, which is commonly referred to as D(C) or chemical diffusion coefficient [6],[7]. A

conventional implicit assumption is that the D(C) remains a constant coefficient of the material and does not change with time under isothermal conditions. Nonetheless, this assumption may not universally hold true. In interdiffusion, variations in the partial molar volumes and the mobility of diffusing substances can result in the uneven distribution of the volume transport of the substances. This phenomenon can be likened to the generation of stress-free strain that is not uniform in which on one side of the diffusion pair, contractions take place, while expansion occurs on the opposite side. The stress field associated with this stress-free strain has not been explicitly considered in the conventional Darken's analysis of interdiffusion [8]. In other words, it is assumed that stress relaxation is rapid and complete, with only convective transport (as seen in the Kirkendall effect) resulting from this relaxation being incorporated into the theory [9-12].

These strains produced during diffusion are referred to as diffusion-induced strain, while the ensuing atomic stress that arises from this strain is termed diffusion-induced stress (DIS). Remarkably, strains within crystals influence atomic diffusion coefficients [13-18]. Consequently, the concentration gradient of a solute within a crystal becomes a determining factor for DIS, which, in turn, governs the diffusion coefficient [11]. Empirical evidence confirms the existence of DIS and its impact on diffusion coefficients [9-19]. Given that the concentration gradient during diffusion changes alongside the solute concentration, and considering the relationship among solute concentration, concentration gradient, DIS, and the diffusion coefficient, it is theoretically reasonable for diffusion coefficients to vary with solute concentration which has also been supported in the literature [6,20].

1.2 Research Motivation

Darken's theory [8], assumes that concentration-dependent interdiffusion coefficients, obtained through experimental solutions with Fick's second law of diffusion, remain constant under isothermal conditions, and do not change over time. However, recent research has unveiled both theoretical and experimental instances that challenge this assumption. These cases indicate that not only concentration-dependent interdiffusion coefficients but also impurity diffusion coefficients can undergo isothermal changes over time. These changes in diffusion behavior have been attributed to various factors that change the concentration gradient during diffusion. Consequently, these changes can impact the stress and strain in the diffusion system, thus influencing the diffusion coefficients.

The presence of DIS has sparked further investigation into the previously accepted notion that there are no time-dependent effects on isothermally concentration-dependent interdiffusion and impurity diffusion coefficients.

Moreover, Olaye and Ojo [20] recently developed a numerical diffusion model which takes into account variable diffusion coefficients while conserving solute. Their model can be integrated with a forward simulation analysis [20] and has been shown to effectively address the significant limitations found in conventional approaches like the Boltzmann-Matano (BM), Sauer-Freise (SF), Hall, and Wagner methods. This integrated approach offers a reliable means of studying the time effects on impurity diffusion and concentration-dependent interdiffusion coefficients D(C)s, which are previously underexplored.

1.3 Research Objectives

The objective of this work is to use a recently developed numerical diffusion model in [20] coupled with a forward simulation analysis to study the effect of time on:

(i) the concentration dependency of interdiffusion coefficients and

(ii) the impurity diffusion coefficients in nickel-copper (Ni-Cu) binary systems.

1.4 Summary of key findings

In this study, data are obtained from a number of experiments that involve diffusion treatment on Cu-Ni systems and Cu-Ni alloys at different temperatures and diffusion holding times. The concentration profiles are determined by using microanalysis techniques, specifically through X-ray energy and wavelength dispersive spectroscopies. A minimum of five concentration profiles are obtained from each sample. The experimental concentration profiles are then analyzed by using a numerical model newly developed by Olaye and Ojo [20] and FSM to extract the concentration-dependent interdiffusion and impurity diffusion coefficients.

To evaluate the extent of uncertainty in the experimentally obtained data and, by implication, determine whether the concentration dependence of the interdiffusion coefficient varies with time, the following steps are carried out.:

(i) diffusion coefficients are compared with concentration by using standard deviation error bars and the *p-values* determined through *t-statistics* testing,

(ii) impurity diffusion coefficients are calculated,

(iii) the average of the diffusion coefficients for each sample investigated is calculated,

(iv) the temperature dependence is determined with an Arrhenius equation,

(v) the effect of solute source concentration is determined, and

(vi) conventional methods reported in the literatures are reviewed.

The analysis is conducted by using D(C) with the standard deviation error bars for the interdiffusion coefficient and estimating the *p-values* of the *t-statistics* for concentration-dependent interdiffusion and impurity diffusion coefficients.

Notably, contrary to traditional findings, it is observed that, not only does concentration dependent interdiffusion vary with diffusion time but also the impurity diffusion coefficient changes with time at constant temperatures. Existing studies in the literatures attributes this time-related effect to DIS. When a change in the concentration gradient occurs under a constant temperature and the diffusion coefficient changes, then DIS is considered to be the responsible factor. This holds true since, in the absence of DIS, changes in the concentration gradient at a constant temperature would not lead to changes in the diffusion coefficient; rather, the diffusion coefficient would remain constant within an experimentally determined statistical range.

1.5 Thesis Organization

This thesis is organized into six chapters, each serving a distinct purpose, as follows.

Chapter One: Introduction

In this opening chapter, an overview of the subject of diffusion and its various applications is presented. Chapter One outlines the motivation behind the research work and presents its objectives. Furthermore, this chapter offers a concise summary of the key findings of this study.

Chapter Two: Literature Review

Chapter Two delves into a comprehensive review of the existing literature. This includes background information on diffusion, an exploration of the diffusion phenomenon, and an examination of the traditional methods for determining interdiffusion coefficients. The chapter

also introduces the concept of DIS and discusses its significance in the context of diffusion research.

Chapter Three: Experimental Methods

Chapter Three details the methods used for sample preparation and data acquisition from the system under investigation. The chapter also discusses the procedures for the numerical method used to determine the interdiffusion coefficient. This chapter concludes with a discussion of the statistical tests used to assess the statistical significance of the experimental data.

Chapter Four: Results and Discussion

The focal point of Chapter Four is the presentation and discussion of the results. These include the validation of the numerical methods used, an exploration of the effect of the variation of time on the interdiffusion coefficients in binary systems, an analysis of the effects of time on the impurity diffusion coefficients, a discussion of the underlying contributing factors of DIS, and an evaluation of the significance of the time effects through a conventional approach.

Chapter Five: Summary and Conclusion

Chapter Five serves as the culmination of this work. The chapter summarizes the findings and conclusions drawn from the research conducted.

Chapter Six: Recommendations for Future Research

Finally, Chapter Six outlines the recommendations for future investigations that could arise from this research work. These recommendations aim to further advance understanding of diffusion processes and related phenomena.

CHAPTER TWO

2 Literature Review

2.1 Background information on diffusion

Diffusion is one of the most fundamental processes that greatly affects the rate of occurrence of many phase transformations. It is commonly assumed that diffusion occurs along the concentration gradients [21]. The driving force of diffusion can be expressed in terms of a chemical potential gradient which can lead to a system attaining equilibrium when the chemical potentials of all of the atoms everywhere remains constant. The ease of measuring concentration differences as opposed to chemical potential differences makes it more easier to establish a relationship between diffusion and concentration gradients.

Materials are often annealed to improve their properties. Atomic diffusion is often involved during annealing. Usually, increasing the rate of diffusion is required, except in a few cases where measures are taken to reduce the rate. One can easily predict the heat-treatment temperatures and times, and / or rates of cooling by adopting the mathematics of diffusion and proper diffusion rate constants. A typical example is steel gear designed with a hardened case, by diffusing excess carbon or nitrogen onto the outer surface layer, which will improve the hardness and resistance to fatigue failure [22].

Moreover, the magnitude of the net flux of any species (ions, atoms, electrons, and molecules), depends on the temperature and concentration gradient [1]. The diffusion process has contributed largely to the development of today's technologies. The effort required to manage the diffusion of atoms is paramount especially in materials processing industries. Understanding the diffusion of different atoms into silicon or other semiconductors involves the diffusion of dopants for

semiconductor devices. Dopants with atomic precision such as antimony (sb) and phosphorus (P) are diffused onto small regions of silicon wafers that are as low as nanometers in sizes to create a *p-n junction*. In addition, the diffusion of water vapour, oxygen or other chemicals can be limited by using coatings and thin films. Some of the other applications and technologies related to diffusion include the electrical conductivity of conductive ceramics, manufacturing of plastics beverage bottles, oxidation of aluminum and thermal barrier coatings for turbine blades in aircraft engines [1].

2.2 Mechanism of diffusion

Materials often have defects, which are defined as vacancies. These vacancies create disorderliness reduce free energy and increases the stability of the thermodynamic properties of crystalline material. Usually, the existence of vacancies in materials causes atoms to jump from one lattice position to another, which is a process called self-diffusion [1]. There are two specific conditions required for an atom to jump:

(i) the availability of an empty adjacent site and

(ii) sufficient vibration energy is required by the atom to break the bonds with the neighboring atoms thereby causing lattice distortion during displacement.

A certain fraction of the total number of atoms also migrates at specific temperatures due to their level of vibration. There are two prominent models of atomic motion proposed for metallic diffusion: vacancy diffusion and interstitial diffusion.

2.2.1 Vacancy diffusion

Atoms migrates from their lattice position to fill a neighbouring vacancy which creates a new unoccupied space in the original lattice position. This interchange of an atom with vacant sites causes vacancy diffusion. At high temperatures, a significant number of vacancies are found on metals. The migration of atoms during diffusion leads to the exchange of positions with vacancies. Consequently, atomic diffusion that occurs in one direction, corresponds to the migration of vacancies in the opposite direction. The number of vacancies increases as temperatures increases which significantly influence both self-diffusion and the interdiffusion of a large number of atoms; for interdiffusion, impurity atoms must substitute for the host atoms [22].

2.2.2 Interstitial diffusion

Interstitial diffusion is the migration of atoms from an interstitial space to an empty neighboring position. The interdiffusion of impurities like hydrogen, carbon, nitrogen, and oxygen is an example of interstitial diffusion because their atoms are smaller and can fit into interstitial positions. Interstitial diffusion takes place much faster in metal alloys as opposed to vacancy diffusion as interstitial atoms are smaller and more mobile. A good example are ceramic structures, which have ionic bonding; that is closed packed anions with cations in the interstitial position, so that the smaller cations easily diffuse faster than the larger anions. Furthermore, interstitial atomic migration is more rapid than vacancy diffusion as there are more neighboring interstitial sites than vacancy sites in crystal structures [22,23].

2.3 Driving force of diffusion

At a specific concentration, the diffusion potential serves as the driving force for diffusion. It is possible that diffusion can be influenced by external forces and the potential driving force. The rate of diffusion can also be affected by several potentials.

Some potentials that affect the driving force of diffusion are discussed below, (equations omitted), including, electrical potential, chemical, thermal and stress gradients.

(a) Electrical potential gradients

Electrical potential gradients can provide the energy to drive the mass diffusion of a particular species. There are two types of electrical potential gradients. One type is from the potential gradient that facilitates the migration of diffused charged ions in ionic conductors. An example are solid-electrolyte batteries. The other type of electrical potential gradients involves interstitial atoms in metals that diffuse due to the influence of an electric current [23]. Additionally, the use of an electrical potential gradient can induce diffusion in metals, which is known as electromigration. This occurs due to a cross-effect between the diffusing species and the flow of conduction electrons. This phenomenon is particularly evident when an electric field is applied to a dilute solution of interstitial atoms in metals.

(b) Chemical potentials

The chemical potential of a component is the amount of reversible work required to introduce a very small amount of that component into a system at equilibrium. This process involves the diffusion of a small amount of interstitial solute atoms within the gaps or spaces between atoms in a host crystal. The process occurs in the presence of a concentration gradient of interstitial atoms. The significantly large solvent atoms

essentially remain stationary in their stable positions and undergo much slower diffusion compared to the highly mobile solute atoms, which diffuse through interstitial diffusion. In this context, it is reasonable to consider the solvent atoms as immobile. In this system, the temperature remains constant (isothermal), so diffusion is not restricted by a network, and it is suitable to use a local C-frame coordinate system [23].

(c) Thermal gradients

In a system where both heat flow and mass diffusion of a sparsely spaced interstitial component are present, thermal gradients can trigger mass diffusion. The interstitial chemical potential depends on the concentration, temperature, or both [23].

(d) Stress potential

Stress impacts a number of different aspects of diffusion, including mobility, diffusion potential, and the conditions at the boundaries. The changes in stress during diffusion have a role in shaping the thermodynamic driving force for diffusion and can lead to both elastic and plastic deformations. [24].

(e) Magnetic potential

In situations where a particle carries a magnetic moment and interacts with a magnetic field, supplementary forces can change the chemical potential force. This phenomenon is referred to as magnetic potential, which has the capacity to impact diffusion processes. Research has delved into the influence of magnetic intensity on carbon diffusion [57], and showed that diffusion declines as the intensity of the magnetic field increases.

2.4 Diffusion coefficient

The diffusion coefficient, often denoted as (D), is a fundamental physical parameter that quantifies the rate at which particles, molecules, or species disperse through a medium due to random thermal motion. This coefficient characterizes the ease and speed of diffusion within a given material and under specific conditions. The diffusion coefficient is influenced by factors such as temperature, concentration gradient, and the properties of the medium through which diffusion occurs. The diffusion coefficient is a crucial parameter in a number of different scientific fields which include materials science, chemistry, engineering, biology and physics, as it governs the migration of substances and their interactions in different systems.

Diffusion coefficients are generally evaluated from the experimental data of concentration profiles as presented in Figure 1.1. The Matano interface, also known as the distance origin, is the plane in the diffusion zone that divides the concentration profile equally, where a mass balance is obtained. However, when dealing with ternary and multicomponent systems, complications arise in the presence of the concentration gradient of other components [26].

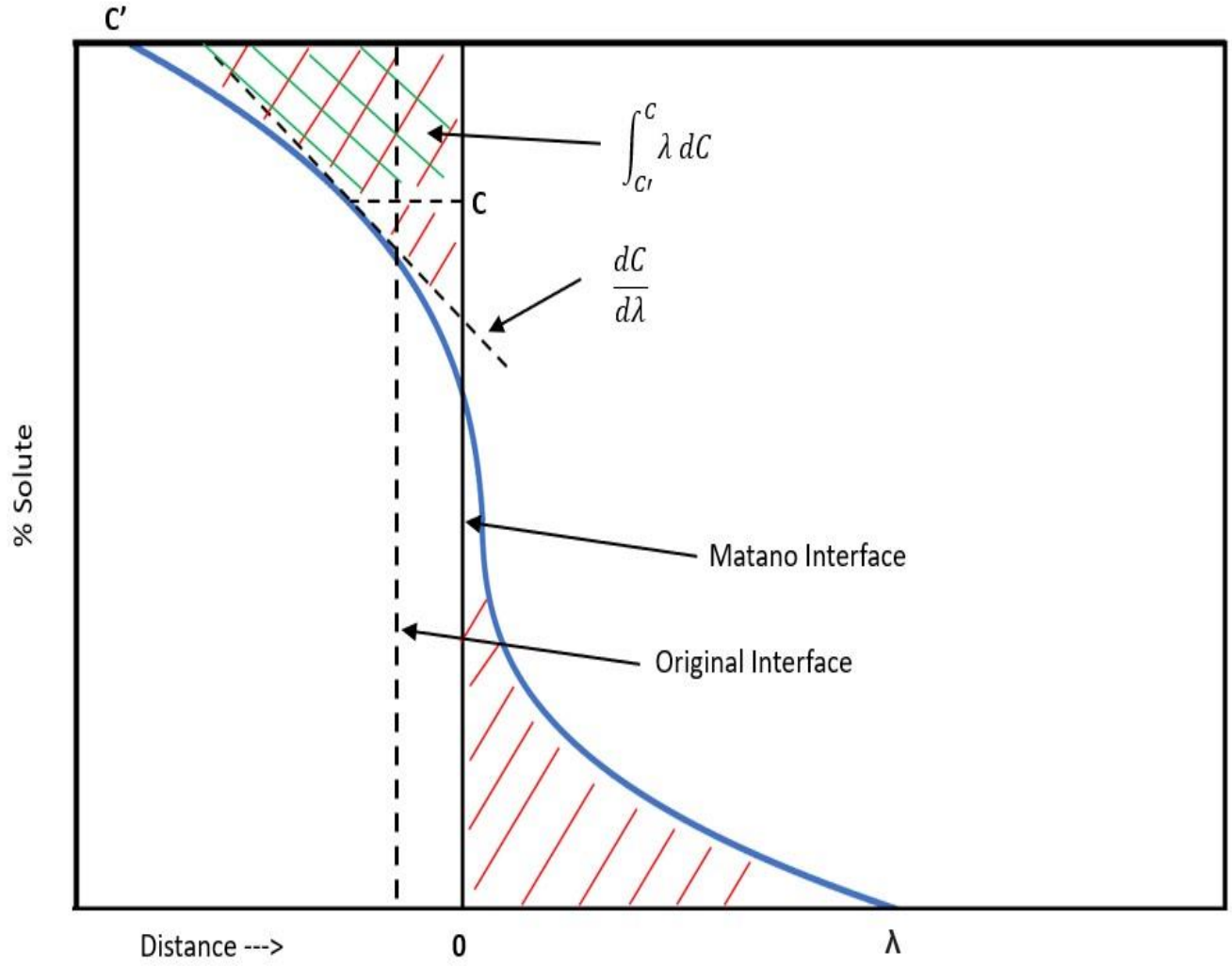

Figure 2.1: Schematic of concentration-dependent diffusion penetration curve in a binary system

2.5 Different types of diffusion coefficients

There are different types of diffusion coefficients, and some of them will be discussed in this section, including:

i) Tracer (self and impurity tracer) diffusion coefficients

ii) Intrinsic diffusion coefficients

iii) Interdiffusion coefficients

iv) Average interdiffusion coefficients

1. Tracer diffusion coefficients

In studies that have focused on diffusion, particularly when investigating trace elements that have radioactivity or isotopic mass, small amounts of the diffusing species, often in the range of parts per million (ppm) or even less, can be used. While a concentration gradient of the trace element is required in a diffusion experiment, it is possible to maintain a low concentration of the total tracer so that the overall concentration of the sample remains practically unchanged throughout the investigation. From an atomistic perspective, this suggests that tracer atoms are not significantly affected by the presence of other tracer atoms. Tracers are suitable for investigating the *self-diffusion* of matrix atoms, and can also be used to study the diffusion of foreign atoms under extremely diluted conditions, a scenario often referred to as *impurity diffusion* [27].

2. Intrinsic diffusion coefficients

The intrinsic diffusion coefficients in a binary alloy system, denoted by D_A^I and D_B^I , show the diffusion of atoms in components A and B in relation to the lattice frame of reference. To determine the intrinsic diffusivities, two measurements are required:

(i) the velocity of the Kirkendall plane and

(ii) the interdiffusion coefficients.

In general, when element A diffuses faster than element B, vacancies are created in the initially abundant region of the more rapidly diffusing element A, thus leading to the loss of mass and contraction in that area. Conversely, vacancies are found in the region initially rich in element B which has less mobility, thus resulting in mass gain and expansion in that region. This cyclic expansion and contraction drive mass flow, ultimately causing the migration of marker particles. The transfer rate of A atoms differs from that of B atoms, thus indicating the existence of two distinct diffusion coefficients: D_A^I and D_B^I. These coefficients are referred to as the intrinsic diffusion coefficients of the respective components.

3. Interdiffusion coefficients

In a binary diffusion couple, the chemical composition of the diffusion zone undergoes changes for a certain distance. Atoms that are undergoing diffusion are subjected to two distinct chemical environments, which lead to the presence of a different type of diffusion coefficient, known as an interdiffusion coefficient. From a broader perspective, the diffusion flux is directly related to the gradient of the chemical potential. There is proportionality between the chemical potential and concentration gradient primarily for

dilute systems or ideal solid solutions. The chemical potential gradient creates an internal driving force, and the mixing of a binary system can be explained with a concentration-dependent interdiffusion coefficient. In the case of a binary alloy, a single interdiffusion coefficient describes the interdiffusion process. This coefficient typically depends on the concentration of the alloy. In essence, interdiffusion can eventually lead to the establishment of an equilibrium concentration of atoms within the material [27].

4. Average interdiffusion coefficient

The concentration profile range of an isothermal diffusion couple in a binary system can indeed be used to calculate the average interdiffusion coefficients. By analyzing the concentration profiles and the rate of diffusion within a diffusion couple, valuable information about the interdiffusion behavior of the two components in the system can be obtained. The data can then be used to calculate the average interdiffusion coefficients, which describe the rate at which the two components mix and diffuse in the system. The D_{ave} or average interdiffusion coefficient is a single diffusion coefficient that enables comparison of interdiffusion behaviour in binary systems at different temperatures and periods of time [28]. In order to determine the D_{ave}, the interdiffusion flux is simply integrated over a range of concentrations along the diffusion zone. The equation is presented below and equivalent to calculating the mean value theorem for interdiffusion against concentration.

$$D_{ave} = \frac{\int_{C_L}^{C_R} D(C)dc}{C_R - C_L} \qquad 2.2$$

where C_R and C_L represent the extreme right and left sides of the concentration profile, respectively.

2.6 Conventional methods of extracting interdiffusion coefficients

There are several conventional methods of extracting interdiffusion coefficients in the literature, a few of them are discussed in this section.

1. *BM*: The Boltzmann-transformed version of Fick's second law is a non-linear ordinary differential equation. This equation can be used to estimate the concentration-dependent interdiffusion coefficient from experimental concentration profiles. In 1933, Japanese scientist Matano proposed appropriate boundary conditions for interdiffusion experiments. [27]. The equation is presented as;

$$D(C) = -\frac{1}{2t} * \frac{\int_{C_L}^{C*}(x - x_m)dC}{\frac{dC}{dx}} \qquad 2.3$$

where x_m is the position of the Matano plane which can be determined by applying a conservation condition expressed as

$$\int_{-\infty}^{x_m}(C(x) - C_L)dx = \int_{x_m}^{\infty}\big(C_R - C(x)\big)dx \qquad 2.4$$

$where\ C_R$ is the concentration of the extreme right-side of the profile and C_L is the concentration of the extreme left-side of the profile. When a binary system is subjected to a diffusion heat treatment for a duration of time *t*, a concentration profile begins to form. This profile can be quantified by conducting an electron microprobe analysis on a cross-section of the diffusion zone. Equation 2.4 is used to determine D for any specific concentration from an experimental concentration profile with raw data. To conduct the analysis, it is essential to determine the position of the Matano plane (denoted as x_m) [27]. Eversole et al. [29] modified the BM method for dilute solutions. They further simplified the integral term in the BM method by parts to change the equation to:

$$D(C) = -\frac{1}{2t} * \frac{(x - x_m)C + \int_{x*}^{+\infty} Cdx}{\frac{dC}{dx}} \qquad 2.5$$

The Matano plane position is then expressed by using the following integral relationship;

$$x_m = \int_0^1 x dC = \int_{-\infty}^{0}\big(1 - C(x)\big)dx + \int_0^{+\infty}\big(1 - C(x)\big)dx \qquad 2.6$$

2. *SF /den Broeder method*: The BM method has also been modified by Sauer and Freise [30] as well as den Broeder [31]. They presented a normalized concentration variable, denoted as Y, with the following definition:

$$Y = \frac{C - C_R}{C_L - C_R} \qquad 2.7$$

Moreover, if there is no volume change during interdiffusion, the SF solution can be expressed as follows:

$$D(C\,) = \frac{1}{2t * \frac{dC}{dx}} * \left[(1 - Y)\int_{x^*}^{\infty}(C^* - C_R)dx + Y\int_{-\infty}^{x^*}(C_L - C^*)dx\right] \qquad 2.8$$

where C^* is the specific concentration at location x^*. The SF approach avoids the need to determine the position of the Matano plane. Consequently, errors related to determining the position are eliminated.

3. *Wagner method*: The equation developed by Wagner is;

$$D(Y_i^*) = \frac{V_m^*}{2t * \frac{dY_i^*}{dx}} * \left[(1 - Y_i^*)\int_{x^{-\infty}}^{x^*}\frac{Y_i}{V_m}dx + Y_i^*\int_{x^*}^{x^{+\infty}}\frac{(1-Y_i)}{V_m}dx\right] \qquad 2.9$$

where Y_i is the normalized concentrations in relation to component *i*, expressed as:

$$Y_i = \frac{N_i - N_i^-}{N_i^+ - N_i^-} \qquad 2.10$$

where N_i^- *and* N_i^+ represent the mole or atomic fraction of the diffusion couple ends that are not affected while V_m denotes the molar volume [32]. The diffusion parameters can be estimated by first converting the concentration profiles to normalized concentration variables.

4. *Hall method:* According to Hall [33], the dependence of diffusion on concentration is exponential, which entails the measurement of slopes and areas of a curve with ordinates and slopes that tend to infinity at the extreme points or limits of the concentration range. Diffusion coefficients calculated accordingly for concentrations close to their limit are therefore subject to considerable uncertainty. The diffusion coefficients of low concentrations are of great importance in terms of diffusion mechanisms for solutions. One element of the diffusion couple is mainly expected to have zero concentration. The following supplementary transformation is introduced in the Hall method (HM) for the dilute end or tail of the concentration profile:

$$C = erfc(u) \qquad 2.11$$

where

$$erfc(u) = \frac{1}{2}(1 + erf(u)) \qquad 2.12$$

$$u = h\lambda + k \qquad 2.13$$

$$\lambda = (x - x_m)\frac{1}{\sqrt{t}} \qquad 2.14$$

Hall [33] assumed that the tail of the concentration profile has linear behavior. The derivative and integral term in the D(C) is evaluated by using [34];

$$\frac{dC}{dx} = \frac{1}{\sqrt{t}}\frac{dC}{d\lambda} = \frac{h}{\sqrt{\pi t}}\exp(-u^2) \qquad 2.15$$

$$\int_0^{C^*}(x - x_m)dC = \sqrt{t}\int_0^{C^*}\lambda dC = -\sqrt{t}\left(\frac{1}{2h\sqrt{\pi}}exp(-u^2) + \frac{kC}{h}\right) \qquad 2.16$$

Combining these equations with the BM equations will yield the HM equation written as:

$$D(C) = \frac{1}{4h^2} + \frac{k\sqrt{\pi}}{2h^2}exp(u^2)erfcu \qquad 2.17$$

where h represent the slope and k denote the intercept of the linear portion of the concentration ratio curve and $u = h\lambda + k$.

5. *Extended Hall Method:* The Extended Hall Method (EHM) was developed to analyse the concentration profile as a whole while the HM was derived to solve for D(C) only at the end of the concentration profile where the concentration approaches zero in linear behavior in the form of a probability plot. Zero concentration at the extreme end remains as the starting point. The development involves combining the basic integration and differentiation steps into the interdiffusion coefficient and calculated at every two neighboring concentration points in a stepwise manner.

   The interdiffusion coefficient for the EHM is given as [35]

   $$D\big(C'(i)\big) = \frac{-1}{2*h'(i)} e^{\{u'(i)\}^2 I(i+1)} \qquad 2.18$$

   where $C'(i) = 0.5\big(C(i) + C(i+1)\big)$

   $u' = h'\lambda' + k'$

   The coefficient of the linear that fits in the equation above are

   $h' = \frac{u(i+1)-u(i)}{\lambda(i+1)-\lambda(i)}$ $\qquad and$

   $k' = \frac{\lambda(i+1)u(i)-\lambda(i)u(i+1)}{\lambda(i+1)-\lambda(i)}$

6. *Method in Sarafianos [36]*: Sarafianos [36] developed an analytical method to determine the different types of diffusion coefficients. He adapted and expanded the analytical technique in Hall [33] to include intermediate concentrations. This modification aimed to formulate an analytical expression capable of determining variable diffusion coefficients across an entire range of concentrations.

The equation considered for three cases (regions of low, medium and high concentrations) is:

$$\frac{-x}{2t}dC = d\left(D\frac{dC}{dx}\right) \quad 2.19$$

(i) For low concentration regions:

$$D = \frac{1}{2t}\exp(u^2)\int_x^{\infty} x\, exp(-u^2)dx \quad 2.20$$

(ii) For high concentration regions:

$$D = -\frac{1}{2t}\exp(u^2)\int_{-\infty}^{x} x\, exp(-u^2)dx \quad 2.21$$

Evaluation of the integral in Equations 2.20 and 2.21 gives

$$D(C) = \frac{1}{4h^2t}\left(1 - k\sqrt{\pi}\, exp(u^2) erfcu\right) \quad 2.22$$

(iii) For intermediate range of concentration:

$$U_{i-\frac{1}{2}} = h_i\left[x_A + (i - \tfrac{1}{2})\Delta x\right] + k_i \quad 2.23$$

7. *The Forward Simulation Method:* Recently, the FSM has been proposed to address the limitations inherent in traditional methods like the SF, BM, HM and Wagner methods [40]. FSM stands out as a robust technique used for extracting both impurity diffusion coefficients and (D(C)s) from experimental concentration profiles. This method is applicable in situations where the interdiffusion coefficient exhibits either strong or weak dependence on the solute concentration and can be used in both infinite and finite systems [37-46]. Moreover, the FSM can be effectively applied in various coordinate systems, including 1-dimensional planar, 2-dimensional cylindrical, and 3-dimensional spherical coordinates. The FSM excels at accurately evaluating the D(C) in systems that show a significant initial solute concentration. [46].

2.7 Concept of DIS

DIS has been the subject of research attention for over a few decades. Prussin [47] reported the mechanism of dislocation generation through stress during the diffusion process and the distribution of such dislocations by solute diffusion.

In both crystalline and non-crystalline solids, the overall interdiffusion process is a complex interplay of various factors. These factors include the diffusive transport of individual chemical components, generation of internal stress, and convective transport resultant of induced deformation. For instance, differences in the partial molar volumes and migration of diffusing species can result in an unequal distribution of volume transport. This unequal distribution is akin to the generation of a non-uniform, stress-free strain, as shown in Figure 2.2. A side of the diffusion couple contracts, while the other side expands. DIS is a consequence of the atomic-scale rearrangement of atoms or molecules within a material. The generation of DIS is somewhat inherent and inevitable when dissimilar atoms engage in mass transfer. Consequently, stress can potentially accumulate within the diffusion system, thus triggering micro and macro-level deformations (for example, the bending of thin films and the Kirkendall effect) and altering the thermodynamic potential. Consequently, this also serves as an added driving force for the process of interdiffusion.

It is noteworthy that the stress field associated with this stress-free strain has been traditionally overlooked in classical Darken analyses of interdiffusion. These analyses assume that stress relaxation occurs rapidly and completely. Consequently, only convective transport, notably the Kirkendall effect resulting from this relaxation, is considered in the theory [8].

Furthermore, the rate at which DIS relaxes is not the same as the rate at which it is generated. This implies that the relaxation process is not swift enough to immediately counterbalance the buildup

of DIS. Consequently, DIS can accumulate near the interface between dissimilar materials. Additionally, the rate at which DIS relaxes is linked to the viscosity of the diffusion couple. In other words, various factors, including the concentration of the diffusion couple, diffusion heat treatment, and more, can significantly affect DIS by altering the viscosity of the diffusion couple. Hence, the presence of DIS can lead to micro and macro deformations as well as stress-induced diffusion.

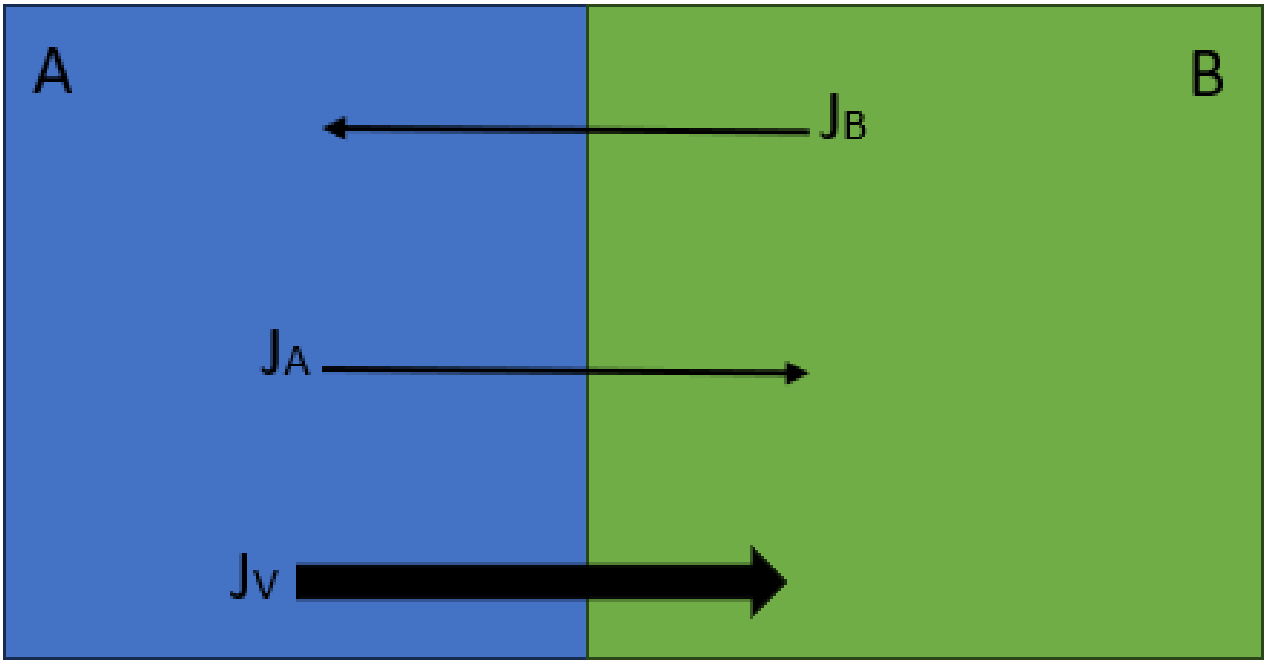

Figure 2.2: Schematic binary diffusion couple for vacancy mechanism

CHAPTER THREE

Methodology

Chapter Three provides details on the methods used for sample preparation and data acquisition from the system under investigation. The procedures for the numerical method used to extract the interdiffusion coefficient are also elaborated. Finally, a discussion of the statistical tests used to assess the statistical significance of the experimental data is provided.

3.1 Materials

The materials used for the sample preparation is pure Cu (100% concentration), pure Ni (100 % concentration), a Cu-based alloy (10 at %Ni) and Ni-based alloy (10 at % Cu), which were all supplied by ACI Alloys Inc. These materials would be later coupled as pure Cu vs pure Ni, pure Cu vs Cu-based alloy, and Cu-based alloy vs pure Ni.

3.2 Cold-rolling

The metals were cold rolled into sheets and cut into cross-sectional dimensions of 12mm x 7mm and thickness of 1.5mm. Cold rolling is a work hardening process that is used to change the structure of metals without the use of heat. This process is usually carried out at room temperature while the metal is subjected to mechanical stress to cause permanent changes to the crystalline structure of the metal which makes the metal stronger. The metals, were fed into large rollers where they were compressed and subjected to high pressure just below their ultimate tensile strength to reduce their thickness.

3.3 Annealing

Following cold rolling, the cross-sectional samples showed a substantial dislocations and residual stress, both of which have a notable influence on interdiffusion. The grain boundaries and dislocations serve as pathways to enhance diffusion, primarily due to the increased migration of the atoms within these defect-rich regions as compared to the regular lattice structure [48-50]. To grow the grains and reduce the internal stress, the samples were then annealed at 1030^0C for 2hrs in vacuumed quartz capsules with backfilled argon gas. The annealing temperature is sufficiently higher to initiate both recrystallization and reduce the stress, thereby preventing any potential grain growth and interference from the residual stress when the diffusion process occurs at a lower temperature [51]. Hence, it is essential to conduct treatments that adequately reduce the stress and grain growth treatments prior to initiating the thermal bonding process.

3.4 Thermal bonding with brazing furnace

The thermal bonding of the samples was conducted by using a LABVAC II brazing furnace produced by (GCA/ Vacuum Industries). Prior to bonding, a meticulous surface preparation procedure was carried out on the samples to expose their surfaces for optimal thermal bonding. The process entailed grinding the samples with 400, 600 and 1200 paper grit, followed by polishing with a liquid diamond suspension.

Then, a Nicrobraz® Green Stop-off pen was applied uniformly to the back side of the polished samples. This Type I solvent prevents the stainless-steel jigs from adhering together to the diffusion couples during the bonding process.

The prepared samples, along with the stainless-steel jigs, were then carefully inserted into the brazing furnace. The furnace was programmed to follow a specific temperature profile, with the bonding temperature set at 600^0C. The bonding process took place over a duration of 1hr under a

high vacuum environment, and a pressure of approximately 10^{-6} Torr was maintained. This controlled environment ensured the accurate and reliable thermal bonding of the samples, which is critical for the success of the experiment.

3.5 Electrodeposition

The thermally bonded couples were subsequently subjected to electrodeposition to enhance their resistance to oxidation during diffusion treatments and also prevent galvanic corrosion which can take place if any of the following three conditions are found: the presence of metals that are electrochemically dissimilar, metals that have electrical contact and metals exposed to the same electrolyte. Electrodeposition is an electrochemical process used to coat or deposit a layer of metal onto the surface of a conductive object. This process is widely used in various industries, including the manufacturing, electronics, jewelry, and automotive industries, to enhance appearance, durability, and functionality.

The components of an electrodeposition process include an anode, cathode, electrolyte and direct current (DC) power supply.

The anode is the conductor where oxidation takes place, and typically made of the same metal that is being deposited, which in this case is Cu. Cu is the source of the metal ions that are deposited onto the samples. The sample metals are deposited onto the cathode which acts as the receiving surface. The electrolyte is a solution that contains metal salts, which provide the source of metal ions for deposition. This solution also contains other chemicals to control the deposition process. Finally, a DC power supply is used to provide the necessary electrical voltage and current to drive the electrochemical reaction.

During electrodeposition, metal ions from the electrolyte migrate toward the cathode (the sample) when a DC is applied. These metal ions gain electrons at the cathode and are reduced to form solid metal atoms. These solid metal atoms then adhere to the surface of the cathode, gradually building a layer of metal. As the electrochemical process continues, the metal atoms are deposited onto the surface of the cathode to form a uniform and adherent metal coating. The thickness of the deposited layer can be controlled by adjusting the electrodeposition time. Afterwards, the coated sample undergo post-processing steps such as being rinsed with distilled water and dried.

3.5.1 Electrodeposition steps

Electrodeposition involves several steps to ensure the successful deposition of a metal coating onto the samples. They include surface preparation, immersion into an electrodeposition solution, electrodeposition, monitoring parameters and completion of electrodeposition.

a) Surface Preparation

- The samples were inserted into a chemical solution of sodium hydroxide (NaOH), sodium carbonate (Na_2CO_3) or disodium phosphate (Na_2HPO_4) at a temperature of 400^0C. This solution helps to remove contaminants and prepare the surface for plating.
- The samples were then rinsed with distilled water.
- The samples were further rinsed with dilute hydrochloric acid (HCl) and dilute sulfuric acid (H_2SO_4) solutions to further clean and activate their surface. This activation step is crucial for ensuring a strong bond between the protective coating and the diffusion couple.

b) Immersion in electrodeposition solution

- The cleaned samples were transferred into a glass vessel that contained an electrodeposition solution of copper(II) sulfate ($CuSO_4$). This solution serves as the source of metal ions for deposition.

c) Electrodeposition.

- A VersaSTAT_3 potentiostat galvanostat was used to control the electrodeposition process. The current density was set to 10mA/cm^2, which determines the rate at which Cu is deposited onto the samples. In this case, the goal is to deposit a specific thickness of 10.3micro-meter of Cu onto the samples.
- During electrodeposition, metal ions from the solution migrated to the surface of the samples and were reduced to form a solid metal layer, which in this case Cu.

d) Monitoring parameters

- Throughout the electrodeposition process, it is essential to monitor the parameters, including the current density and plating time, to achieve the desired thickness and ensure the quality of the deposited layer of Cu.

e) Completion of electrodeposition

- Once the desired thickness of Cu has been deposited onto the samples, the electrodeposition process is completed. The samples can then be carefully removed from the plating solution and subjected to any necessary post-processing steps, such as rinsing with distilled water and drying.

3.6 Isothermal diffusion treatment

Following the electrodeposition process, all of the bulk planar samples were sealed in vacuumed quartz capsules filled with argon gas in preparation for the subsequent diffusion heat treatments.

Tables 3.1 to 3.3 list the details of the diffusion couples: pure Cu vs pure Ni, pure Cu vs Cu-based alloy, and pure Cu vs Ni-based alloy diffusion couples, respectively.

Table 3.1 : Pure Cu vs pure Ni diffusion couple

Temp/Time	5 hrs	25 hrs	75 hrs	150 hrs	450 hrs
900^0C	√	√	√	√	√
940^0C	√	√	√	√	√
980^0C	√	√	√	√	√
1020^0C	√	√	√	√	√

Table 3.2: Pure Cu vs Cu-based alloy (with 10 at %Ni) diffusion couple.

Temp/Time	25 hrs	150 hrs
900^0C	√	√
1020^0C	√	√

Table 3.3: Pure Ni vs Ni-based alloy (with 10 at %Cu) diffusion couple.

Temp/Time	25 hrs	150 hrs
900^0C	√	√
1020^0C	√	√

3.7 Metallographic sample preparation

The effective preparation of samples in metallographic laboratories remains a skill-based endeavor. Given the increasing importance of accreditation in the field of metallography, it has become essential to incorporate systematic evaluations of procedures and establish standard documentation alongside empirically developed techniques. In the following discussion, some of the fundamental aspects involved with the preparation of the samples in this study are reviewed.

1.) *Sampling:* A crucial step in the preparation of samples, and essential to choose the appropriate technique tailored to the specific material and its unique conditions. Ensuring meticulous control over the results is imperative to avoid any potential artifacts. The technique used is electron discharge machining (EDM), a metal fabrication process whereby the desired shape is obtained by using electrical discharging (spark machining).

2.) *Mounting*: Done in Kemet conductive phenolic (bakelite) resin, primarily chosen for its suitability for small-sized samples. A mounting press is utilized along with a hot compression mounting process which subjects the sample to heat and pressure, thus securely fixing the sample. Mounting the samples offers several advantages, including improved handling during the grinding and polishing stages, and the convenience of labeling or marking for straightforward identification.

3.) *Grinding:* An essential step in the preparation process. Typically, the surface of a cut cross-section shows a significant degree of irregularity, which is systematically eliminated through a series of grinding steps. Emery paper, coated with silicon carbide (SiC) particles, is used for this purpose. The emery paper used are meticulously graded from coarse to fine, with a particle size that varies between P400 to P1200. This gradual progression of abrasiveness helps to give the sample a smoother and more uniform surface finish.

4.) *Polishing:* A crucial step to attain a surface that is free from artifacts. Polishing involves the removal of the rough layer from the sample. While it is generally possible to create surfaces that are free of scratches, mechanically polishing a surface until there are no flaws can be challenging, if not impossible. Diamond polishing paste was applied to the samples, beginning with a relatively coarse grade of 6 microns and progressing to a finer grade of 1 micron. This use of a progressively finer abrasive contributes to the desired level of surface smoothness and quality.

5.) *Optical microscopy*: Serves as a method for investigating the microstructure, particularly in the case of metallic materials, which are typically opaque. Consequently, the predominant approach in metallography is to examine the planar cross-sections by using an incident light. An optical microscope is used for optical microscopy in this study, which uses a visible light and a series of lenses to produce enlarged images of the samples. The samples were positioned on the stage of the microscope and connected to a computer to capture the micrographs. The optical microscope plays a crucial role in the grinding and polishing process by allowing observations of the sample when it is completely polished and free from any surface irregularities. The microscope allows for quality control and accuracy during sample preparation.

3.8 Scanning Electron Microscopy

Scanning electron microscope is one of the most versatile methods for microstructural analysis which uses a scanning electron microscope (SEM). The operational principle of scanning electron microscopy is relatively straightforward: an electron beam scans the surface of the sample, which is similar to how a cathode-ray tube displays an image [52]. These electrons are typically emitted

from a heated tungsten cathode. The SEM offers several imaging techniques for studying metallic microstructures, and a few of them are discussed as follows.

Secondary Electron (SE) Mode is a mode of scanning electron microscopy and used to reveal the surface topography and, in favorable cases, provides information on the atomic number and crystal orientation contrast with high resolution. The SE mode is particularly useful for obtaining information from a shallow depth just beneath the surface.

Backscattered Electron (BE) Mode is a mode of scanning electron microscopy that provides topographic details and substantial material contrast from a more significant depth and width beneath the surface of the sample. However, the BE mode typically results in reduced resolution compared to the SE mode. The JEOL JSM-5900LV SEM is specifically designed for scanning electron microscopy applications. This SEM is a specialized instrument used for high-resolution imaging and microstructural analysis of various materials, including metallic samples. This SEM is equipped with features and capabilities that enable researchers and scientists to study the microstructures of materials at different scales, which make it a valuable tool in the field of materials science and microstructural analysis.

The ability of SEM to offer multiple imaging modes makes it an invaluable tool for the comprehensive analysis of microstructures in metallic materials.

3.9 Data Measurement

The diffusion couple samples were cross sectioned by using the EDM as discussed earlier. It is important to accurately acquire the data for a proper understanding of the characteristics of the diffusion behaviour in the Cu-Ni system under investigation. The samples were mounted on a bakelite purposefully to hold them tightly for ease of surface preparation. The goal was to clean

the surface of the cross-section so that it would be free from particles that could prevent the accurate measurement of concentration profiles across the diffusion zone. Furthermore, the samples were carefully positioned on the JEOL JSM-5900LV SEM and concentration profiles were acquired by using EDS.

3.10 Data Smoothening and Analysis

To minimize errors when calculating the interdiffusion coefficients with the use of a concentration profile, it is a good practice to acquire a number of concentration profiles. When approximately five concentration profiles are used for each sample, the accuracy and reliability of the calculations can be enhanced through data redundancy and statistical analysis. Additionally, a number of concentration profiles allows assessment of the consistency of results across different measurements, thus improving the overall confidence in these findings. The profiles were smoothened by using the simple moving average technique [53] to minimise the noise and randomness of the data. The average of the five smoothened profiles were then calculated into a single profile for each sample to represent their corresponding concentration profile. The average concentration profile was subsequently analysed by using the recently developed model in [54-55].

3.11 Numerical model governing equations

The numerical model in Olaye and Ojo [20,54-55] for extracting interdiffusion coefficients from experimental data uses a hybrid approach. They used a fully explicit finite difference analysis with the Leapfrog/Dufort-Frankel scheme. This combination is used to avoid the need for non-trivial simplifications that could potentially reduce the accuracy of fully implicit solutions. By doing so, the model provides a more accurate and comprehensive understanding of the interdiffusion process

based on the experimental data, while maintaining numerical stability and minimizing the impact of simplified assumptions. The detailed derivations can be found in [20, 54-55]

The governing equations used for the numerical model are:

$$r^{\lambda-1}\frac{\partial c(r,t)}{\partial t} = \frac{\partial}{\partial r}\left(r^{\lambda-1}D_A[c(r,t)]\frac{\partial c(r,t)}{\partial r}\right) \qquad 0 \le r \le s(t) \qquad 3.1$$

$$r^{\lambda-1}\frac{\partial c(r,t)}{\partial t} = \frac{\partial}{\partial r}\left(r^{\lambda-1}D_B[c(r,t)]\frac{\partial c(r,t)}{\partial r}\right) \qquad s(t) \le r \le R \qquad 3.2$$

$$D_A[c(r,t)]\frac{\partial c(r,t)}{\partial r}\Big|_{r=s(t)^-} - D_B[c(r,t)]\frac{\partial c(r,t)}{\partial r}\Big|_{r=s(t)^+} = [C_B - C_A]\frac{ds}{dt} \qquad r = s(t) \qquad 3.3$$

Equations 3.1 to 3.3 usually apply to a two-phase system but are now being adapted for use in the single-phase system under investigation in this study. This adaptation involves tailoring the model to accommodate the specific characteristics and behavior of the single-phase system, thus allowing for a more accurate analysis of the system's interdiffusion properties of the system. Equations 3.1 and 3.2 denote the diffusion of the solute in Phases A and B, respectively, while Equation 3.3 describes the migration along the interface. The diffusion coefficients in Phases A and B are D_A and D_B respectively while λ represent the geometrical ratio which is 1 for planar, 2 for cylindrical and 3 for spherical geometries.

3.12 Leapfrog/Dufort-Frankel scheme

The Dufort-Frankel scheme effectively combines the attributes of the Euler explicit and Crank Nicholson schemes and capitalizes on their stability and rapid convergence. Consequently, the Dufort-Frankel scheme boasts unconditional stability and a convergence rate that is twice as fast as that of the Crank-Nicholson scheme. This is primarily due to the diminishing ratio of the change

in time to the change in position, a characteristic often utilized for solving parabolic equations via the finite difference method [78].

Moreover, the Dufort-Frankel scheme can be used to calculate diffusion coefficients, regardless of whether they are constant or variable. The scheme is particularly well-suited for solving single-phase systems devoid of continuous interface boundaries. However, in cases where the advective term that represents interface boundary migration is present, the Leapfrog approach is used to analyze this scenario. Drawing from the findings reported in [54, 55], the Leapfrog/Dufort-Frankel algorithm is implemented to solve the finite difference scheme for Equations 3.1 and 3.2. Given that the system under investigation is a single-phase, either of the discretized equations, that is Equation 3.1 or 3.2, can be used.

3.13 Forward simulation procedures

The FSM is an iterative technique that calculates D(C)s accurately through an inverse relationship between the concentration gradients and diffusion coefficients. To execute the FSM, numerical models that can solve Fick's law in single or multi-phase systems are necessary. The numerical models used to apply Fick's second law for simulation in this research work has been extensively discussed [20,54,55,56-59].

In this study, the numerical inverse method for forward simulation is used to calculate the interdiffusion coefficients for cases that involve a non-uniform initial solute distribution and those without a non-uniform initial solute distribution. This method is commonly used in scenarios that involve diffusion processes, which are often found in fields like materials sciences and aerospace engineering. The steps of this method are outlined as follows:

1. First, the concentration profiles are prepared after SEM observation. They are smoothened to remove noise or irregularities.
2. The initial estimate for the interdiffusion coefficient function, denoted as D = exp(f(C)), is made based on a conventional method such as the BM, or SF method. This function relates the diffusion coefficient (D) to the concentration (C).
3. Using the assumed interdiffusion coefficient function and a numerical model capable of solving Fick's second law, the behavior of the system over time is simulated. This procedure also works for cases with significant initial solute distributions.
4. Following the simulation of the diffusion process, a comparison is made between the calculated concentration profiles and experimentally obtained concentration profiles. The least squares method is frequently used to quantify the differences between the simulated and experimental profiles. If the error is below a predefined tolerance value of 0.001, the process is considered to be acceptable.
5. If the error is not within the acceptable tolerated value, the interdiffusion coefficient function is adjusted. The interdiffusion coefficient is adjusted by multiplying, by the ratio of the inverse concentration gradient of the experimental and simulated profiles, respectively. Equations 3.4 is used to adjust the interdiffusion coefficient.

$$D(C)_{new} = D(C)_{old} * \frac{\left.\frac{dx}{dC}\right|_{experiment}}{\left.\frac{dx}{dC}\right|_{simulated}} \qquad 3.4$$

6. Steps 3 through 5 are repeated iteratively until a preset accepted level of error is reached. This involves refining the interdiffusion coefficient function with each iteration, to converge to a solution that is in good agreement with the experimental data.

In summary, the numerical inverse method for forward simulation is used to estimate the interdiffusion coefficients by iteratively adjusting an estimated coefficient function until the simulated concentration profiles match the experimental profiles within a specified tolerance value. This approach is valuable for understanding and characterizing diffusion processes in materials and other systems.

3.14 *T*-statistics test

To further evaluate the significant differences in the data obtained in this study, it is imperative to use a statistical analysis. The *t*-statistics method is commonly used because comparisons of the means between two groups can be implemented. This method is frequently used to test hypotheses to determine whether a particular process or treatment has a discernible impact on the population of interest or if there are significant differences between two groups. The *t*-statistics and the degrees of freedom (denoted as "d") in the t-test are expressed as follows [79]:

$$t = \frac{D(C)|_2 - D(C)|_1}{\sqrt{\frac{S_2^2}{n_2} - \frac{S_1^2}{n_1}}} \quad 3.5$$

$$d = n_2 + n_1 - 2 \quad 3.6$$

where n_2 and $n_1$represent the sample size, $D(C)|_2$ and $D(C)|_1$ denote the mean values of the interdiffusion coefficients and S_2 and S_1 represent the standard deviations.

To facilitate the *t*-test analysis, statistical software is integrated with Excel spreadsheets. This built-in function takes the raw data and calculates the *t*-value, which is subsequently compared to a

critical value. Additionally, the *p*-value is calculated which allows for a quick assessment of the statistical difference in the dataset. The recommended threshold for significance is typically set at $p < 0.001$, which indicates that the data are considered statistically and significantly different when $p < 0.001$, while $p > 0.2$ suggests that the compared datasets are statistically similar.

CHAPTER FOUR

Results and Discussion

This chapter presents the results and discussion on the time variation effect on concentration dependent interdiffusion and impurity diffusion coefficients in Cu-Ni system. The underlying contributing factor of DIS and the significance of time variation of diffusion coefficients are also discussed.

4.1 Validation of numerical model

Olaye and Ojo [54, 55] developed numerical diffusion model to analyze a system with two concentration profiles which allows for the determination of D(C), through the use of these two experimental concentration profiles. This is a numerical inverse method that can estimate the concentration dependency of the interdiffusion coefficient when there is a non-uniform solute distribution in the system. In situations where there is a pre-existing non-uniform solute distribution, conventional methods like BM, SF, Hall, and Wagner methods, typically used to determine diffusion coefficients from experimental concentration profiles, are not applicable. The reason for this limitation lies in the common assumption that a material does not have a non-uniform solute distribution prior to the diffusion process. This implies that there is an initial step function in space by the solute concentrations [35, 60-61].

Moreover, a number of material processes like sintering, brazing, coating, age-hardening, etc. require diffusion-controlled treatments with multiple steps because of the multiple steps of diffusion at various temperatures. During the modelling of diffusion-controlled processes with multiple steps, it is common to use concentration-dependent diffusion coefficients for modeling diffusion behavior at different temperatures with standardized techniques that involve no non-

uniform initial solute distribution. The conventional methods cannot effectively estimate the concentration dependent interdiffusion coefficient in materials with a non-uniform solute distribution before diffusion treatment. Hence, the numerical diffusion model used conveniently estimate the D(C) when there is pre-existence of non-uniform solute distribution prior to diffusion. The numerical model uses the solution of Fick's second law as a means to calculate the interdiffusion coefficients, ultimately yielding the simulated concentration profiles. The FSM is used with the model to calculate the interdiffusion coefficient with a non-uniform initial solute distribution which then calculates the interdiffusion coefficient needed to obtain the final experimental concentration profile by using the initial concentration profile as the initial condition. In order to validate the results of the numerical model used in this study, the FSM was used to adjust the interdiffusion coefficient function until an acceptable error margin was attained. A litmus test to confirm the accuracy of the final results of the D(C) produced was used to compare the final simulated concentration profile with the final experimental concentration profile as presented in Figures 4.1 and 4.2. It can be observed in the figures that the simulated final concentration profile is somewhat in agreement with the final experimental profile. Hence, using conventional analytical methods to calculate the D(C) for cases that have a pre-existing non-uniform initial solute distribution can result in significant errors.

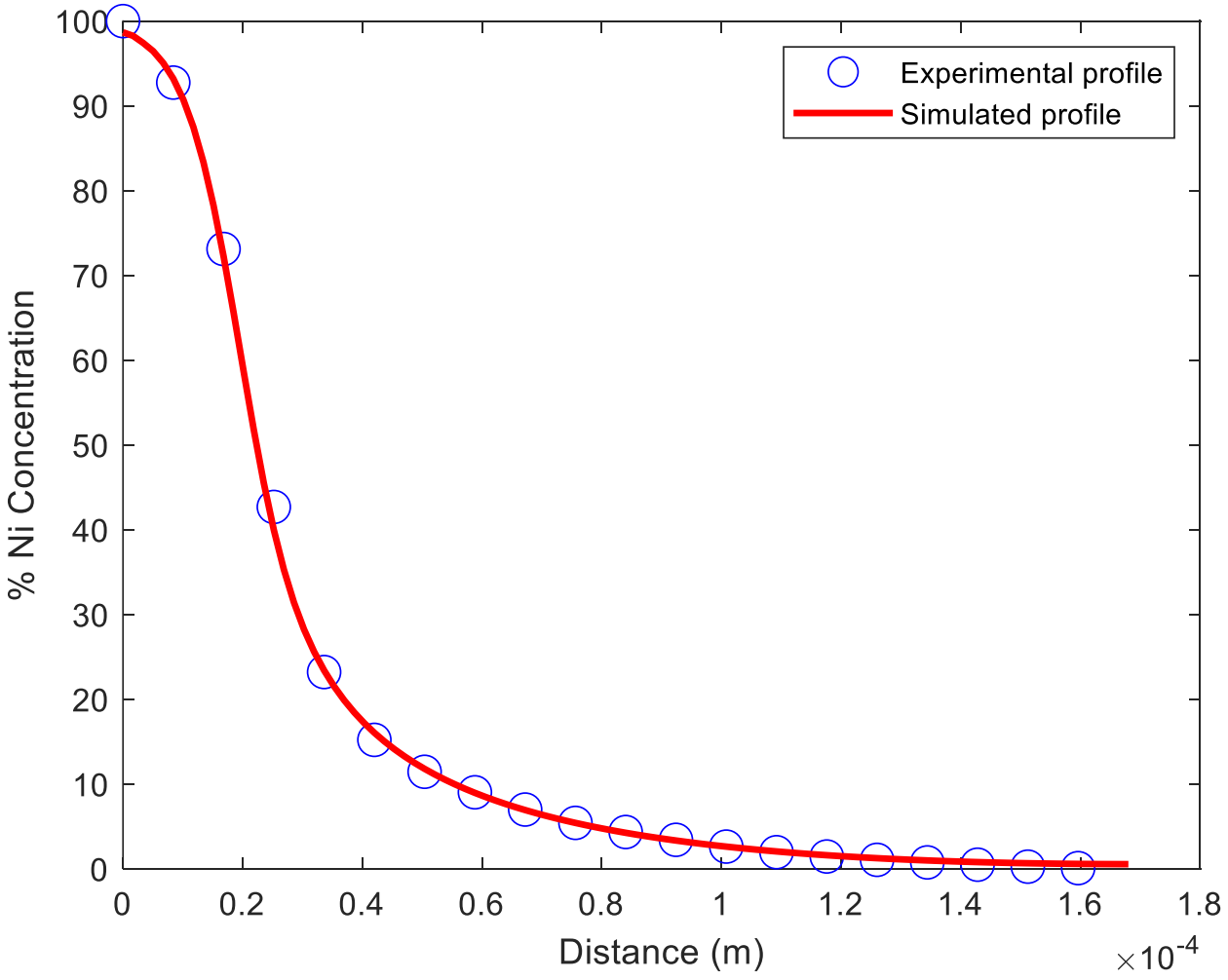

Figure 4.1: Variation of experimental profile with simulated profile for pure Cu-Ni between 5-25 hrs at 900^0C.

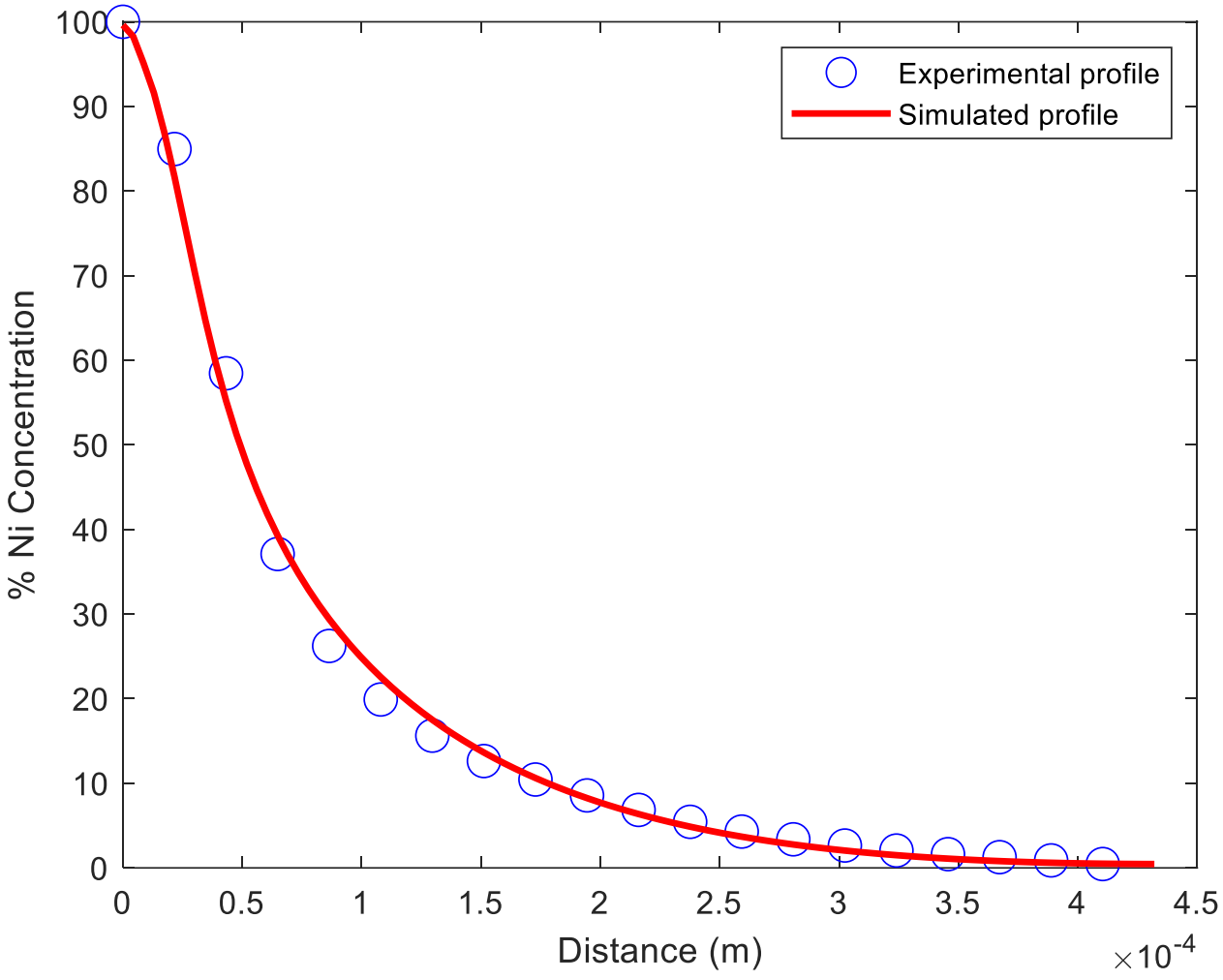

Figure 4.2: Variation of experimental profile with simulated profile for pure Cu-Ni between 150-450 hrs at 900^0C

4.2 Effect of Time on Interdiffusion Coefficients

Validating the effect of time on interdiffusion coefficients is a crucial factor for understanding how the rate of diffusion changes over different periods of time. This validation process involves experimental, theoretical, and computational approaches to assess how various factors, such as concentration gradients, temperature, and material properties, influence the diffusion process over time.

Experimental verification in this research entails conducting diffusion experiments under controlled conditions and measuring the concentration profiles of diffusing species of a pure Cu-Ni binary system and its alloys at different time intervals. The collected data were then analyzed to observe how the diffusion rate changes with time. If the observed diffusion behavior deviates from traditional models or expectations, this may suggest the presence of time-dependent effects.

Theoretical modeling and computational simulations also play a significant role in verifying time effects on diffusion. A recently developed mathematical model and numerical simulations that incorporate the relevant factors that affect diffusion and running them over different time intervals was used to compare the simulated results with experimental data to help validate whether time-dependent effects are at play.

Furthermore, statistical analysis, such as the calculation of standard deviation error bars, *p-values* of the *t-statistics* used in this study will provide insights into the significance of observed changes in diffusion behavior over time.

Ultimately, the validation of time effects on diffusion contributes to a better understanding of how diffusion processes evolve and are influenced by various factors. Validation will also allow researchers to refine existing theories and models to better capture real-world diffusion phenomena.

4.2.1 Effect of Time on Interdiffusion Coefficient in Pure Cu-Ni system at 900^0C

A pure Cu-Ni diffusion couple was annealed at a constant temperature of 900^0C and different time intervals of 5-25 hrs, 75-150 hrs and 150-450 hrs. The numerical model in [20] was coupled with the FSM to produce interdiffusion coefficients that vary with solute concentration as shown in Figures 4.3 - 4.5. The results show the concentration dependency of D(C) operative between two isothermal concentration profiles; for instance, a diffusion time interval of 5-25 hrs means an initial non-uniform solute distribution obtained at 5 hrs and a final experimental concentration profile obtained after 25 hrs. This contradicts the conventional techniques such as the BM, SF and Hall-methods, because the results of the D(C)s obtained through these conventional methods can conveniently solve diffusion couple between the diffusion period and time zero; that is, the host material has no solute atoms and no specific diffusion time. However, Figure 4.3 statistically reveals variation in time as the D(C) changes from 5 to 25 hrs to 25 to 75 hrs. At the Cu-rich region, the difference is highly significant, and then steadily reduces until the difference is no longer obvious. Similarly, the *p-values* of the *t-statistics* in Table 4.1 shows a range of concentration points between 11 at % Ni – 30 at % Ni that are statistically similar while the majority of the concentration points reveals a statistically reliable result that confirms the data of the D(C) varies as the time interval of diffusion changes.

The calculated average diffusion coefficient D_{ave} as shown in Table 4.2 shows a significant variation of about 72% increase in diffusivity as the diffusion process progresses from 5-25 hr. Likewise, about 34% and 81% increases in the average diffusivity occur during a diffusion time of 25-75 hrs to 75-150 hrs and period of 75-150 hrs to 150-450 hrs respectively. These results show a significant variation of time of the D(C) through the emerging non-uniform initial solute distribution which conflicts the general assumption that it does not change with time.

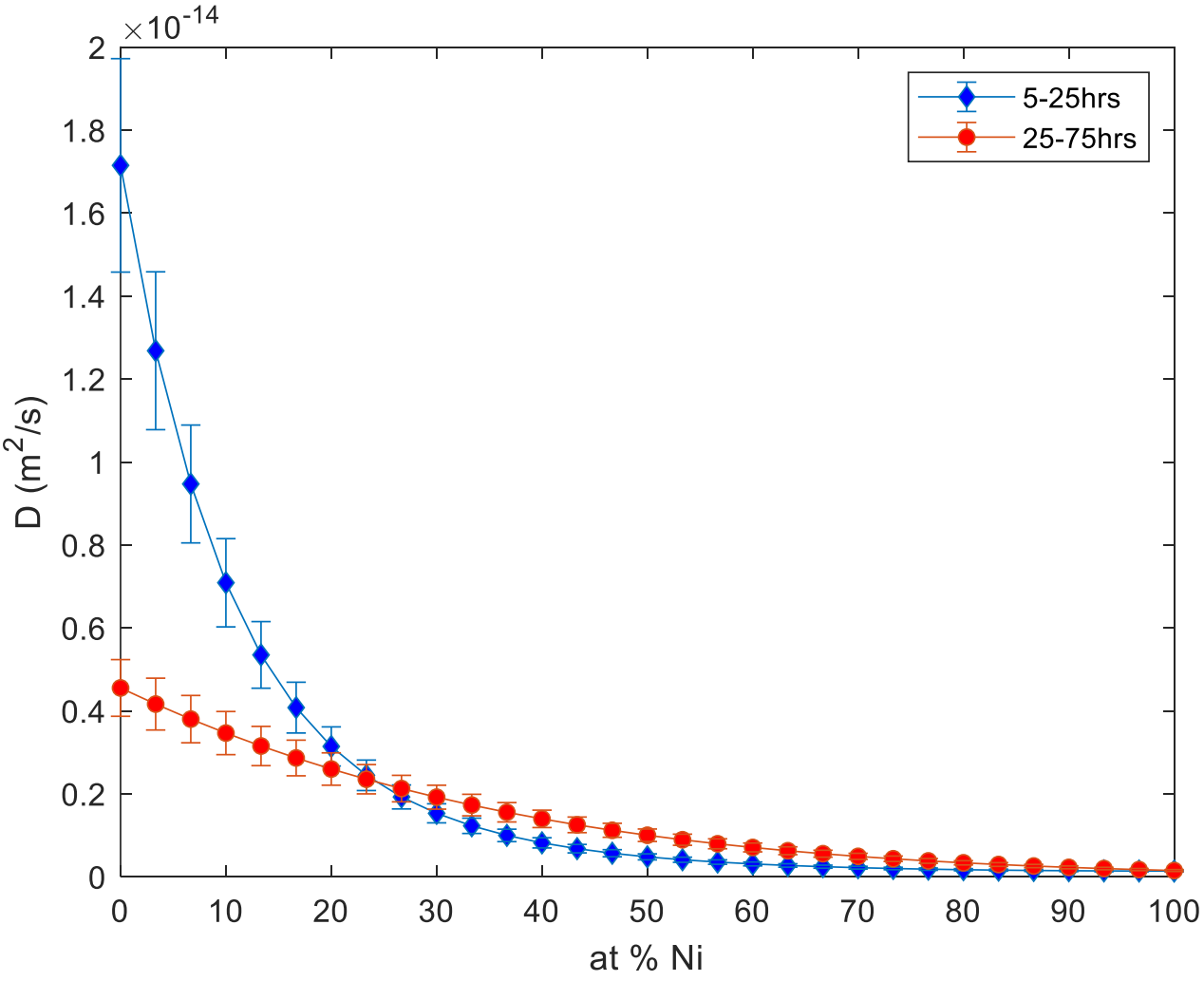

Figure 4.3: Concentration-dependent interdiffusion coefficients of pure Cu-Ni at 900^0C for holding times of 5-25 hrs versus 25-75 hrs.

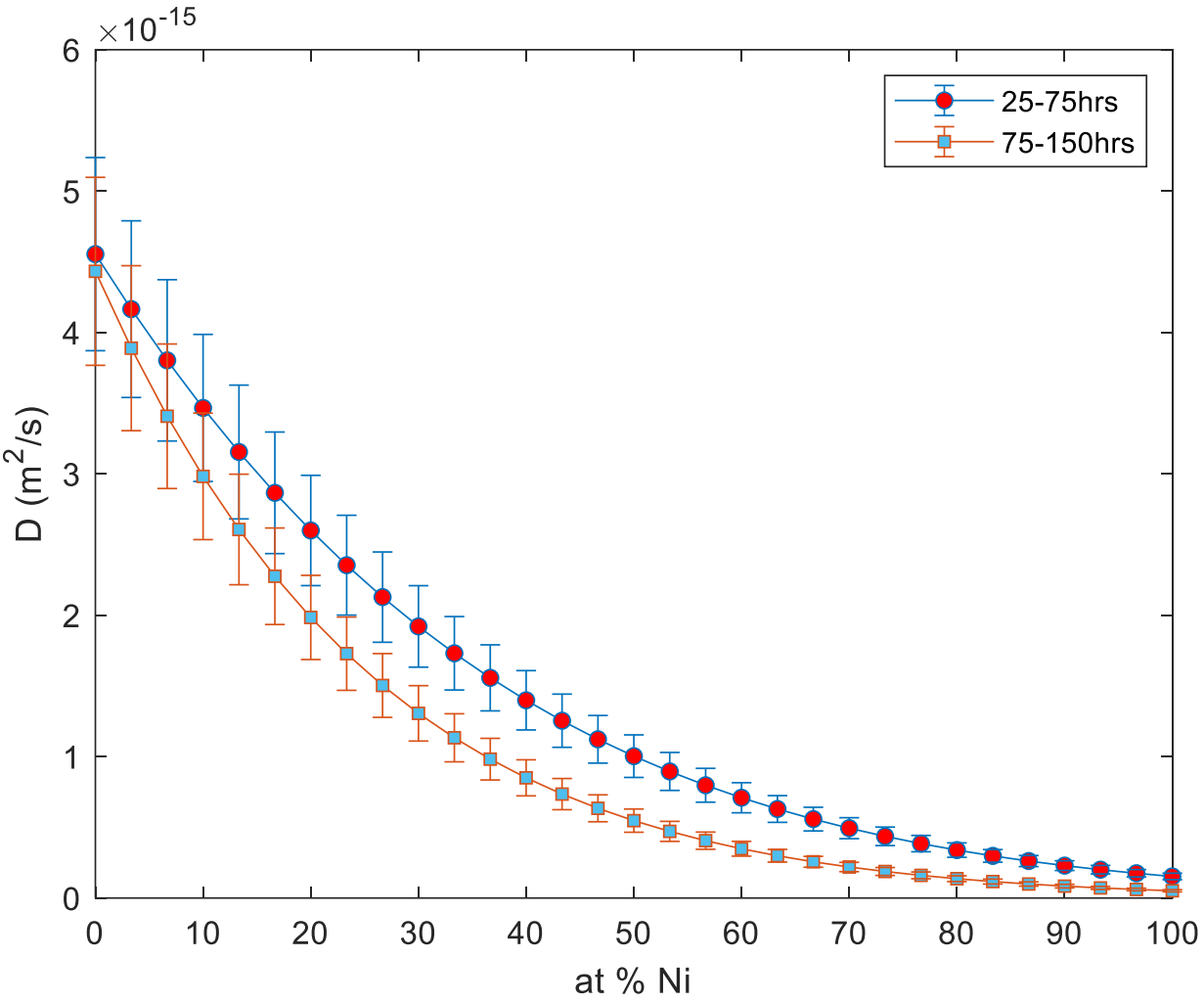

Figure 4.4: Concentration-dependent interdiffusion coefficients of pure Cu-Ni at 900^0C for holding times of 25-75 hrs versus 75-150 hrs.

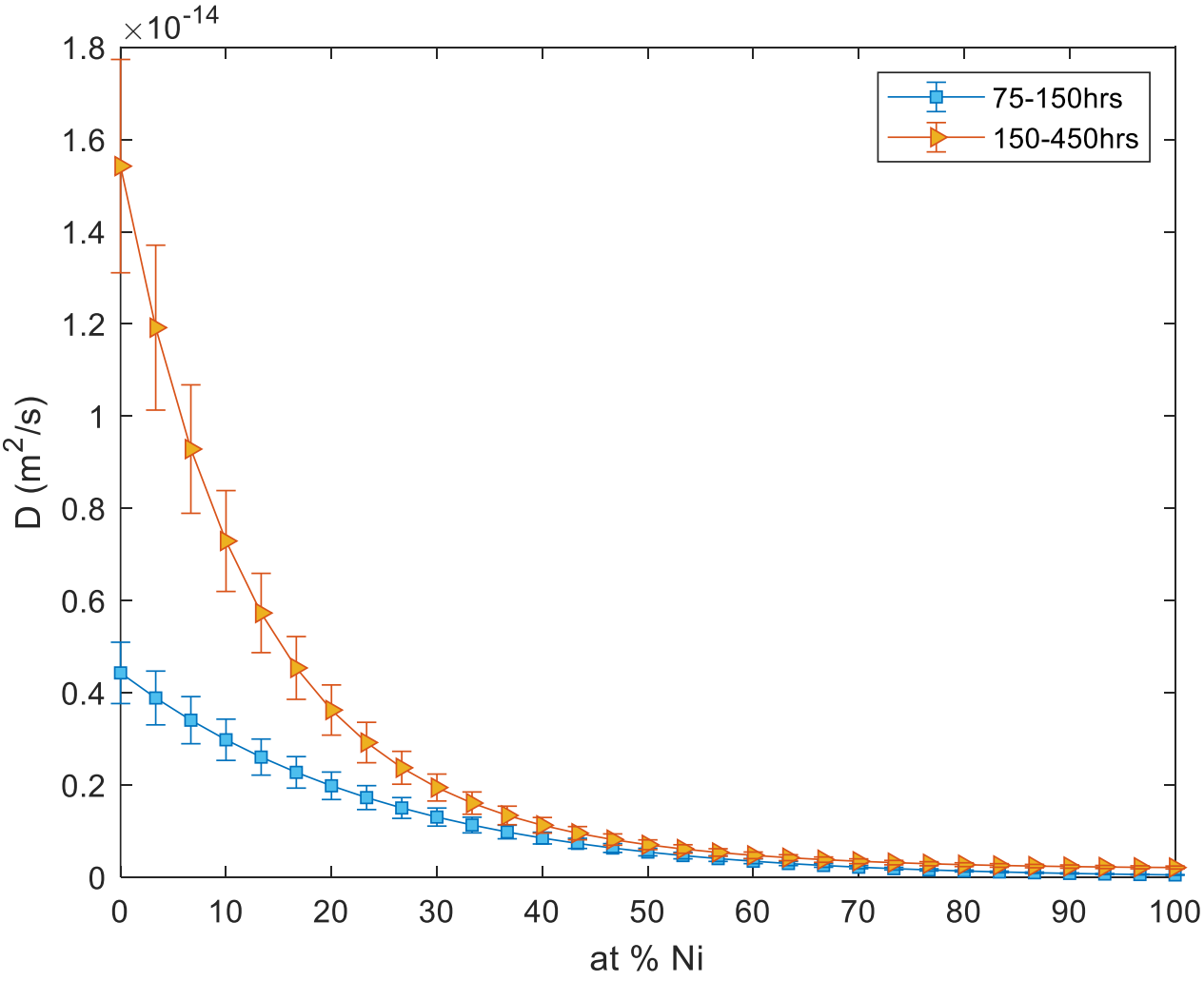

Figure 4.5: Concentration-dependent interdiffusion coefficients of pure Cu-Ni at 900^0C for holding times of 75-150 hrs versus 150-450 hrs.

Table 4.1: *p*-values of *t-statistics* for pure Cu-Ni diffusion couple at 900^0C

Ni at. %	**0**	**5**	**10**	**15**	**20**	**25**	**30**
5-25 h vs 25-75 h	0.001	0.001	0.001	0.013	0.058	> 0.2	> 0.2
25-75 h vs 75-150 h	0.132	> 0.2	> 0.2	> 0.2	0.074	0.030	0.025
75-150 h vs 150-450 h	0.001	0.001	0.001	0.001	0.001	0.001	0.003
Ni at. %	35	40	45	50	55	60	65
5-25 h vs 25-75 h	> 0.2	0.135	0.099	0.032	0.026	0.039	0.032
25-75 h vs 75-150 h	0.018	0.018	0.029	0.023	0.019	0.031	0.027
75-150 h vs 150-450 h	0.013	0.009	0.012	0.020	0.015	0.024	0.020
Ni at. %	70	75	80	85	90	95	100
5-25 h vs 25-75 h	0.042	0.038	0.081	> 0.2	> 0.2	> 0.2	> 0.2
25-75 h vs 75-150 h	0.029	0.021	0.030	0.033	0.032	0.035	0.031
75-150 h vs 150-450 h	0.013	0.019	0.015	0.013	0.014	0.011	0.013

Table 4.2: D_{ave} for different time intervals at 900^0C and variations

Time interval (hrs)	**D_{ave} (m^2/s)**	**Percentage increase (%)**
5-25	2.58E-15	-
25-75	1.50E-15	-
75-150	1.12E-15	-
150-450	2.03E-15	-
25-75 and 5-25	-	72
75-150 and 25-75	-	34
75-150and 150-450	-	81

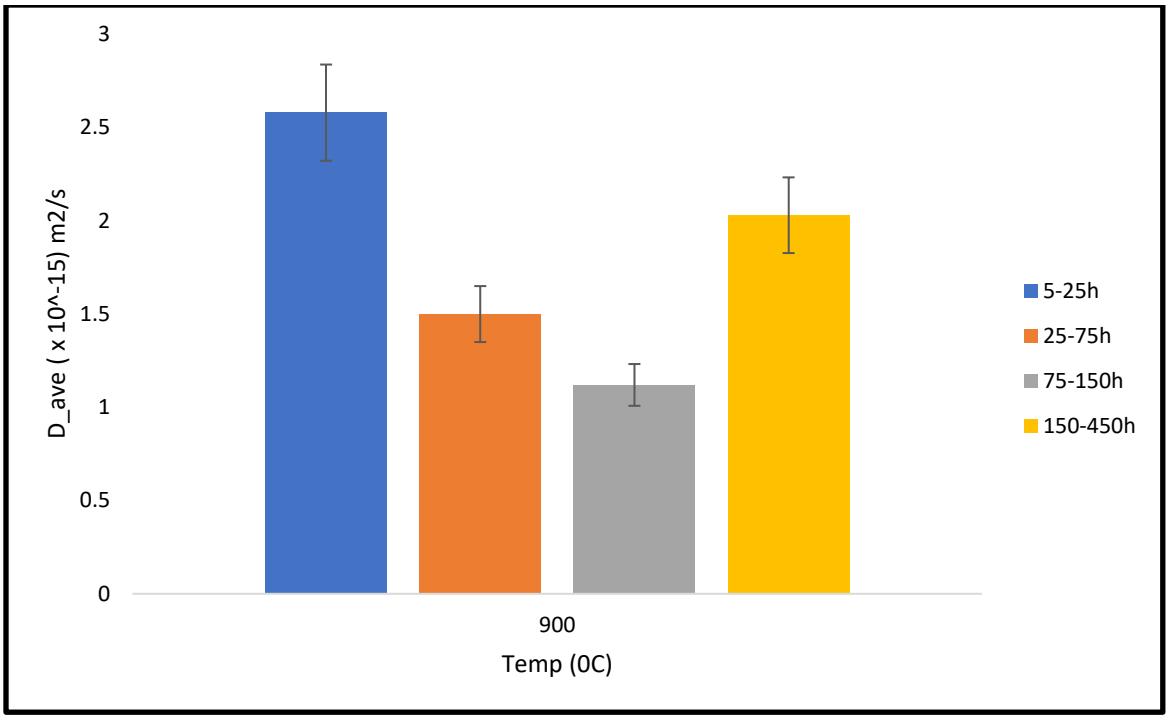

Figure 4.5a: Average interdiffusion coefficients at different times for pure Cu-Ni at 900^0C

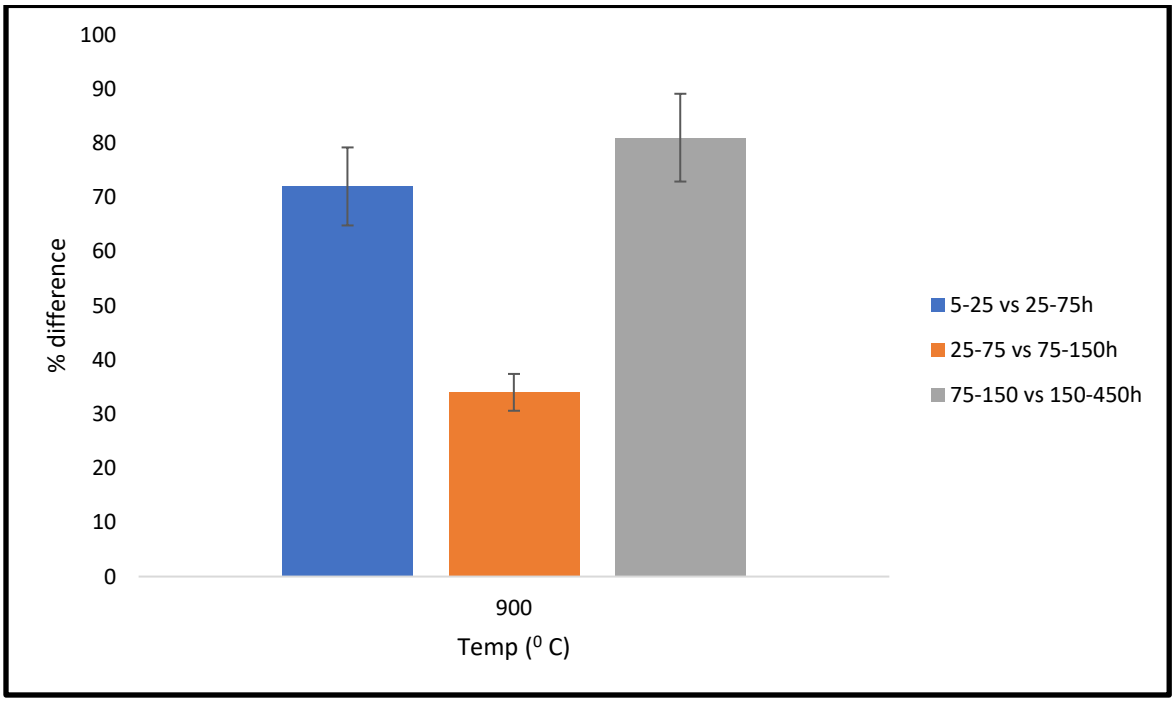

Figure 4.5b: Percentage difference between diffusion time at 900^0C

4.2.2 Effect of Time on Interdiffusion Coefficient in Pure Cu-Ni system at 940^0C

Solid-solid interdiffusion in a single-phase system of pure Cu-Ni subjected to heat treatment at 940^0C for 5 hrs, 25 hrs, 75 hrs, 150 hrs and 450 hrs was used to investigate the effect of time on the interdiffusion coefficient. Figures 4.6 - 4.8 show the plotted D(C) curves with standard deviation error bars that compare the diffusion period. The variations in the curves show the effect of time on interdiffusion. As reported in [62] ,these results further confirm that the pattern of large variations in the Cu-rich interdiffusion region at 900^0C is valid. Figures 4.6 and 4.7 show a similar trend, but Figure 4.8 shows a significant variation except at the region around 20 at %Ni concentration. Accordingly, it is reasonable to affirm that the interdiffusion coefficient could vary with concentration and time. To corroborate this observation, the results of the *p-values* of the *t-statistics* in Table 4.3 shows that although few concentration points are within the statistical range of an acceptable benchmark, but during a longer diffusion period, a large statistical range of difference is observed as shown in Figure 4.8. The average diffusivity calculated in Table 4.4 shows a closer value between the diffusion period and that percentage increase is as low as 9% between 75 hrs and 150 hrs when compared to 150-450 hrs. This is below the empirically derived 15%, which means that they are statistically similar. Overall, both the graphical and statistical results confirm that the interdiffusion coefficients change with diffusion time which demonstrates the effect of time on the interdiffusion coefficients for the pure Cu-Ni system at 940^0C.

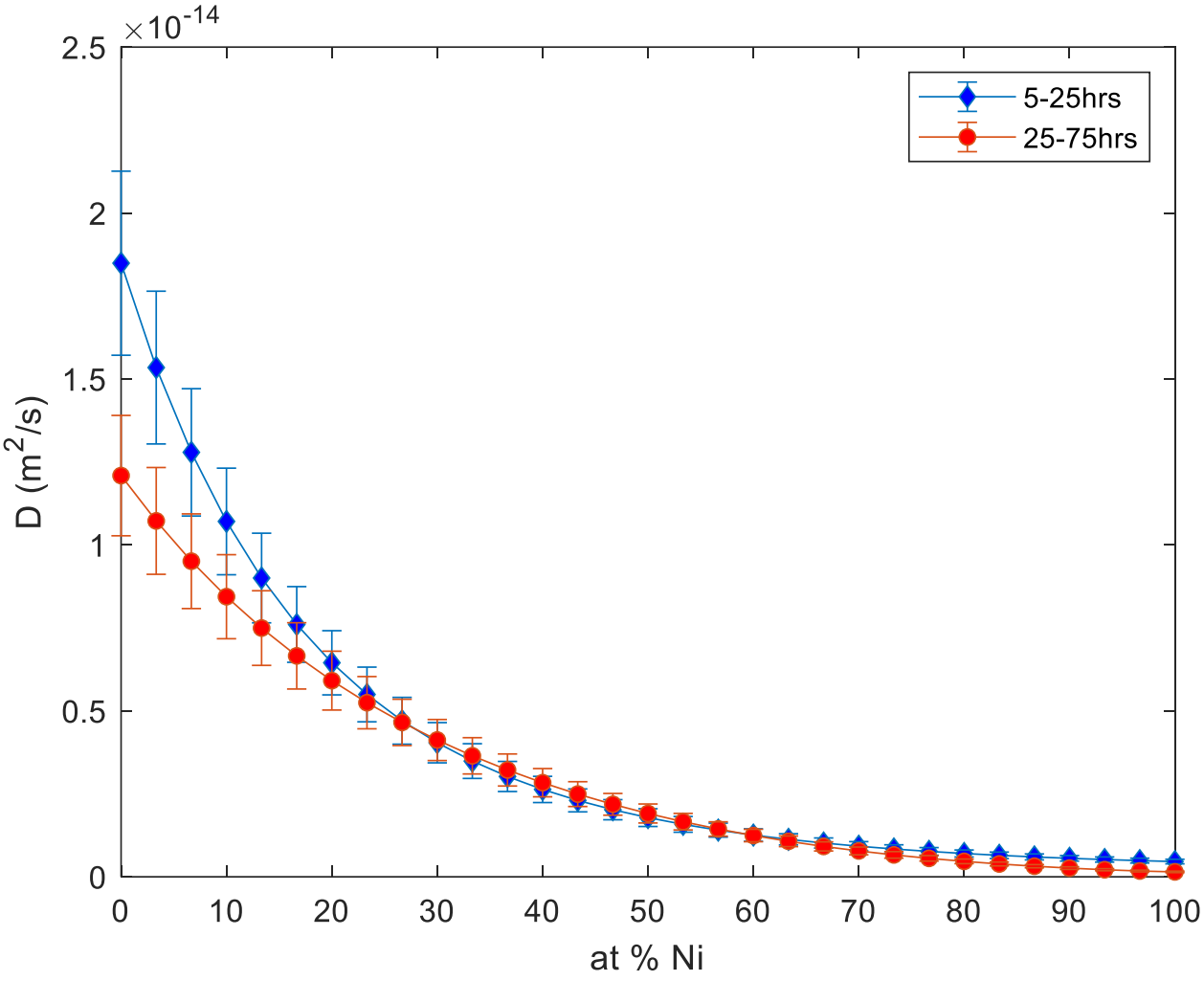

Figure 4.6: Concentration-dependent interdiffusion coefficients of pure Cu-Ni at 940^0C for holding times of 5-25 hrs versus 25-75 hrs.

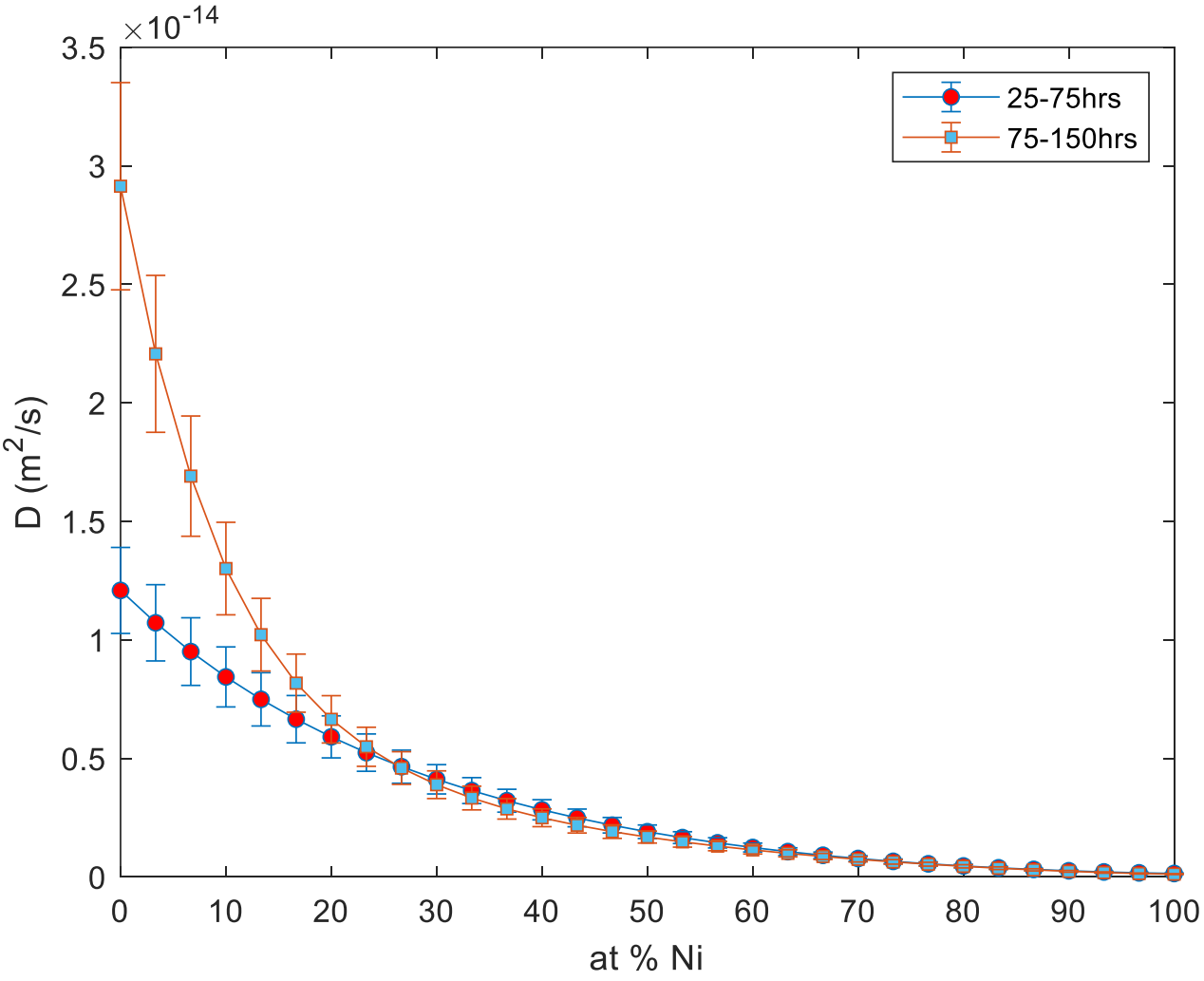

Figure 4.7: Concentration-dependent interdiffusion coefficients of pure Cu-Ni at 940^0C for holding times of 25-75 hrs versus 75-150 hrs.

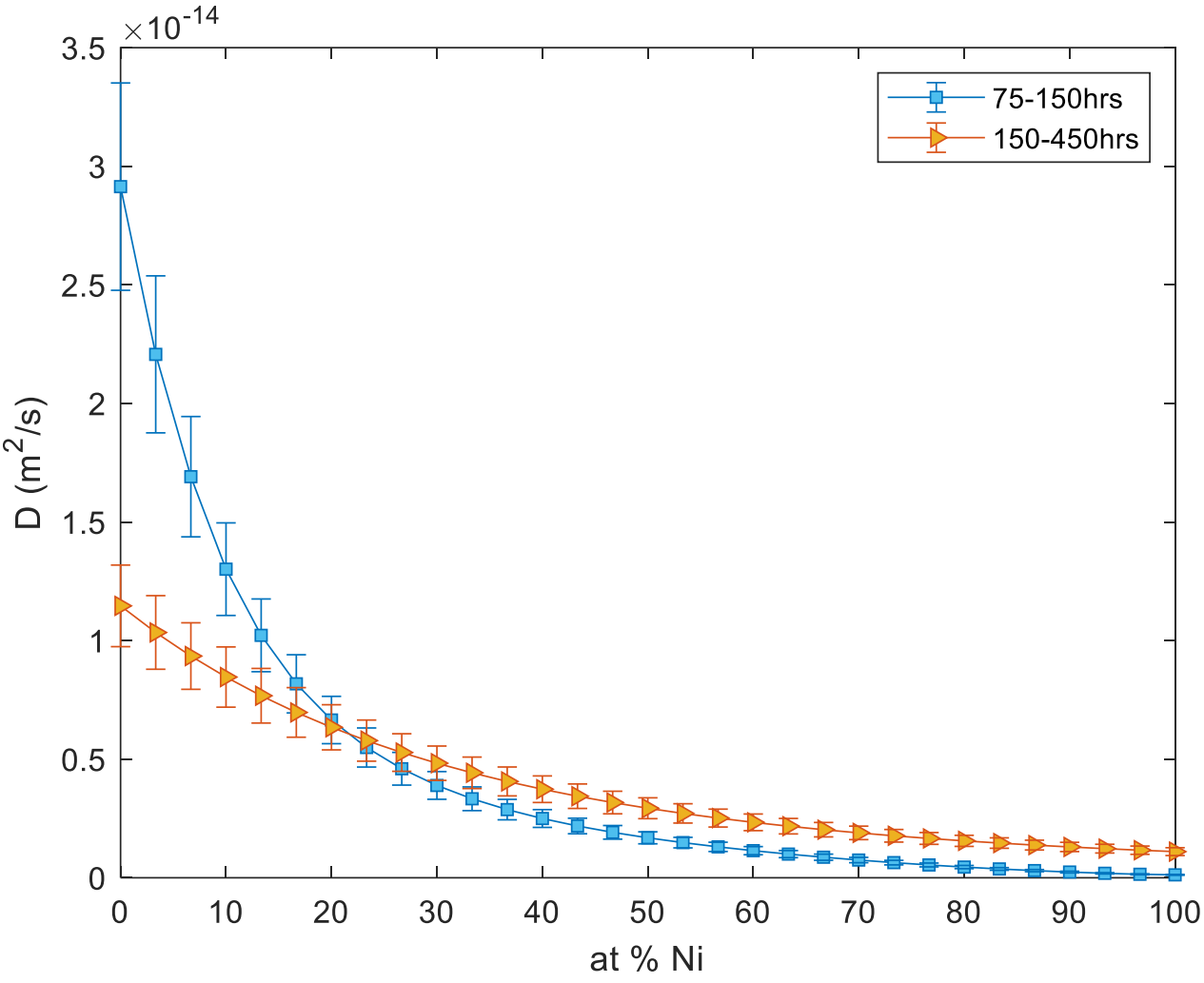

Figure 4.8: Concentration-dependent interdiffusion coefficients of pure Cu-Ni at 940^0C for holding times of 75-150 hrs versus 150-450 hrs.

Table 4.3: *p*-values of *t-statistics* for pure Cu-Ni diffusion couple at 940^0C

Ni at. %	**0**	**5**	**10**	**15**	**20**	**25**	**30**
5-25 h vs 25-75 h	0.008	0.011	0.013	0.012	0.053	0.135	> 0.2
25-75 h vs 75-150 h	0.046	0.033	0.022	0.025	0.054	0.074	> 0.2
75-150 h vs 150-450 h	0.010	0.010	0.034	0.120	> 0.2	> 0.2	> 0.2
Ni at. %	35	40	45	50	55	60	65
5-25 h vs 25-75 h	> 0.2	> 0.2	0.140	0.080	0.060	0.023	0.013
25-75 h vs 75-150 h	> 0.2	> 0.2	> 0.2	> 0.2	> 0.2	> 0.2	> 0.2
75-150 h vs 150-450 h	> 0.2	> 0.2	> 0.2	0.162	0.158	0.069	0.032
Ni at. %	70	75	80	85	90	95	100
5-25 h vs 25-75 h	0.026	0.019	0.016	0.019	0.029	0.060	0.087
25-75 h vs 75-150 h	> 0.2	> 0.2	> 0.2	> 0.2	> 0.2	> 0.2	> 0.2
75-150 h vs 150-450 h	0.023	0.009	0.003	0.002	0.001	0.001	0.001

Table 4.4: D_{ave} for different time intervals at 940^0C and their variation

Time interval (hrs)	**D_{ave} (m^2/s)**	**Percentage increase (%)**
5-25	4.14E-15	-
25-75	3.29E-15	-
75-150	4.35E-15	-
150-450	3.98E-15	-
25-75 and 5-25	-	26
25-75 and 75-150	-	32
150-450 and 75-150	-	9

4.2.3 Effect of Time on Interdiffusion Coefficients in Pure Cu-Ni system at 980^0C

The plot of concentration dependent interdiffusion coefficients for pure CuNi at 980^0C for different diffusion times are shown in Figures 4.9 - 4.11. To verify if the D(C) varies with time in these results, the standard deviation of the interdiffusion coefficients versus concentration for diffusion times of 5-25 hrs, 25-75 hr, 75-150 hrs and 150-450 hrs show trends of where there is no overlapping between the error bars on the individual time intervals especially in Figures 4.9 and 4.11, which shows that D(C) changes with time. Note that Figure 4.10 only shows a slight variation at the Cu-rich region of the diffusion process. Also, the calculated average of the interdiffusion concentration coefficients as revealed in Table 4.6 shows that based on [63], the increase in percentage between the D_{ave} calculated for diffusion times of 5-25 h and 25-75 h is 31%; 25-75 h and 75-150 h is 6%; and 75-150 h and 150-450 h is 71%. The maximum change in the D_{ave} is ideally an uncertainty of 15% in experimentally measured diffusion coefficients. The data show that the interdiffusion coefficient varies significantly with concentration for two of the holding times except for 25-75 h and 75-150 h which has a 6% difference. The *p-values* for 75-150 hr vs 150-450 hr in Table 4.5 shows a significant statistical difference that is observed in Figure 4.11 and *p-values* less than .001 which is the benchmark used. On the other hand, the holding times of 25-75 h vs 75-150 h only show a slight difference which is reflected by the increase in percentage of the D_{ave}.

Overall, although the D_{ave} differs for each time interval, not all the isothermal variations of D_{ave} have more than a 15% experimental uncertainty. Most of the data clearly show that the D(C) isothermally changes with time, as confirmed by the result which is based on the standard deviation error bar.

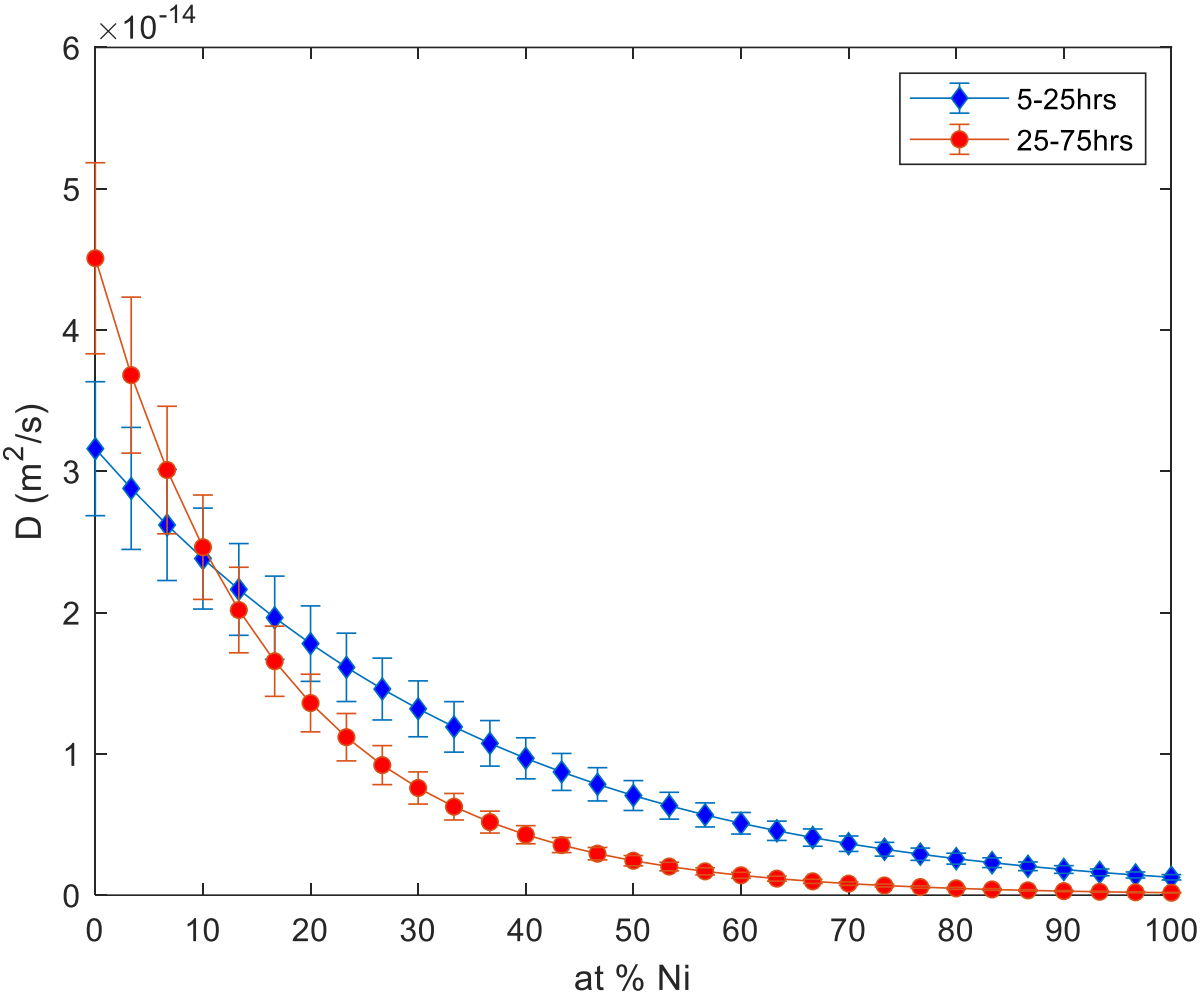

Figure 4.9: Concentration-dependent interdiffusion coefficients of pure Cu-Ni at 980^0C for holding times 5-25hrs versus 25-75hrs.

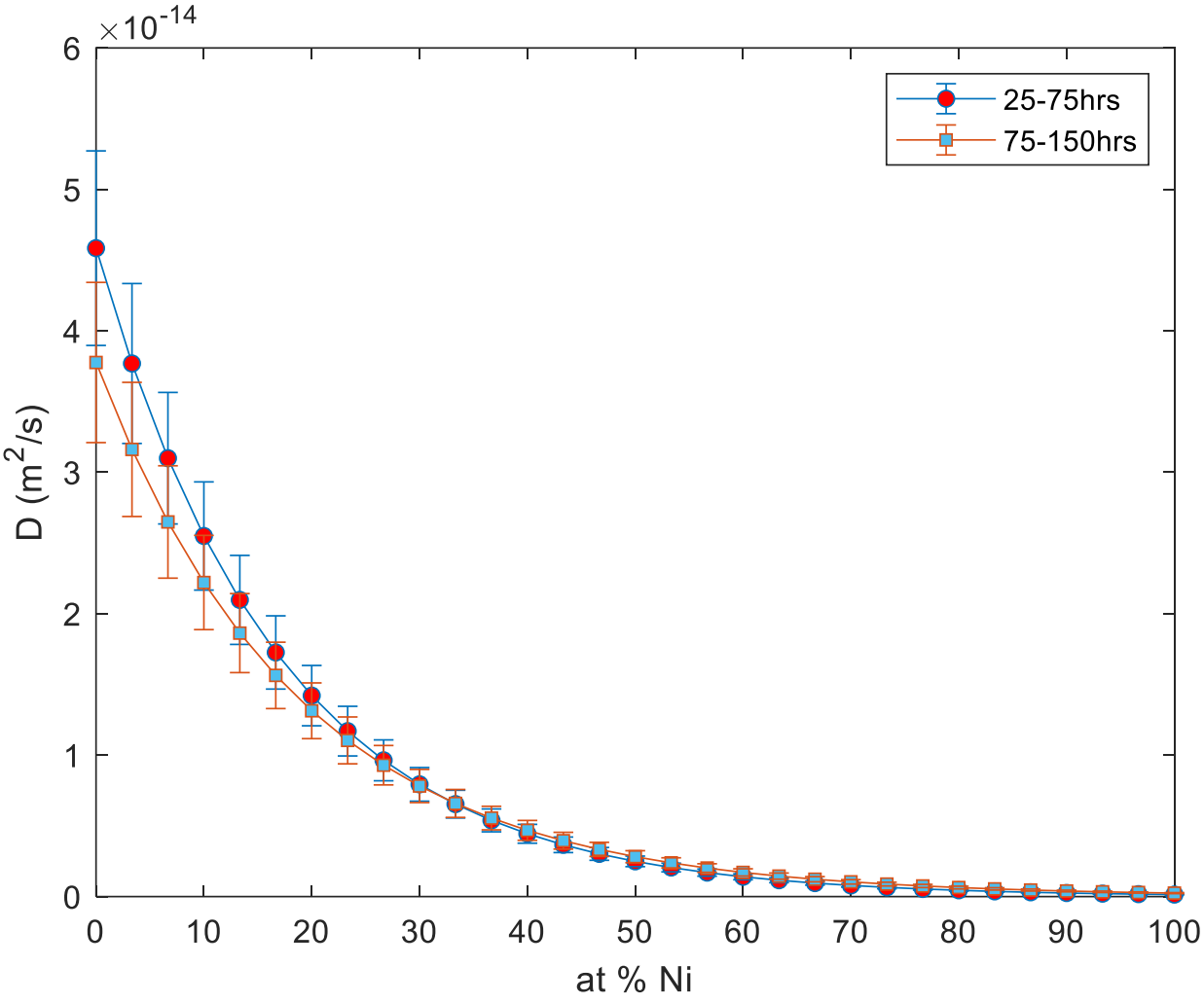

Figure 4.10: Concentration-dependent interdiffusion coefficients of pure Cu-Ni at 980^0C for holding times of 25-75 hrs versus 75-150 hrs.

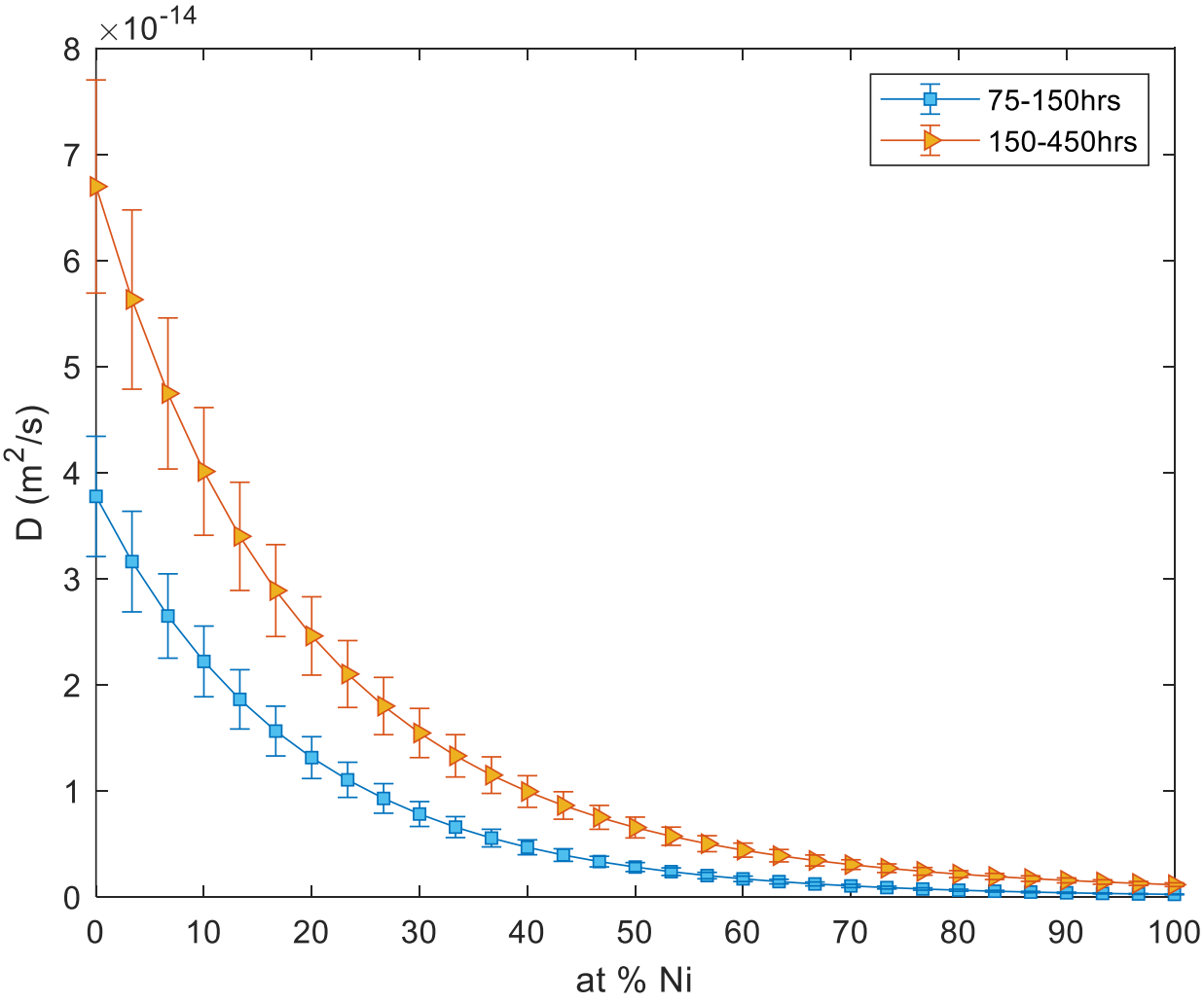

Figure 4.11: Concentration-dependent interdiffusion coefficients of pure Cu-Ni at 980^0C for holding times 75-150 hrs versus 150-450 hrs.

Table 4.5: *p*-values of *t-statistics* for pure Cu-Ni diffusion couple at 980^0C

Ni at. %	**0**	**5**	**10**	**15**	**20**	**25**	**30**
5-25 h vs 25-75 h	0.116	0.718	0.597	0.115	0.024	0.010	0.003
25-75 h vs 75-150 h	0.044	0.021	0.008	0.006	0.100	0.120	> 0.2
75-150 h vs 150-450 h	0.043	0.040	0.016	0.004	0.003	0.001	0.001
Ni at. %	35	40	45	50	55	60	65
5-25 h vs 25-75 h	0.002	0.001	0.001	0.001	0.001	0.001	0.001
25-75 h vs 75-150 h	> 0.2	> 0.2	> 0.2	> 0.2	> 0.2	> 0.2	> 0.2
75-150 h vs 150-450 h	0.001	0.001	0.001	0.003	0.002	0.002	0.002
Ni at. %	70	75	80	85	90	95	100
5-25 h vs 25-75 h	0.001	0.001	0.001	0.003	0.004	0.008	0.014
25-75 h vs 75-150 h	> 0.2	> 0.2	> 0.2	> 0.2	> 0.2	> 0.2	> 0.2
75-150 h vs 150-450 h	0.003	0.006	0.010	0.020	0.035	0.071	0.119

Table 4.6: D_{ave} for different time intervals at 980^0C and their variation

Time interval (hrs)	**D_{ave} (m^2/s)**	**Percentage increase (%)**
5-25	8.88E-15	-
25-75	7.66E-15	-
75-150	7.26E-15	-
150-450	1.24E-14	-
25-75 and 5-25	-	31
75-150 and 25-75	-	6
75-150 and 150-450	-	71

4.2.4 Effect of Time on Interdiffusion Coefficients in Pure Cu-Ni system at 1020^0C

Again, at a higher temperature, the effect of time was investigated for the specified diffusion times and the results are presented in Figures 4.12 - 4.14. At an average concentration of 40 at %Ni, there are no obvious overlapping areas as represented by the standard deviation error bars. This indicates that as the Ni solute diffuses into Cu, the magnitude of the diffusion coefficient differs. For a high temperature of 1020^0C which is little lower than the melting temperature of Cu (by 65^0C), the D(C) is expected to be constant and not change with time as previously concluded in the literature. However, the findings in this study contradicts that in current studies. The D(C)s appear to have similar value even at extreme values from 50 at %Ni to 100 at% Ni, however, Figures 4.12 to 4.14 do not show complete overlap of the two compared D(C)s at the diffusion times studied. To further explain for this finding, the *p-values* reported in Table 4.7 clearly show statistical significance difference of $p < .001$ and $p \geq .2$(for statistically similar data) except for 41-50 at% Ni and 61-70 at% Ni for different diffusion intervals of 5-25 hrs vs 25-75 hrs and 75-150 hrs vs 150-450 hrs respectively. The extreme values confirm that the data are statistically significant. The calculated average of the D(C)s of these diffusion times vary despite isothermal conditions and the increase in percentage shows a significantly large difference as presented in Table 4.8. For the D(C) operators of the diffusion time intervals of 25-75 hrs and 75-150 hrs, the % increase is about 112%. If the D(C) is isothermally constant and does not vary with time, as generally assumed, the opposite would have been observed.

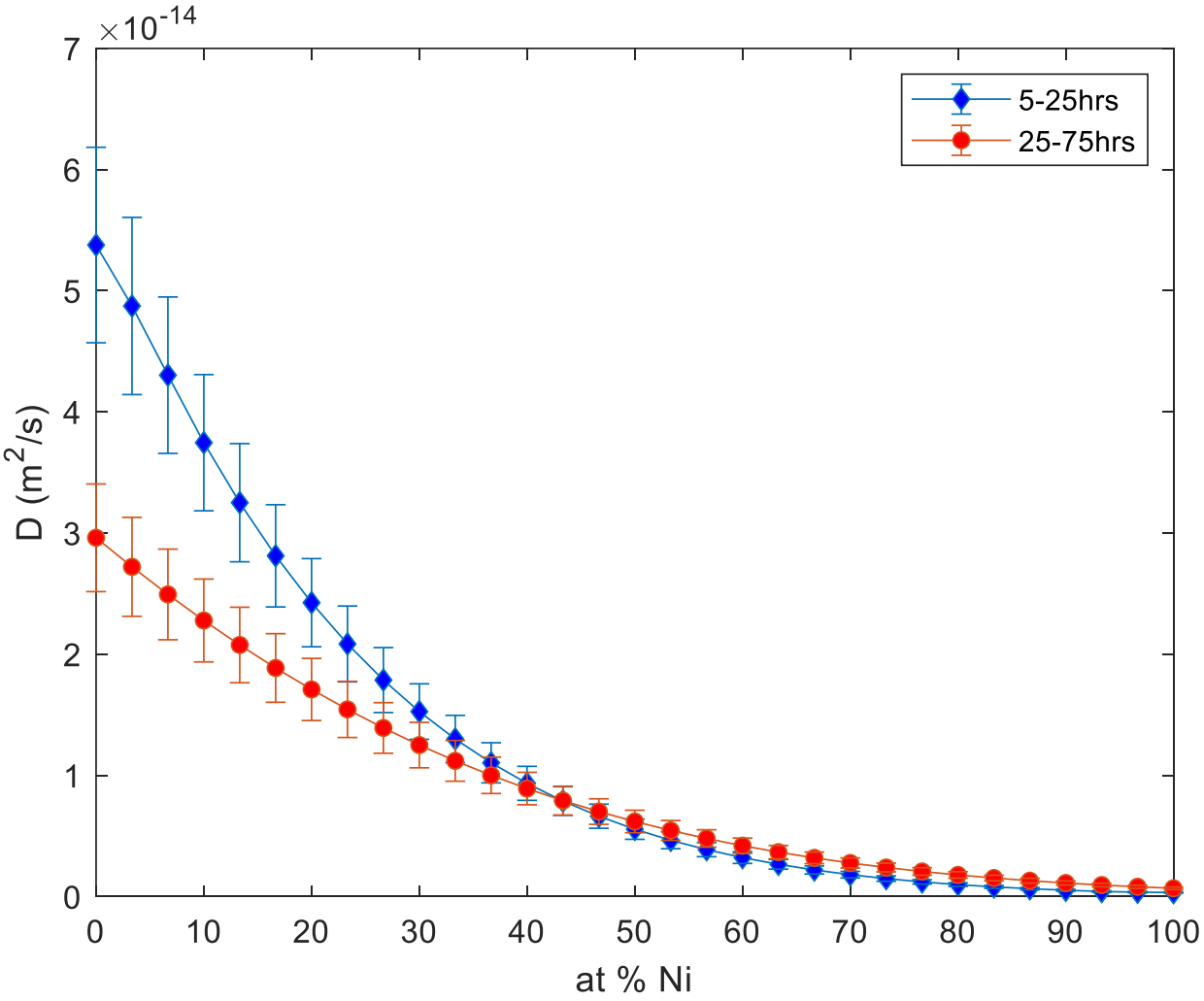

Figure 4.12: Concentration-dependent interdiffusion coefficients of pure Cu-Ni at 1020^0C for holding times 5-25 hrs versus 25-75 hrs.

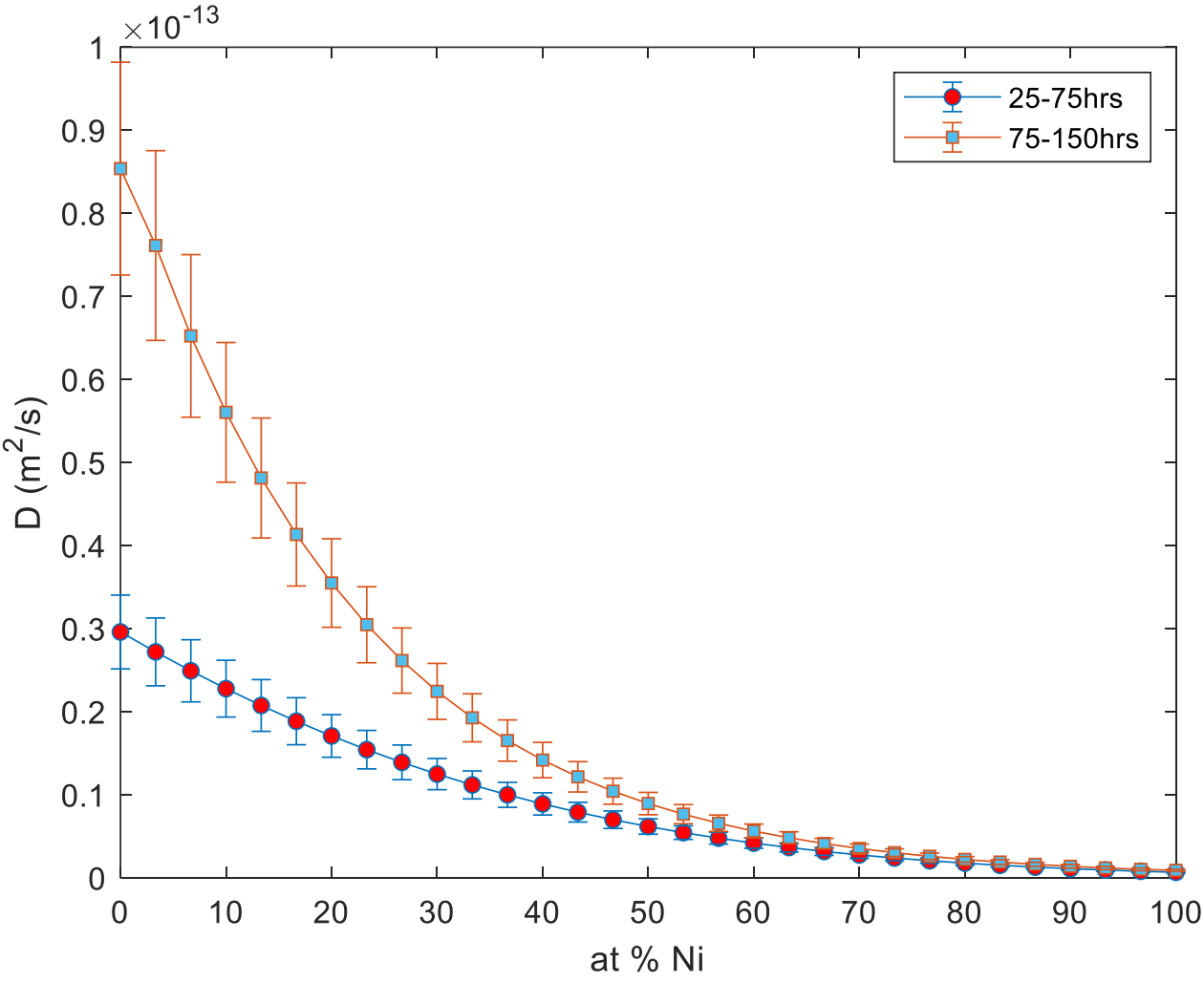

Figure 4.13: Concentration-dependent interdiffusion coefficients of pure Cu-Ni at 1020^0C for holding times 25-75 hrs versus 75-150 hrs.

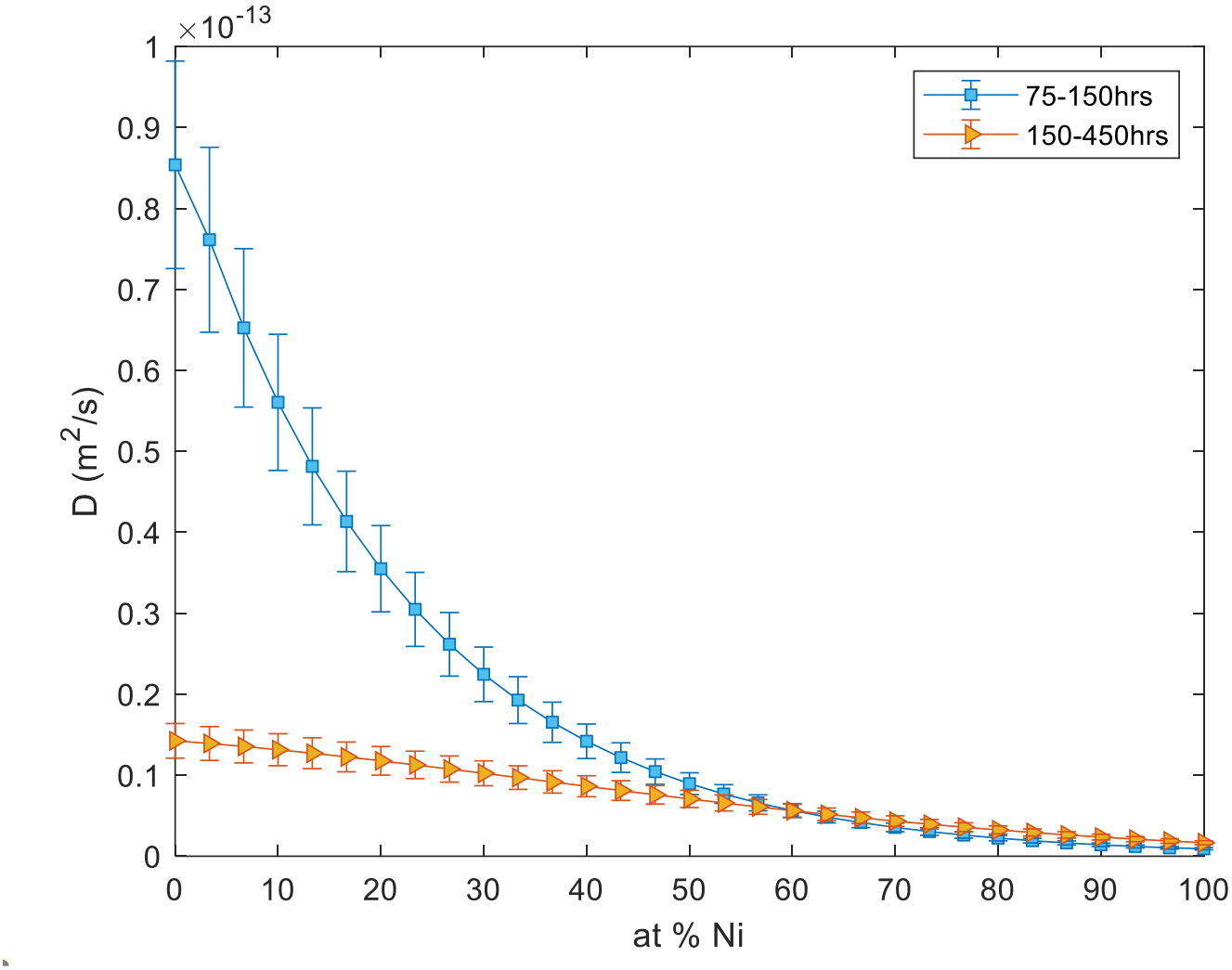

Figure 4.14: Concentration-dependent interdiffusion coefficients of pure Cu-Ni at 1020^0C for holding times 75-150 hrs versus 150-450 hrs.

Table 4.7: *p*-values of *t-statistics* for pure Cu-Ni diffusion couple at 1020^0C

Ni at. %	**0**	**5**	**10**	**15**	**20**	**25**	**30**
5-25 h vs 25-75 h	0.118	0.035	0.025	0.010	0.009	0.004	0.006
25-75 h vs 75-150 h	0.001	0.001	0.001	0.001	0.001	0.001	0.001
75-150 h vs 150-450 h	0.007	0.003	0.002	0.000	0.001	0.001	0.002
Ni at. %	35	40	45	50	55	60	65
5-25 h vs 25-75 h	0.012	0.085	0.160	> 0.2	> 0.2	> 0.2	> 0.2
25-75 h vs 75-150 h	0.002	0.002	0.003	0.003	0.005	0.002	0.002
75-150 h vs 150-450 h	0.003	0.004	0.008	0.009	0.021	0.013	0.022
Ni at. %	70	75	80	85	90	95	100
5-25 h vs 25-75 h	> 0.2	> 0.2	> 0.2	> 0.2	> 0.2	> 0.2	> 0.2
25-75 h vs 75-150 h	0.002	0.002	0.003	0.003	0.011	0.024	0.041
75-150 h vs 150-450 h	0.068	0.116	> 0.2	> 0.2	> 0.2	> 0.2	> 0.2

Table 4.8: D_{ave} for different time intervals at 1020^0C and their variation

Time interval (hrs)	**D_{ave} (m^2/s)**	**Percentage increase (%)**
5-25	1.26E-14	-
25-75	9.12E-15	-
75-150	1.93E-14	-
150-450	1.03E-14	-
25-75 and 5-25	-	38
25-75 and 75-150	-	112
150-450d 75-150	-	88

4.3 Activation energy and frequency factor of concentration-dependent interdiffusion

The D(C) and temperature can be closely related by using the Arrhenius law:

$$D = D_0 exp\left(\frac{-Q_d}{RT}\right) \quad 4.1$$

where D_0 and Q_d represent a temperature independent pre-exponential factor and the activation energy for diffusion respectively, and R and T are a gas constant and the absolute temperature. These parameters can be determined by using the previously calculated interdiffusion coefficients at various temperatures and diffusion times investigated in this study.

The plot of the natural logarithm of the interdiffusion coefficient versus the reciprocal temperature at a magnitude of 10^4 can be used to verify the Arrhenius plot where the temperature dependence of the interdiffusion coefficient follows the Arrhenius law. Figures 4.15 - 4.18 show the relationship between the interdiffusion coefficients and temperature. At a constant temperature, the interdiffusion coefficients are not the same, when observed at 20 at% of Ni. A line of best fit in the figures is used to calculate the slope from the equations of the line which show the extent of the activation energy and the intercept which illustrates the size of the pre-exponential factor. Olaye and Ojo [55] reported that for effectiveness, it is important to exclude errors that may arise from the possibility of the presence of an initial solute distribution by using an experimental concentration profile obtained after a certain diffusion time as a reference to determine the D(C) between the reference and final experimental concentration profiles. This investigation uses 5 hrs as the reference profile for each temperature, therefore, the numerically obtained D(C) at longer diffusion intervals is for 5 and 25 hrs, 5 and 75 hrs, 5 and 150 hrs, and 5 and 450 hrs in the pure Cu-Ni system. The calculated interdiffusion coefficients were then used to show their temperature dependence in Figures 4.15 - 4.18.

Consequently, the values of the activation energy and pre-exponential factor of these concentration profiles with the reference profiles are calculated and the results are presented in Figures 4.19 and 4.20. It is obvious that the activation energy and pre-exponential factor change with time. The literature has reported that temperature increases can influence the frequency factor of diffusion and/or affect the activation energy at a certain temperature due to the specific mechanism of diffusion which occurs significantly at such critical temperatures. However, the variation of the time effect of the interdiffusion coefficients is responsible for the changes in Q and D_0 with diffusion time. A list of activation energies and pre-exponential factors for Ni-Cu interdiffusion in Table 4.10 shows that the findings of this study are in agreement with those in the literature.

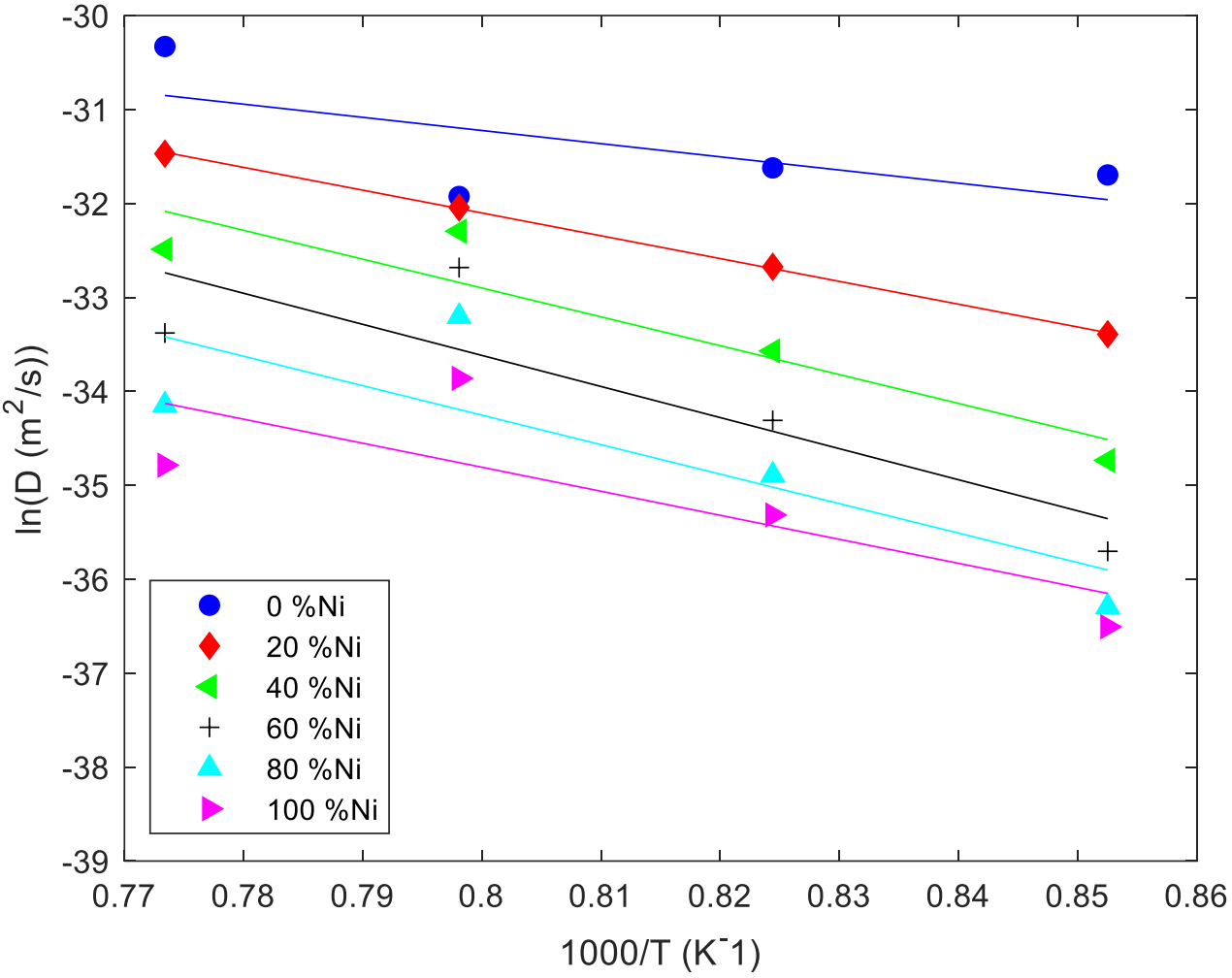

Figure 4.15: Temperature dependence of interdiffusion coefficients for diffusion time of 5-25 hrs in Cu-Ni system (Arrhenius plot)

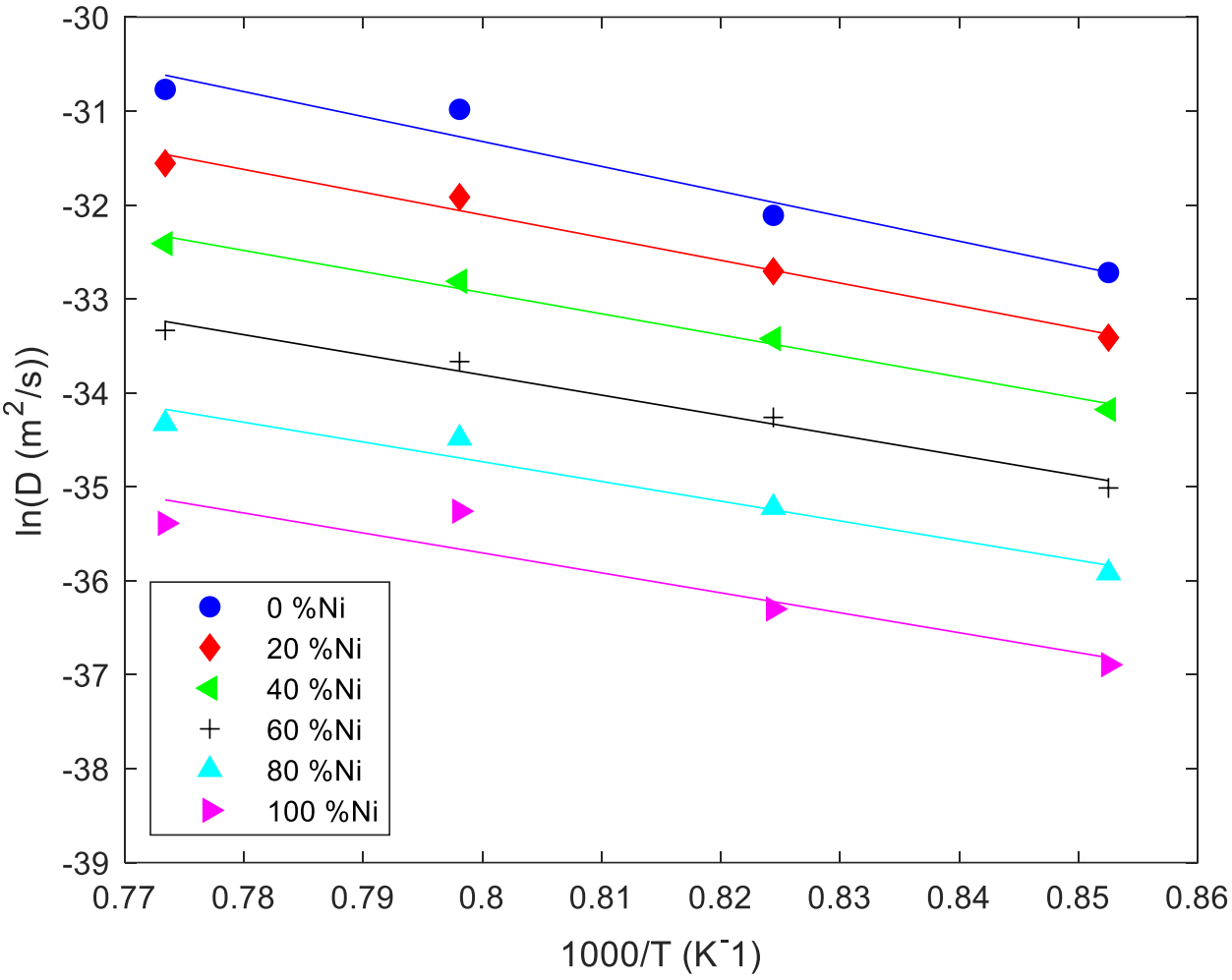

Figure 4.16: Temperature dependence of interdiffusion coefficients for diffusion time of 5-75 hrs in Cu-Ni system (Arrhenius plot)

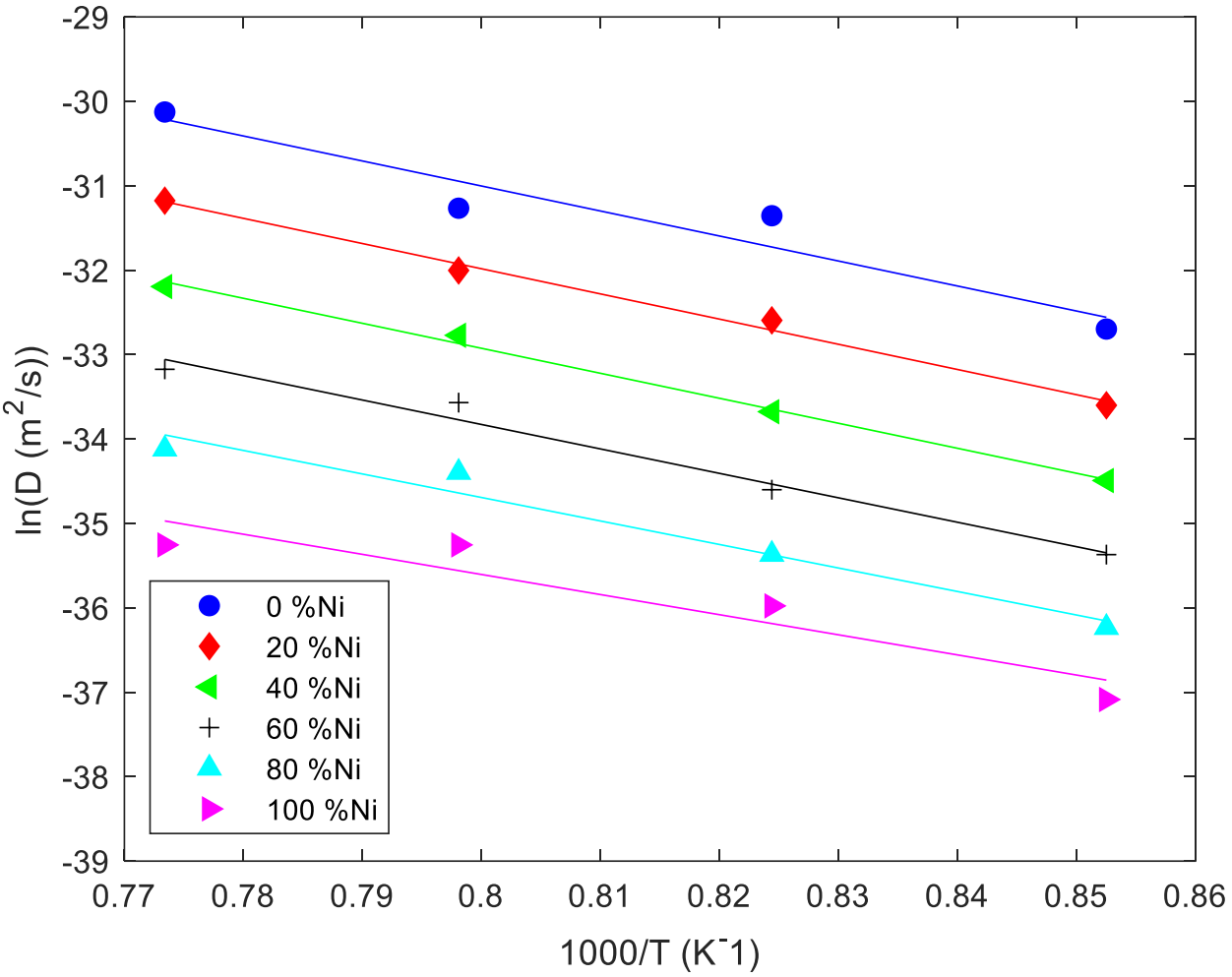

Figure 4.17: Temperature dependence of interdiffusion coefficients for diffusion time of 5-150 hrs in Cu-Ni system (Arrhenius plot)

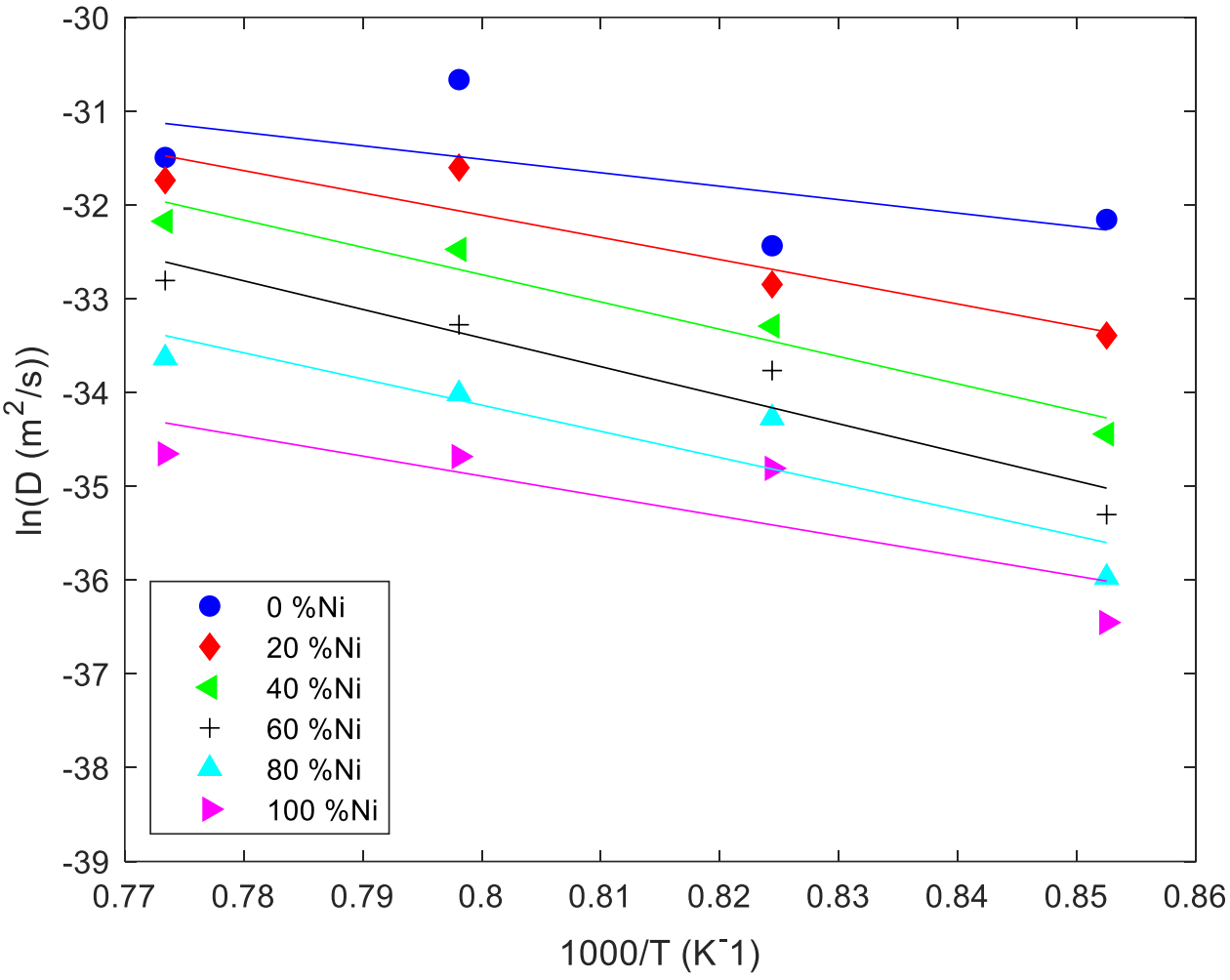

Figure 4.18: Temperature dependence of interdiffusion coefficients for diffusion time of 5-450 hrs in Cu-Ni system (Arrhenius plot)

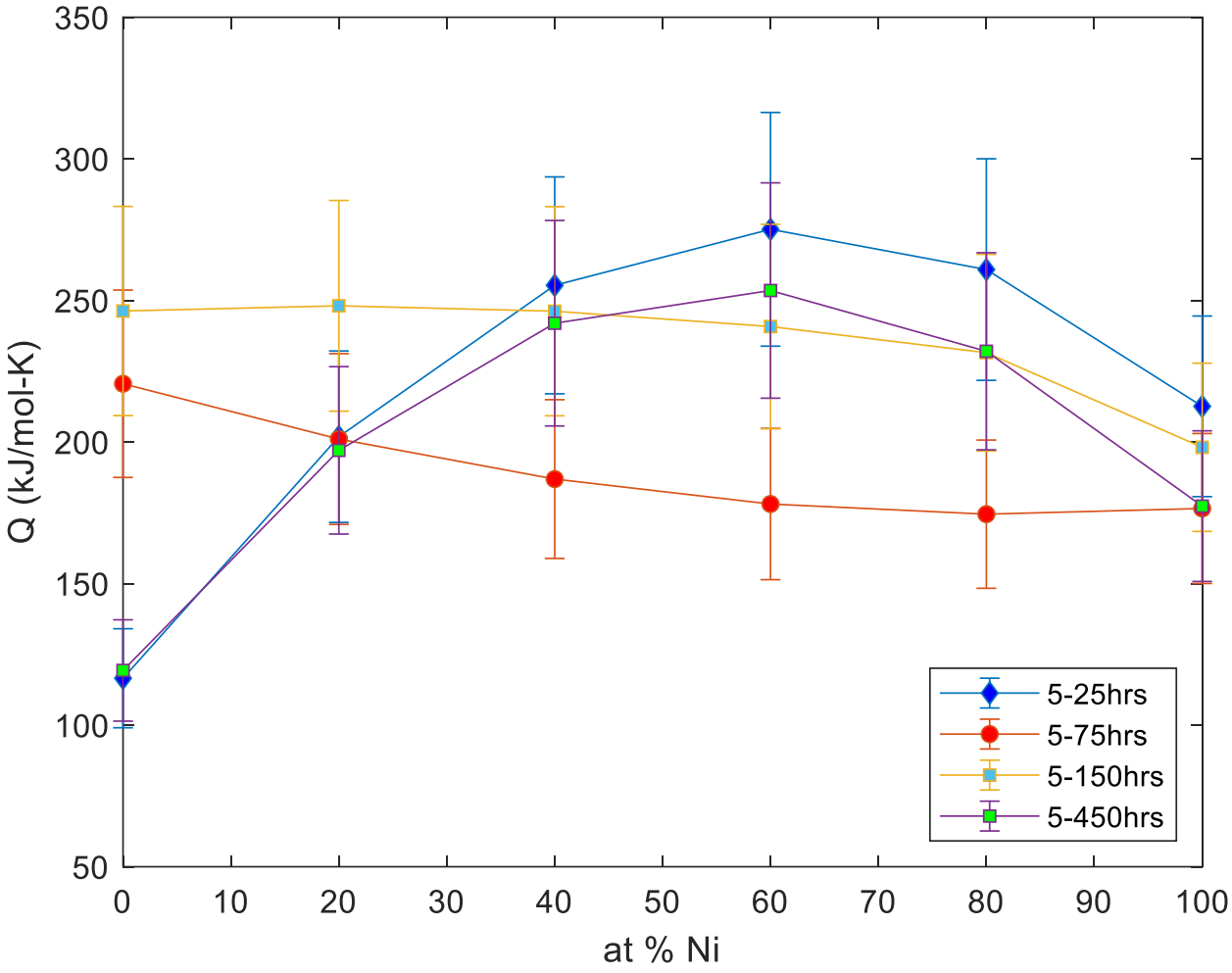

Figure 4.19: Concentration dependence of activation energy for interdiffusion of Cu-Ni diffusion couple

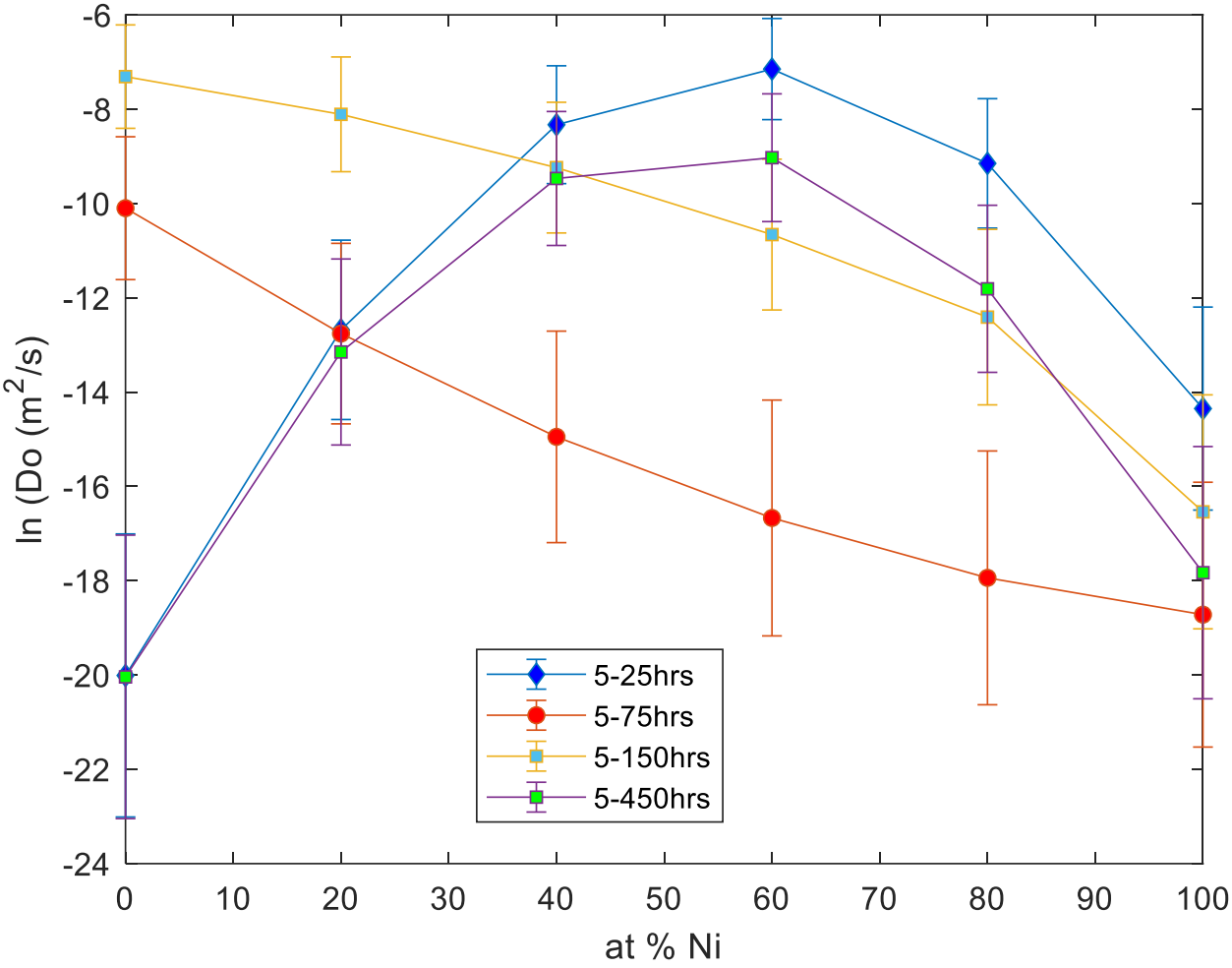

Figure 4.20: Concentration dependence of frequency factor for interdiffusion of Cu-Ni diffusion couple

Table 4.9: Activation energy Q (kJ/mol K) and frequency factor D_0 (m^2/s) for 20 at% Ni and different diffusion times

Conc.	5-25 hrs		5-75 hrs		5-150 hrs		5-450 hrs	
% Ni	Q	$\ln(D_0)$	Q	$\ln(D_0)$	Q	$\ln(D_0)$	Q	$\ln(D_0)$
0	116.56	-20.01	220.57	-10.1	246.26	-7.31	119.31	-20.04
20	201.86	-12.68	201.03	-12.76	248.09	-8.11	197.04	-13.15
40	255.32	-8.33	186.90	-14.95	246.18	-9.24	241.94	-9.47
60	275.11	-7.15	178.09	-16.67	240.77	-10.66	253.49	-9.03
80	260.89	-9.15	174.51	-17.94	231.54	-12.41	232.04	-11.81
100	212.59	-14.35	176.51	-18.72	198.12	-16.54	177.34	-17.83

Table 4.10: Activation energies and pre-exponential factors for Ni-Cu interdiffusion

Temperature range (^{0}C)	Activation energy (kJ/mol)	Pre-exponential factor (m^2/s)	References
250-450	130.5	-	[64,65]
200-630	131.8	-	[66]
550-650	41-221	-	[67]
650-850	31-53	-	[68]
750-950	108.8	-	[69]
950-1050	217.6	-	[69]
450-550	228.7	2×10^{-5}	[70]
300-504	133.1	2.6×10^{-10}	[71]
400-600	79-90	1.18×10^{-11}- 8.86×10^{-11}	[72]
695-1061	237.7	3.8×10^{-4}	[73]
947-1054	108.8	1.5×10^{-10}	[74]
850-1050	255.2	7.24×10^{-5}	[75]
775-1050	255.2	2.7×10^{-5}	[76]
900-1020	187 - 243	7.4×10^{-6} - 3.4×10^{-3}	Present study

4.4 Effect of time on impurity diffusion coefficients

One unique aspect of this research work is the numerical study of the effect of time on impurity diffusion coefficients. Fortunately, the numerical model in [20] is shown to be reliable in calculating the impurity diffusion coefficients aside from the commonly used technique of radioactive tracing. This technique was coupled with forward simulation to calculate the D(C)s for the Cu-Ni system. The same experimental data were also used in the SF method to show that for the extreme values of Ni concentrations, using the FSM to obtain the impurity diffusion coefficients is more reliable compared to the SF method. This model was then used to determine the D(C)s from the Cu-Ni system at different temperatures and different holding times in order to study the effect of time on the impurity diffusion coefficients of Ni solute in the Cu solvent and calculate the increase in percentage and correspondingly for the Cu solute in the Ni solvent. The impurity diffusion coefficients are observed to change with time with the Ni solute in the Cu solvent, with the smallest increase in percentage of 13% for intervals of 25-75 hrs vs 75-150 hrs. However, this is still higher than the 10% reported in the literature [32, 80, 81] as the benchmark of experimental uncertainty. This shows a significant variation of time with D(C)s at constant temperatures for impurity diffusion coefficients. The same trends are observed in Tables 4.12 - 4.14 at different temperatures. The assumption that D(C)s are a constant parameter and do not change with time isothermally does not hold true in the present analysis which may render the data erroneous when a factor of accuracy in design is required and used in the industry. Obviously, in this investigation, the D(C)s not only change with time but the impurity diffusion coefficients show variation of time with D(C)s isothermally.

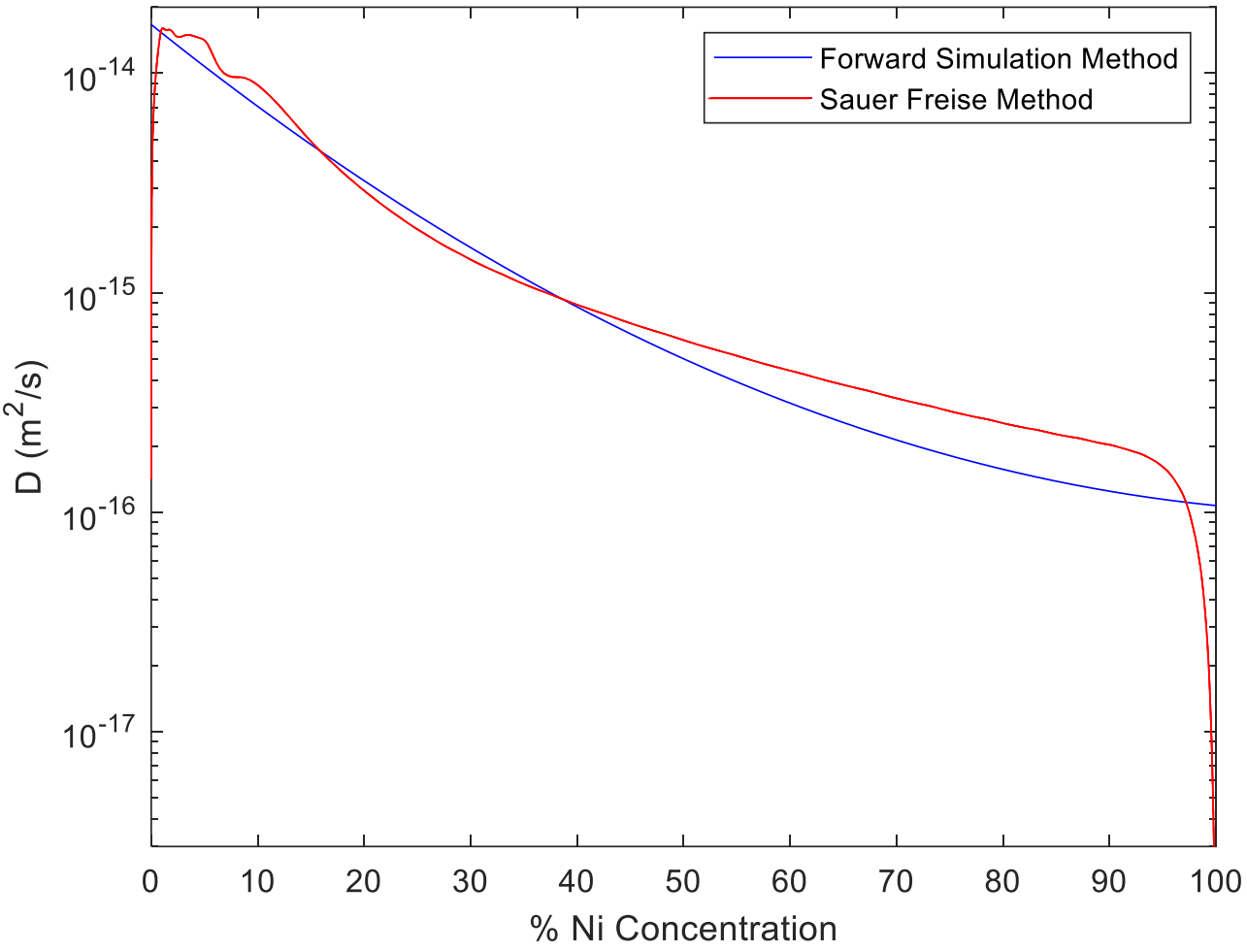

Figure 4.21: Concentration-dependent interdiffusion coefficients for pure Cu-Ni at 900^0C for holding time of 5-25 hrs: FSM vs SF method

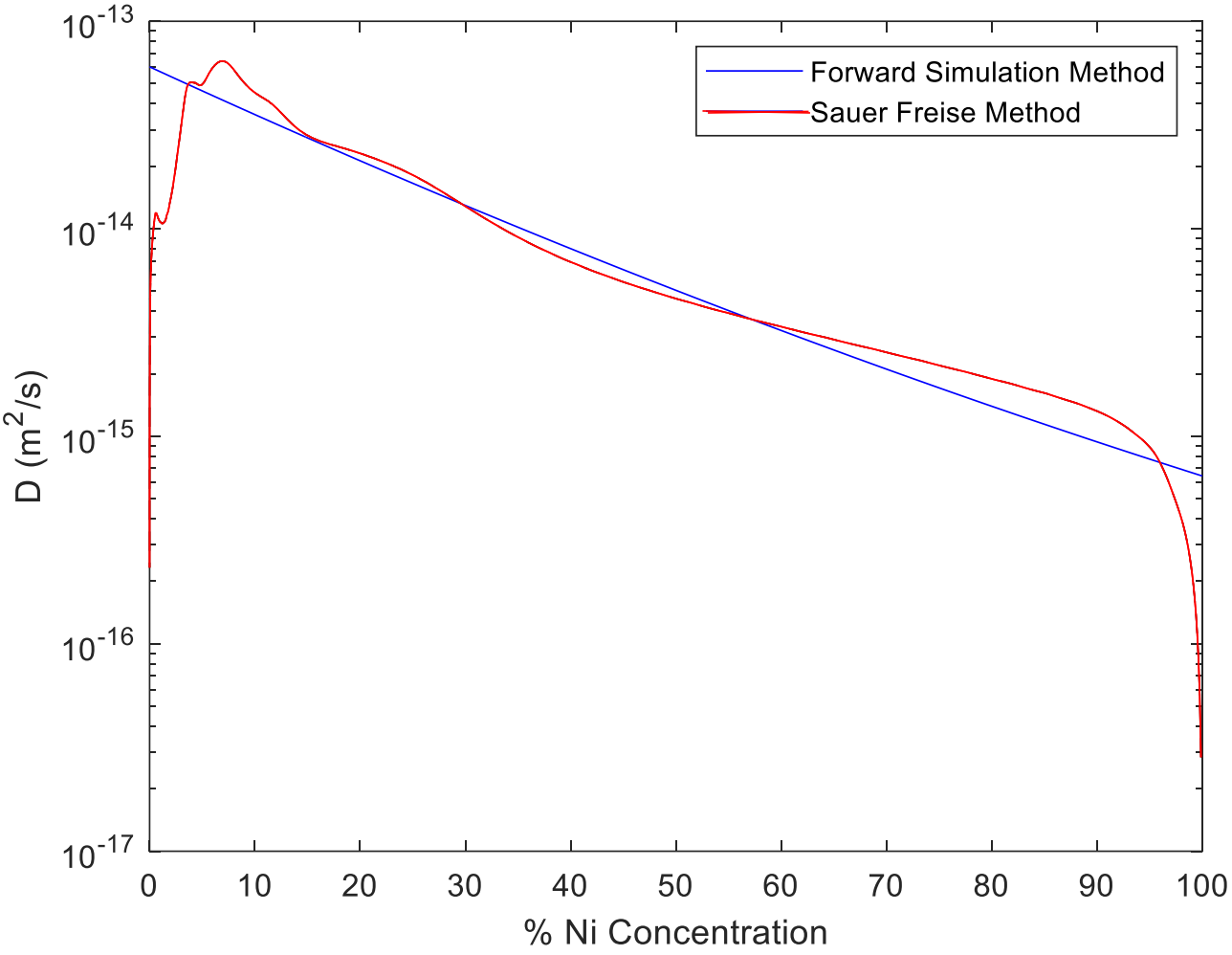

Figure 4.22: Concentration-dependent interdiffusion coefficients for pure Cu-Ni at 1020^0C for holding time of 5-25 hrs: FSM vs SF method

Table 4.11: Impurity diffusion coefficients of Ni solute in Cu solvent and Cu solute in Ni solvent and their corresponding increase in percentage for pure Cu-Ni at 900^0C

Time interval (hrs)	Ni in Cu	(%) increase	Comparison of time intervals (hrs)	Cu in Ni	(%) increase	Comparison of time intervals (hrs)
5-25	1.70E-14	-	-	1.40E-16	-	-
25-75	4.40E-15	286	5-25 vs 25-75	1.52E-16	9	5-25 vs 25-75
75-150	3.90E-15	13	25-75 vs 75-150	9.50E-17	60	25-75 vs 75-150
150-450	1.07E-14	174	75-150 vs 150-450	1.15E-16	21	75-150 vs 150-450

Table 4.12: Impurity diffusion coefficients of Ni solute in Cu solvent and Cu solute in Ni solvent and their corresponding increase in percentage for pure Cu-Ni at 940^0C

Time interval (hrs)	Ni in Cu	(%) increase	Comparison of time intervals (hrs)	Cu in Ni	(%) increase	Comparison of time intervals (hrs)
5-25	1.97E-14	-	-	1.95E-16	-	-
25-75	1.22E-14	61	5-25 vs 25-75	1.48E-16	32	5-25 vs 25-75
75-150	2.91E-14	139	25-75 vs 75-150	1.23E-16	20	25-75 vs 75-150
150-450	1.15E-14	154	75-150 vs 150-450	1.10E-15	89	75-150 vs 150-450

Table 4.13: Impurity diffusion coefficients of Ni solute in Cu solvent and Cu solute in Ni solvent and their corresponding increase in percentage for pure Cu-Ni at 980^0C

Time interval (hrs)	Ni in Cu	(%) increase	Comparison of time intervals (hrs)	Cu in Ni	(%) increase	Comparison of time intervals (hrs)
5-25	3.16E-14	-	-	1.27E-15	-	-
25-75	4.15E-14	31	5-25 vs 25-75	2.05E-16	520	5-25 vs 25-75
75-150	3.34E-14	24	25-75 vs 75-150	1.24E-16	65	25-75 vs 75-150
150-450	6.70E-14	101	75-150 vs 150-450	1.16E-15	835	75-150 vs 150-450

Table 4.14: Impurity diffusion coefficients of Ni solute in Cu solvent and Cu solute in Ni solvent and their corresponding increase in percentage for pure Cu-Ni at 1020^0C

Time interval (hrs)	Ni in Cu	(%) increase	Comparison of time intervals (hrs)	Cu in Ni	(%) increase	Comparison of time intervals (hrs)
5-25	5.40E-14	-	-	3.40E-16	-	-
25-75	2.85E-14	89	25-75 vs 5-25	8.00E-16	135	5-25 vs 25-75
75-150	8.50E-14	198	25-75 vs 75-150	9.50E-16	19	25-75 vs 75-150
150-450	1.43E-14	496	150-450 vs 75-150	1.66E-15	75	75-150 vs 150-450

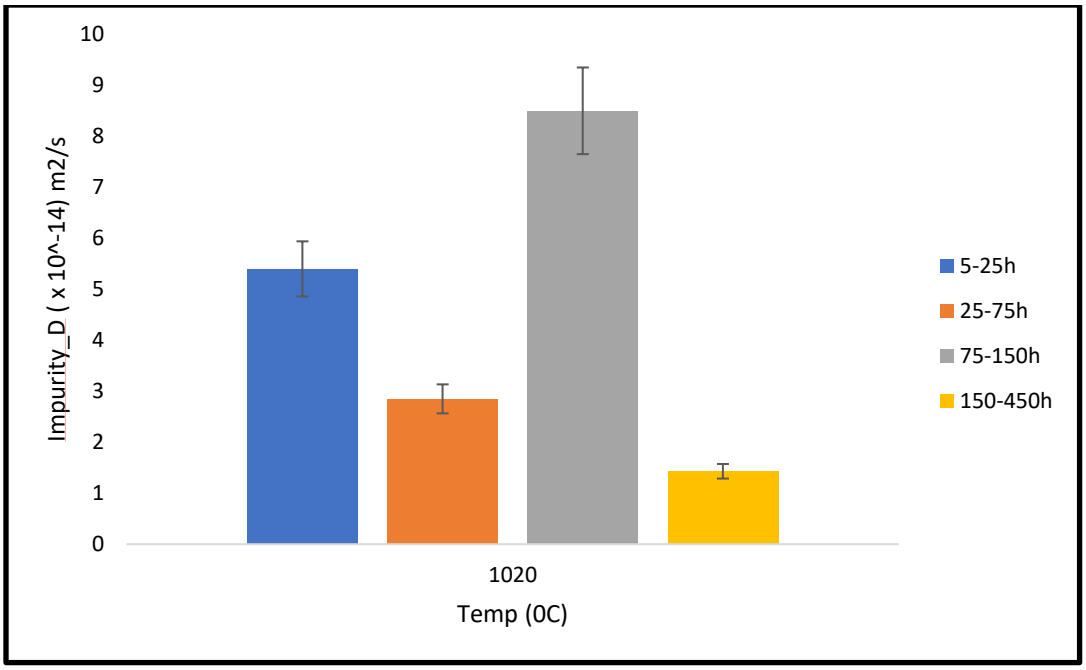

Figure 4.22a: Impurity diffusion coefficient of Ni in Cu at different times at 1020^0C

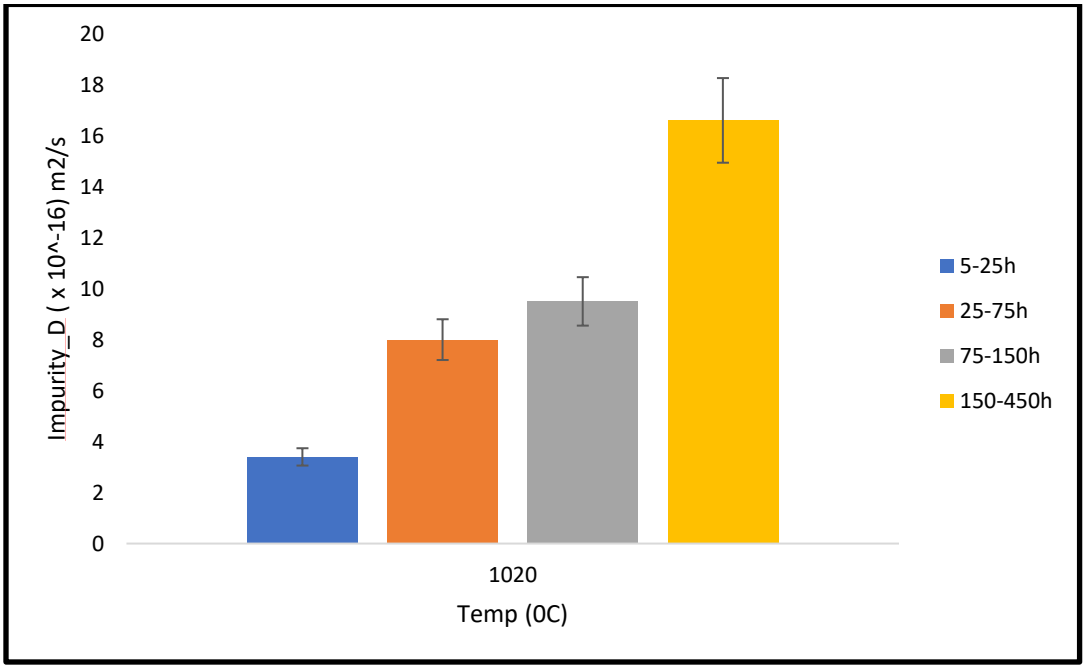

Figure 4.22b: Impurity diffusion coefficient of Cu in Ni at different times at 1020^0C

4.5 Underlying Factor of Diffusion-induced Stress

DIS has been discussed in the literature as a factor that can change the concentration gradient which then affects the solute concentration dependence of the interdiffusion coefficient. The report generated in this research shows a change in the D(C)s at constant temperatures and different diffusion times. This finding challenges the general assumption that the D(C) does not change with time.

Fundamentally, the atomic mismatch caused by the difference between the atomic size of the Ni solute and Cu solvent changes the lattice parameter of the host material at the occurrence of diffusion. The solute concentration gradient is induced by diffusion and further leads to variations of the lattice parameters in the crystal structure. This result in stress formation on one side and relaxation on the other side of the material host. Hence, the solute concentration gradient is a factor that influences DIS which implies that diffusion coefficients can be somewhat influenced. The concept is that during diffusion, the concentration gradient influences the DIS which controls the diffusion coefficient; hence, diffusion coefficients can vary with solute concentration.

Time is an important factor during diffusion. Several researchers [75,76] have repeatedly calculated diffusion coefficients and in spite of the different results, acknowledge them as material constants that do not change with time.

In order to extend work on DIS as the underlying factor for changes in D(C)s which causes time variation in diffusion systems, two attributable facts will be discussed:

(i) the effect of the solute source concentration, and

(ii) occurrence of anomalous temperature behaviour

4.5.1 Effect of solute source concentration on interdiffusivity

During the diffusion process, the solute concentration gradient changes in the crystal lattices lead to diffusion-induced strain, thus giving rise to DIS [59]. However, comparisons of the theoretical and experimental D(C)s of a pure metal/pure metal couple and a pure-metal/alloy couple are rarely done in the literature. The numerical model in [20] was used to examine the effects of the solute source concentration on interdiffusivity. The diffusivity of 10 at% Ni pure Cu and 100 at% Ni-pure Cu was observed at a constant time and constant temperature but different concentration gradients. Figures 4.23 and 4.24 show that the interdiffusivity changes, which contradicts the general assumption in the literature that interdiffusivity does not change with time. The results of the standard deviation errors for $Cu_{10}Ni_{90}$ and 100%Cu for 900^0C and 1020^0C in Figures 4.25 and 4.26 respectively show the experimental difference between the D(C)s of $Cu_{10}Ni_{90}$ and 100% Cu. Table 4.15 lists the changes in the calculated average interdiffusivity of different solute source concentrations.

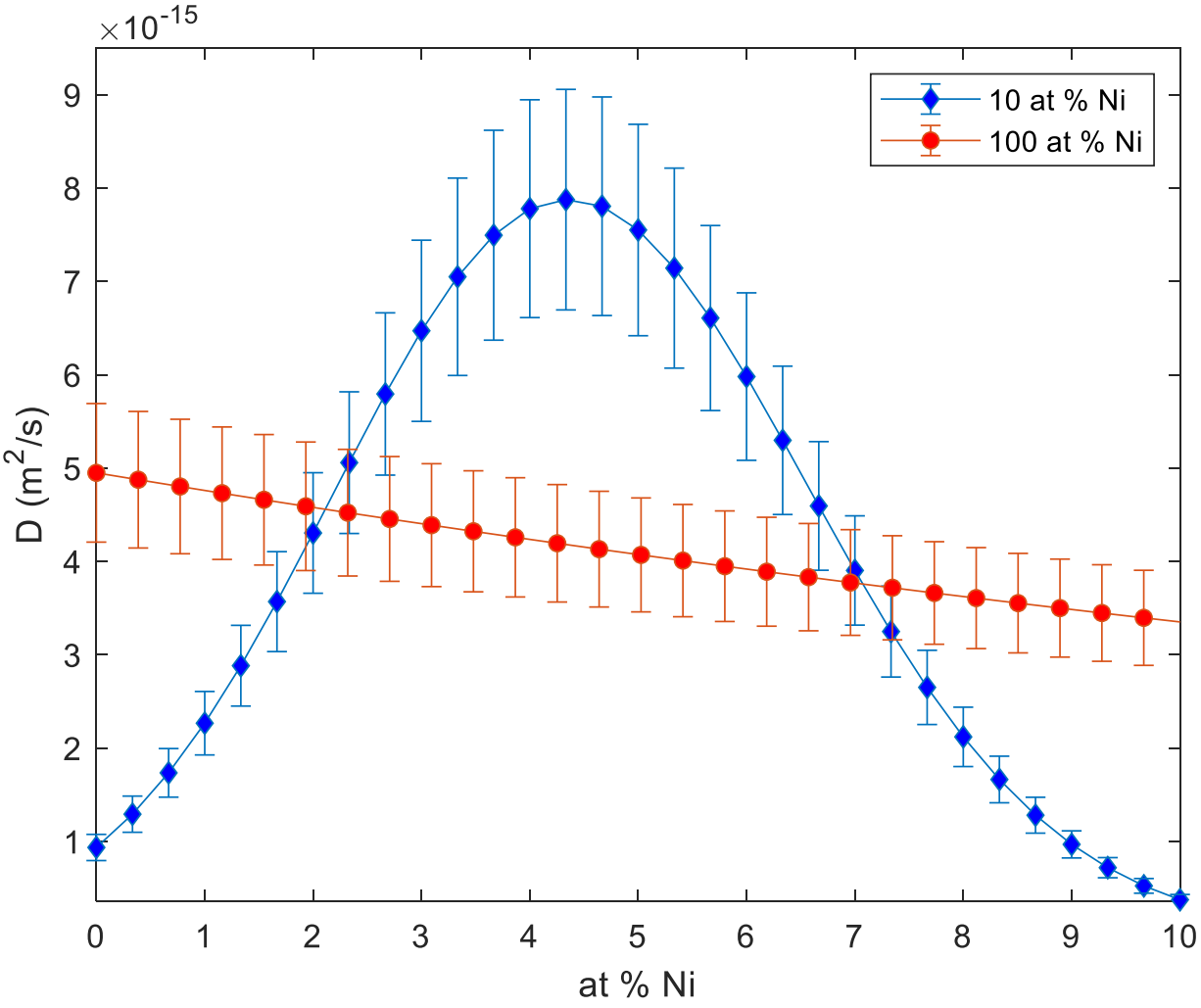

Figure 4.23: Concentration dependence of interdiffusion coefficient for 10 at% Ni and 100 at% Ni between 25-150 hrs for holding temperature of 900^0C.

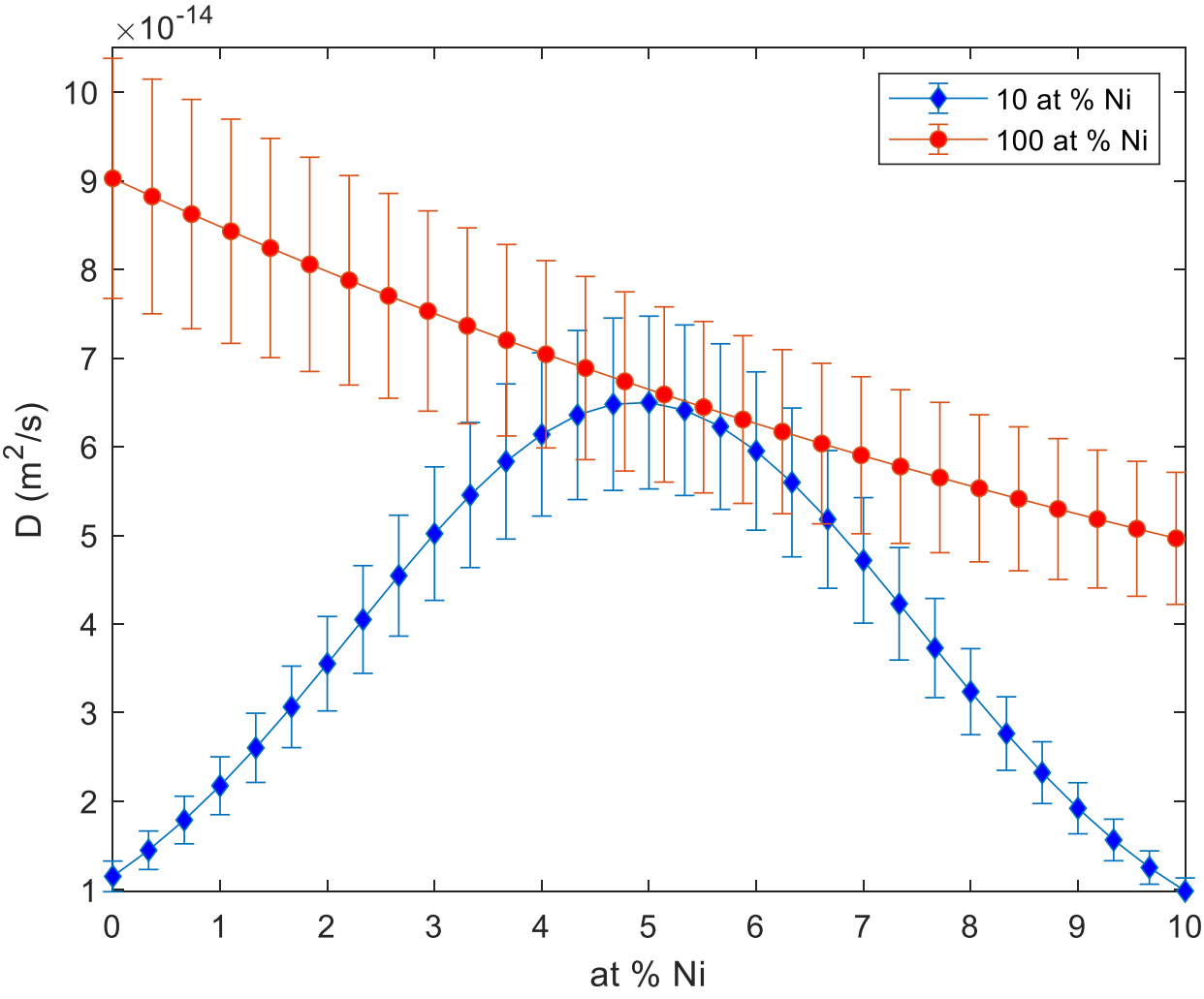

Figure 4.24: Concentration dependence of interdiffusion coefficient for 10 at% Ni and 100 at% Ni between 25-150 hrs for holding temperature of 1020^0C.

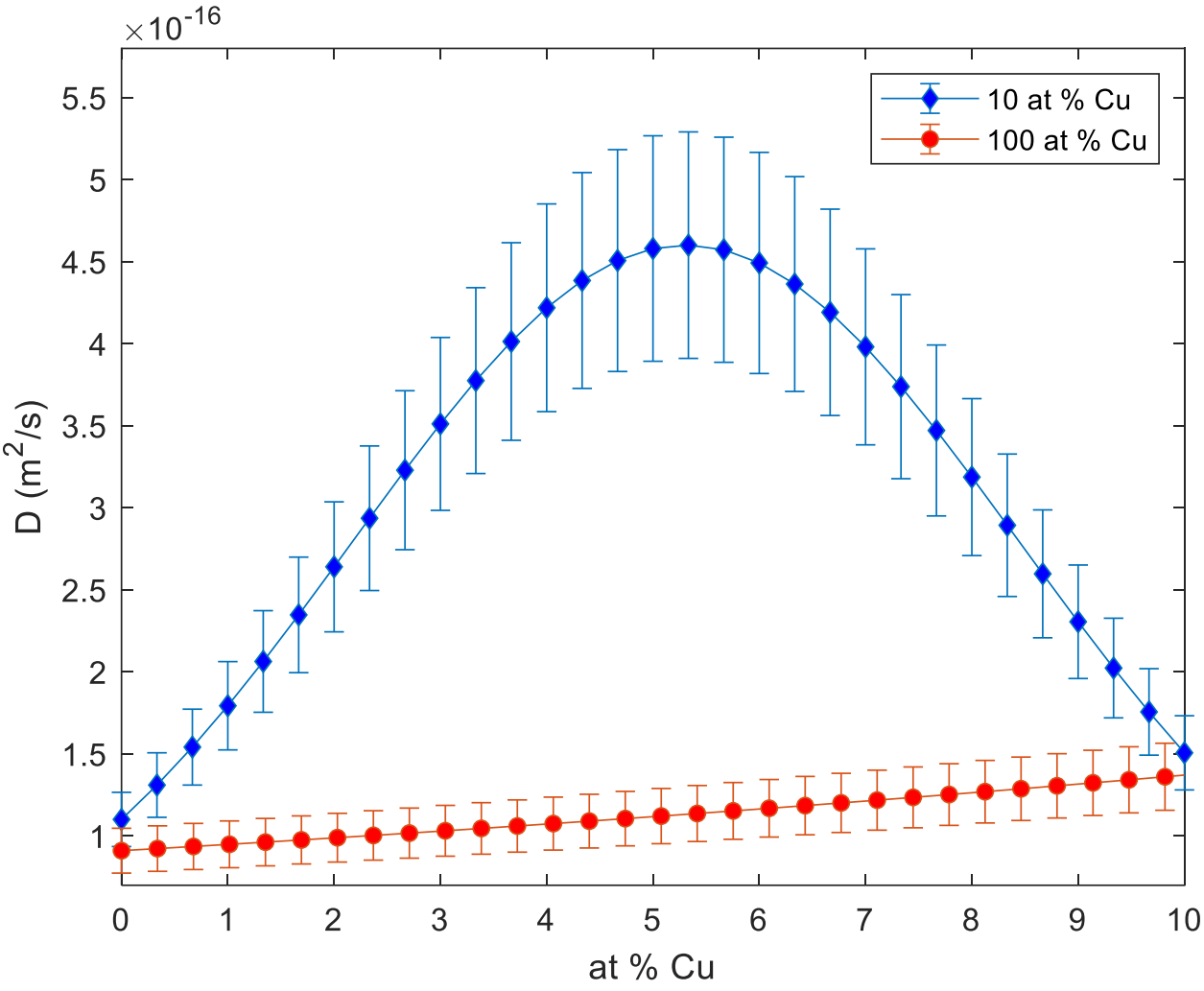

Figure 4.25: Concentration dependence of interdiffusion coefficient for 10 at% Cu and 100 at% Cu between 25-150 hrs for holding temperature of 900^0C.

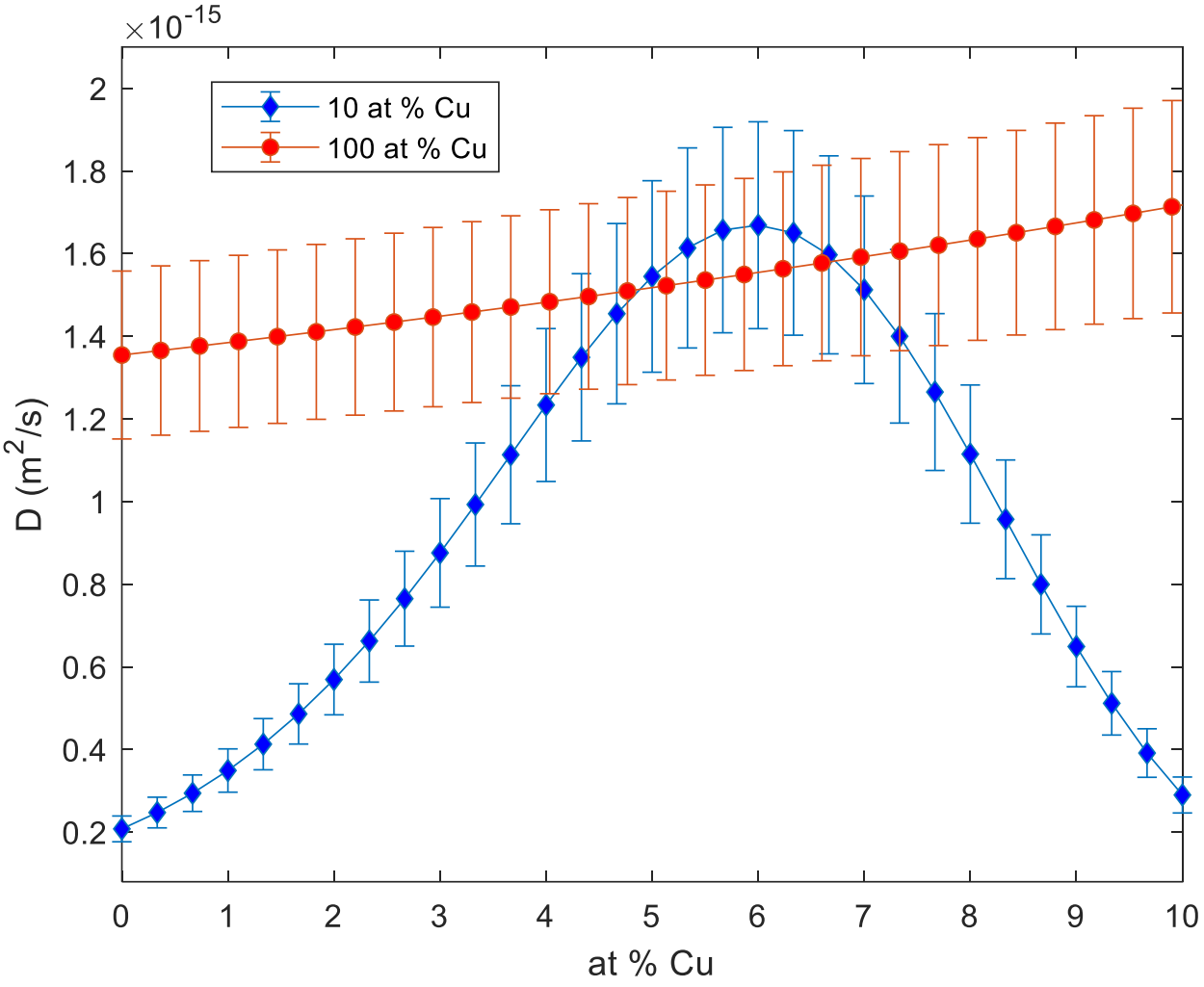

Figure 4.26: Concentration dependence of interdiffusion coefficient for 10 at% Cu and 100 at% Cu between 25-150 hrs for holding temperature of 1020^0C.

4.5.1.2 Effect of solute source concentration on impurity diffusivity of Ni solute in Cu solvent at different holding temperatures

The concentration profiles at 25 hrs and 150 hrs were used to determine the D(C) operator between two isothermal profiles of 25-150 hrs. The result in Table 4.16 illustrates the differences in the impurity diffusion coefficient of the Ni solute in pure Cu. Furthermore, the % increase of the impurity diffusion coefficient is about 429% at 900^0C which is higher than the highest uncertainty of 15% found experimentally.

4.5.1.3 Effect of solute source concentration on impurity diffusivity of Cu solute in Ni solvent at different holding temperatures

Likewise, the result in Table 4.17 follows the pattern found in Table 4.16. Thus the % increase recorded for the impurity diffusion coefficient shows that the values are higher than the 15% uncertainty found experimentally. These experimental findings unequivocally confirm that changing the constant solute source concentration within systems can lead to substantial changes in D(C)s. This is because the changes impact the distribution of the concentration gradients, thereby affecting the DIS, which is found to have an impact on D(C)s.

Table 4.15: Calculated average of interdiffusivity of different solute source concentrations

Temp(^{0}C)	Time interval	Ni 10 at% in Cu	Ni 100 at% in Cu	%increase
900	25-150 hrs	4.27E-15	1.28E-15	232%
1020	25-150 hrs	4.04E-14	1.66E-14	143%

Table 4.16: Impurity diffusion coefficient of different % of Ni solute source concentration in Cu

Temperature(^{0}C)	**Time interval (hrs)**	**Ni 10 at% in Cu**	**Ni 100 at% in Cu**	**(%) increase**
900	25-150	9.35E-16	4.95E-15	429
1020	25-150	3.75E-15	9.03E-14	2308

Table 4.17: Impurity diffusion coefficient of Cu in different % of Ni solute source concentration

Temperature(^{0}C)	**Time interval (hrs)**	**Cu in Ni 10%**	**Cu in Ni 100%**	**(%) increase**
900	25-150	3.76E-16	9.10E-17	313
1020	25-150	5.19E-15	1.36E-15	282

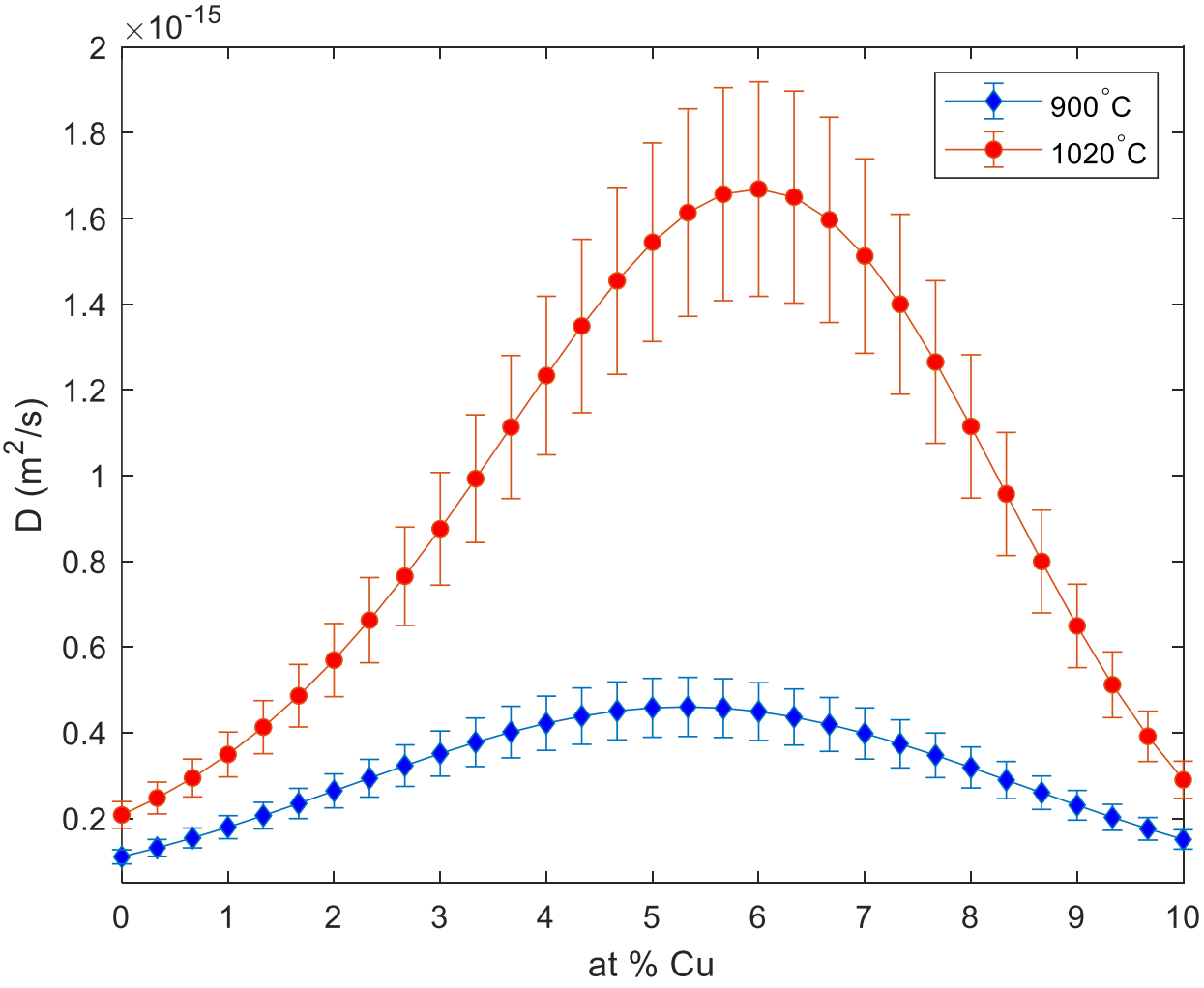

Figure 4.27: Plot of concentration dependence of interdiffusion coefficient for Ni-based alloy (with 10 at% Cu) and pure Ni between 25-150 hrs for 900^0C and 1020^0C holding temperatures.

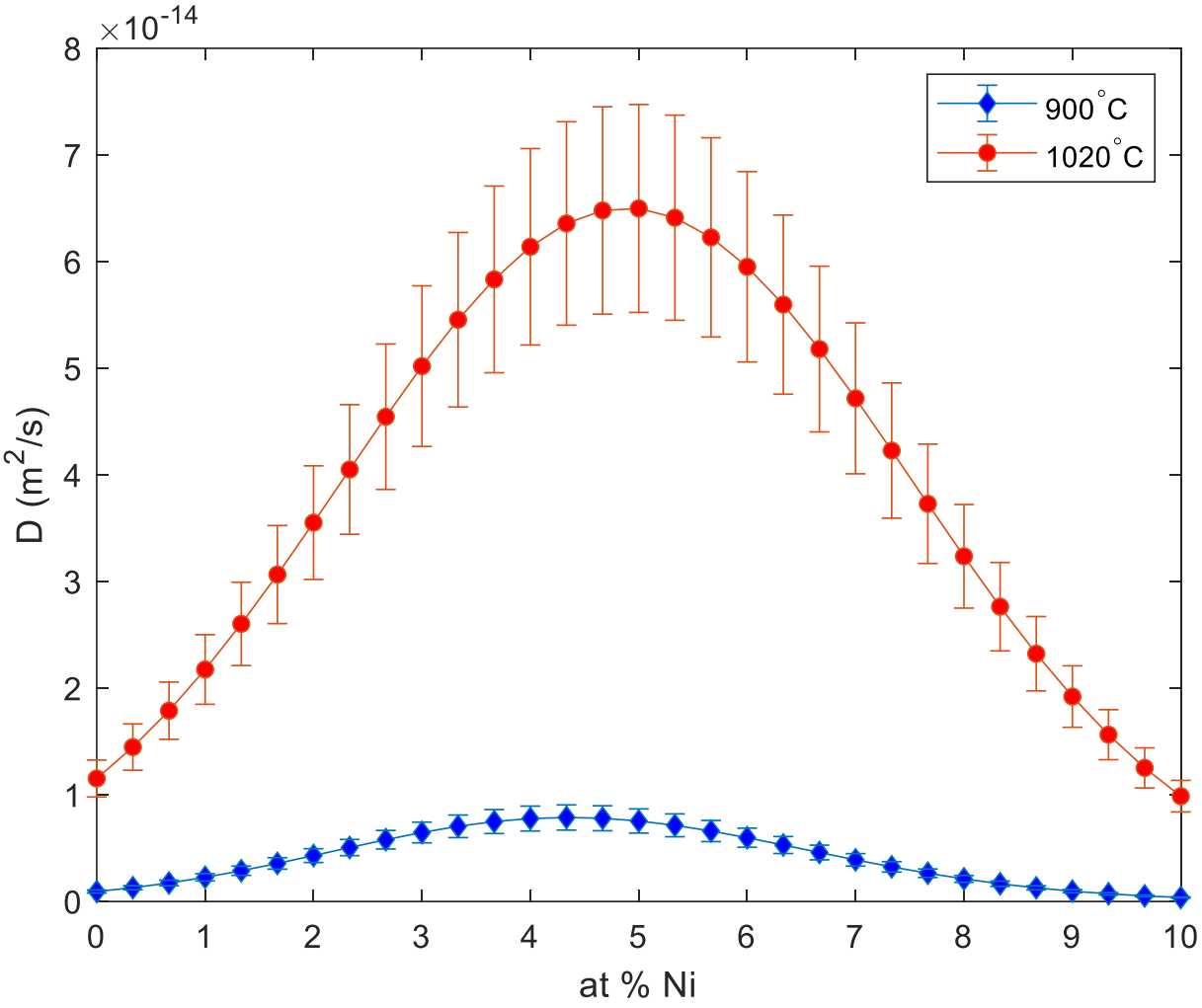

Figure 4.28: Plot of concentration dependence of the interdiffusion coefficient for Cu-based alloy (with 10 at% Ni) and pure Cu between 25-150 hrs for holding temperatures of 900^0C and 1020^0C.

4.5.2 Anomalous behaviour of temperature on D(C)s

Another less conventional way to understand that DIS is found in a system when the D(C)s change, is through the anomalous behaviour of temperature on D(C)s, which can be observed under two circumstances:

(a) occurrence of anomalous behaviour of temperature at a certain concentration, and

(b) occurrence of anomalous behaviour of temperature at a certain diffusion time.

4.5.2.1 Occurrence of anomalous behaviour of temperature at certain concentrations

Figure 4.29 shows temperature increases with larger D(C)s; however, at 46 at% of Ni this relationship changes so that D(C)s at a lower temperature of 980^0C are larger than those at a higher temperature of 1020^0C. This obvious anomaly only occurs at certain concentrations and shows that DIS is found in a system. Likewise, a similar pattern is observed in Figure 4.30 for 13 at% of Ni and Figure 4.32 for 1.2 at%, 6.6 at% and 46 at% of Ni.

4.5.2.2 Occurrence of anomalous behaviour of temperature at certain diffusion time

The second scenario where a system shows anomalous behaviour of the temperature is at a certain diffusion time. In Figure 4.29, anomalous behavior of the temperature can be observed between 980°C and 1020°C. Normally, D(C)s should become larger with rising temperature, but within the range of 0 to 40 at% Ni, the DCs behave differently. Similarly, the concentration between 0 and 18 at% Ni shows a larger D(C) at 980°C, but a lower D(C) at 1020°C. This anomaly is not found in Figure 4.32, as the plot follows the expected pattern in Figure 4.30. However, Figure 4.32 does exhibit anomalies between 980°C and 1020°C, 900°C and 1020°C, as well as 900°C and 940°C.

These anomalous temperature effects on the D(C) are evidently due to the presence of DIS in the Cu-Ni system.

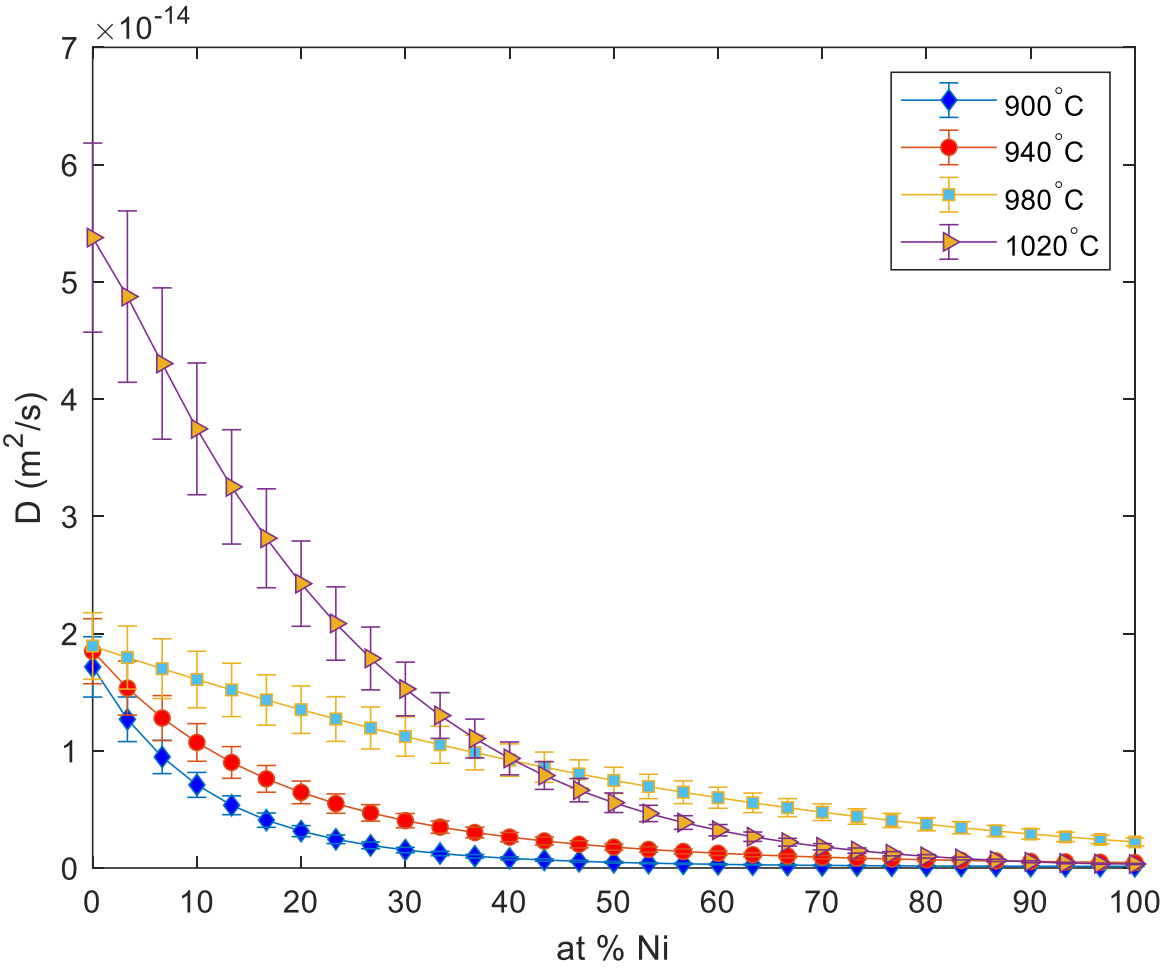

Figure 4.29: Concentration dependence of interdiffusion coefficients for pure Cu-Ni between 5-25 hrs for different holding temperatures

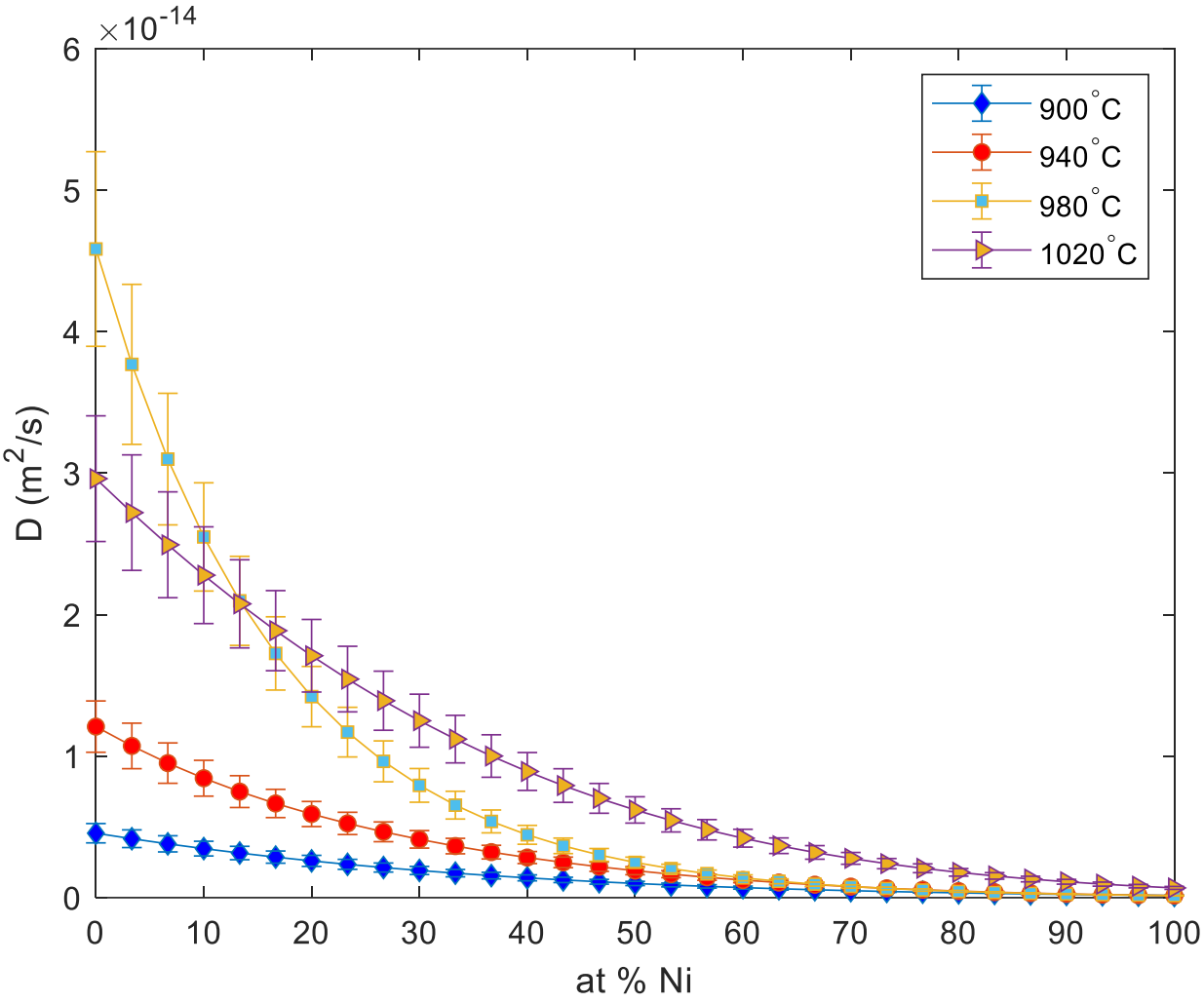

Figure 4.30: Concentration dependence of interdiffusion coefficients for pure Cu-Ni between 25-75 hrs for different holding temperatures

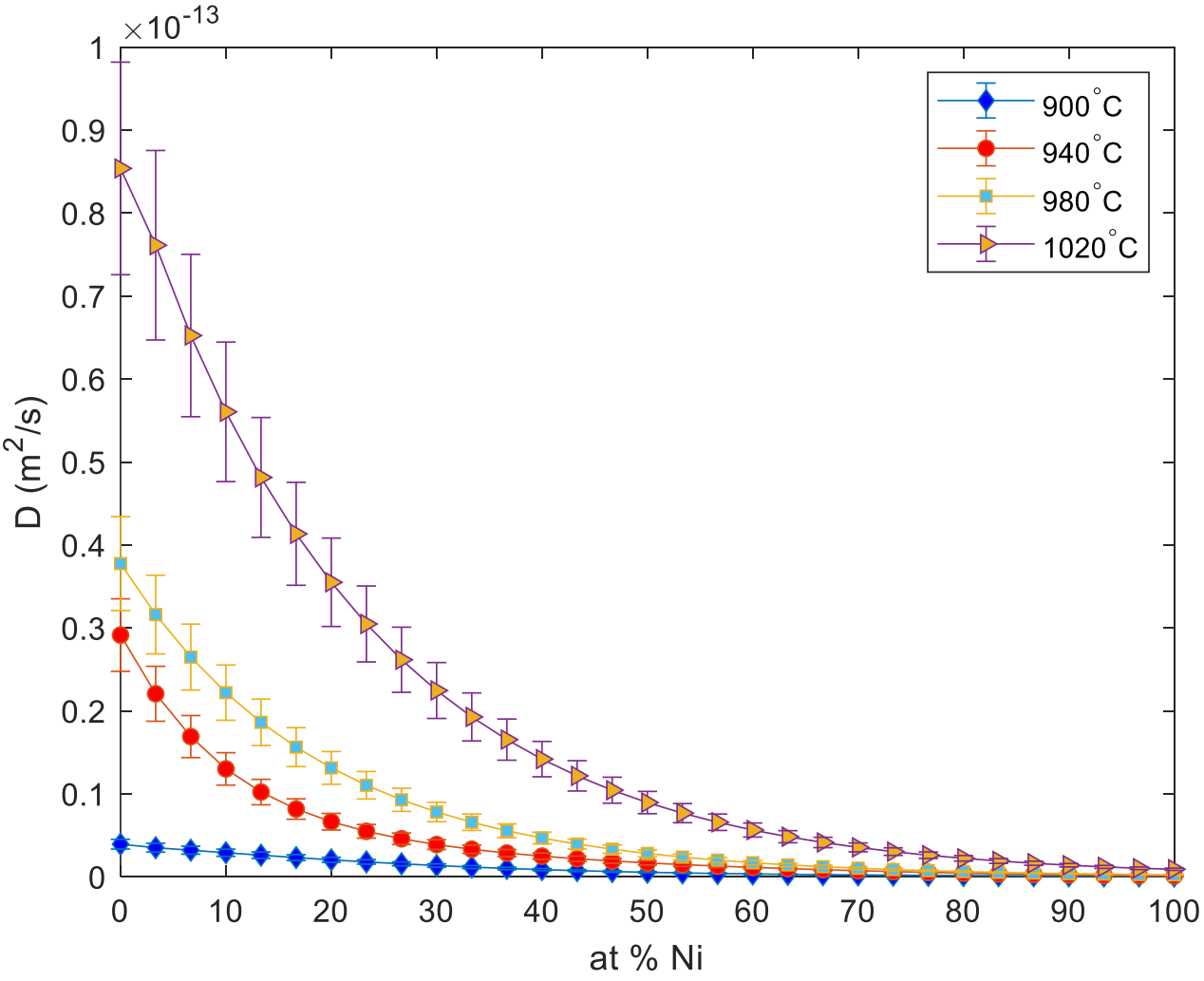

Figure 4.31: Concentration dependence of interdiffusion coefficients for pure Cu-Ni between 75-150 hrs for different holding temperatures

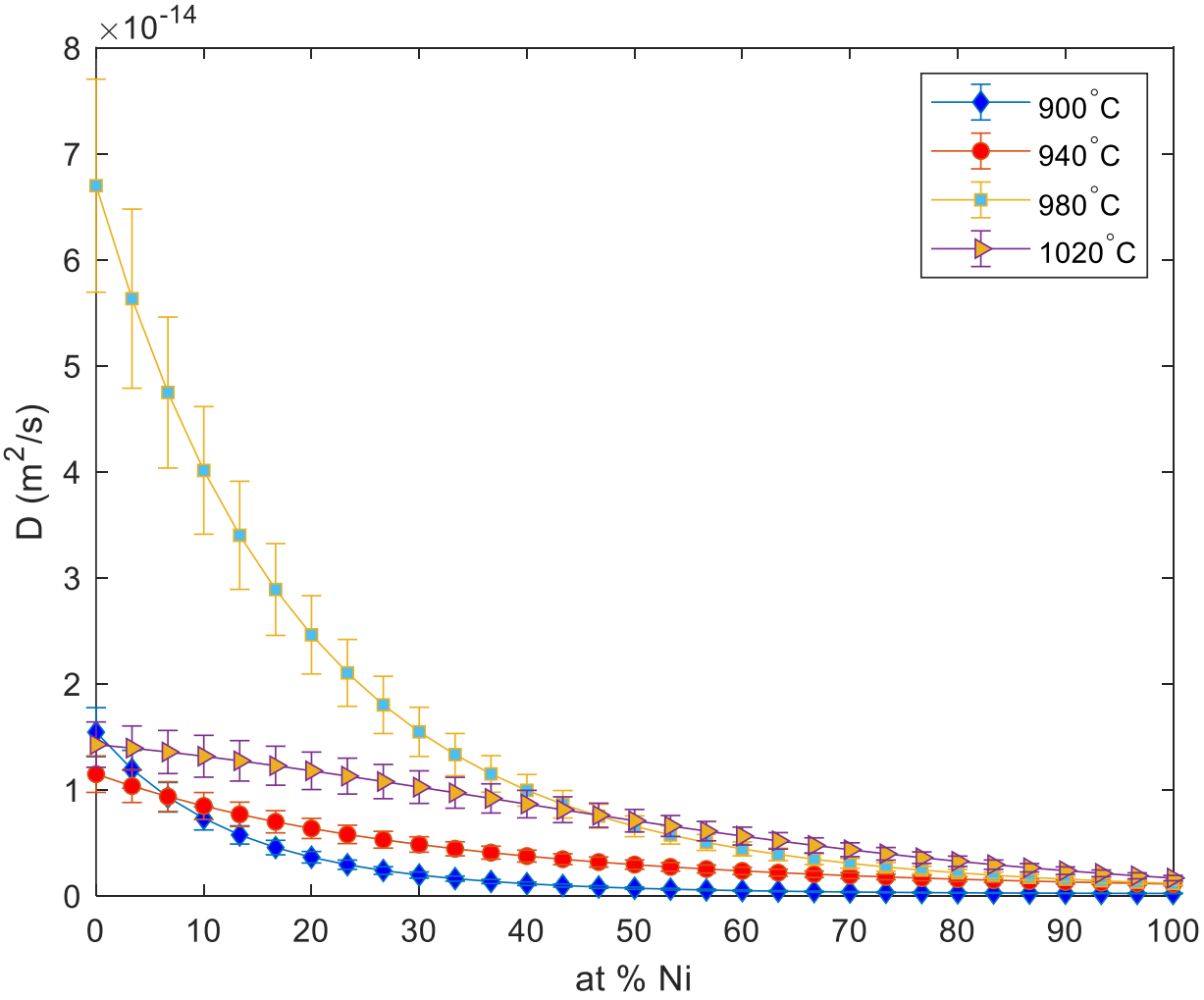

Figure 4.32: Concentration dependence of interdiffusion coefficient for pure Cu-Ni between 150-450 hrs for different holding temperatures

4.5.2.3 Anomalous behaviour of temperature for interdiffusion coefficients and impurity diffusion coefficents

Having explored and observed the anomalous behaviour of temperature on D(C)s that occur at certain concentrations and certain diffusion times as evidence of the presence of DIS in the system, this anomaly can be further investigated by using the calculated average of the interdiffusion time. In Figure 4.33, the relationship between D_{ave} and temperature for pure Cu and pure Ni can be observed at various temperatures. However, an unusual pattern emerges within the time interval of 150-450 hours, where the D_{ave} decreases between 980°C and 1020°C. Additionally, during 5-25 hours and 75-150 hours, the D_{ave} increases significantly between temperatures of 980°C and 1020°C beyond expectations, respectively.

Likewise, a similar trend is clearly evident in Figures 4.34 and 4.35, which show the impurity diffusion coefficients of Ni solute in Cu solvent. The increase in temperature is accompanied by an abnormal trend or anomalous behavior in the size of the impurity diffusion coefficient. This abnormality is observed at specific temperatures and during certain diffusion times. The trend serves as compelling evidence that DIS indeed exists within the system.

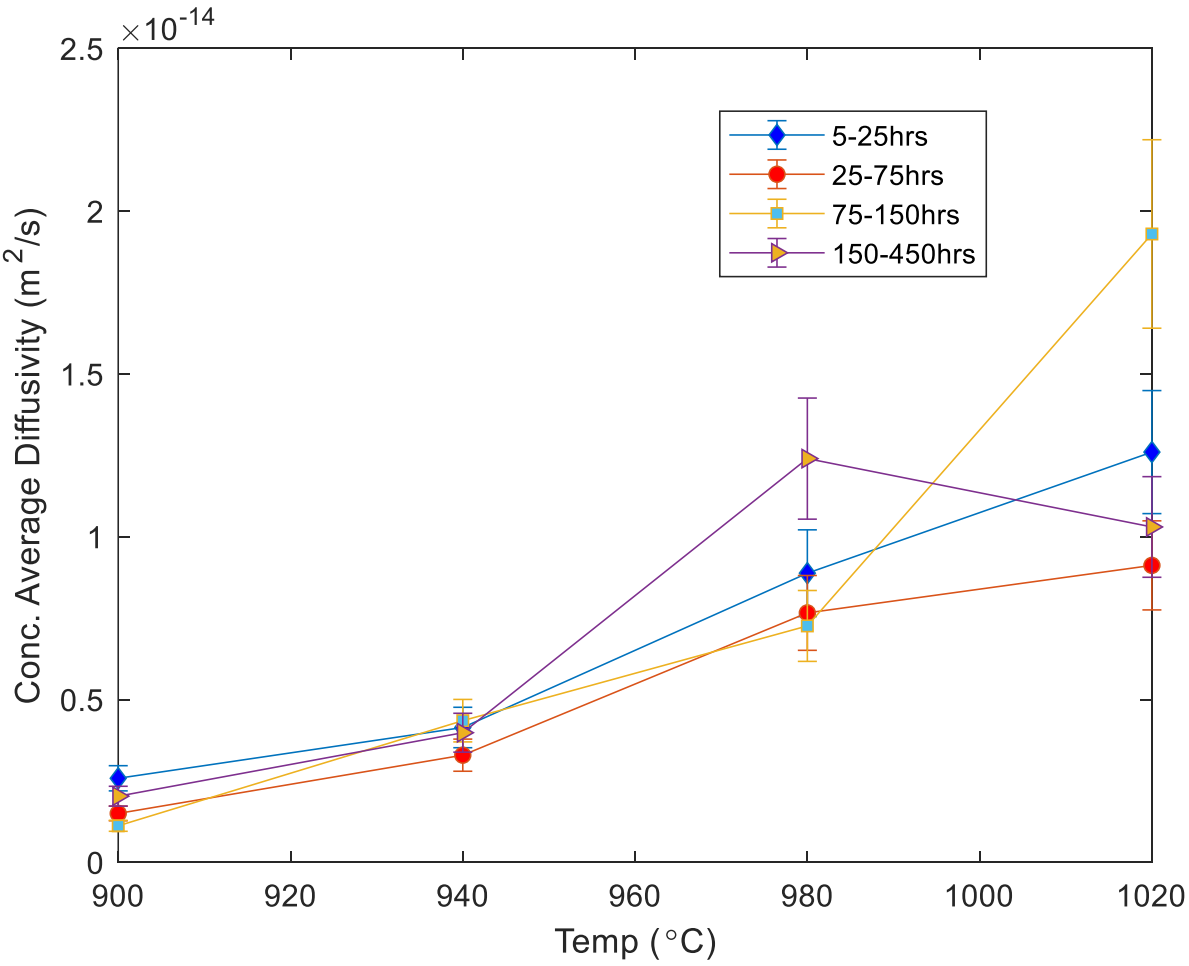

Figure 4.33: Calculated average of diffusivity vs temperature of pure Ni-Cu for different diffusion times

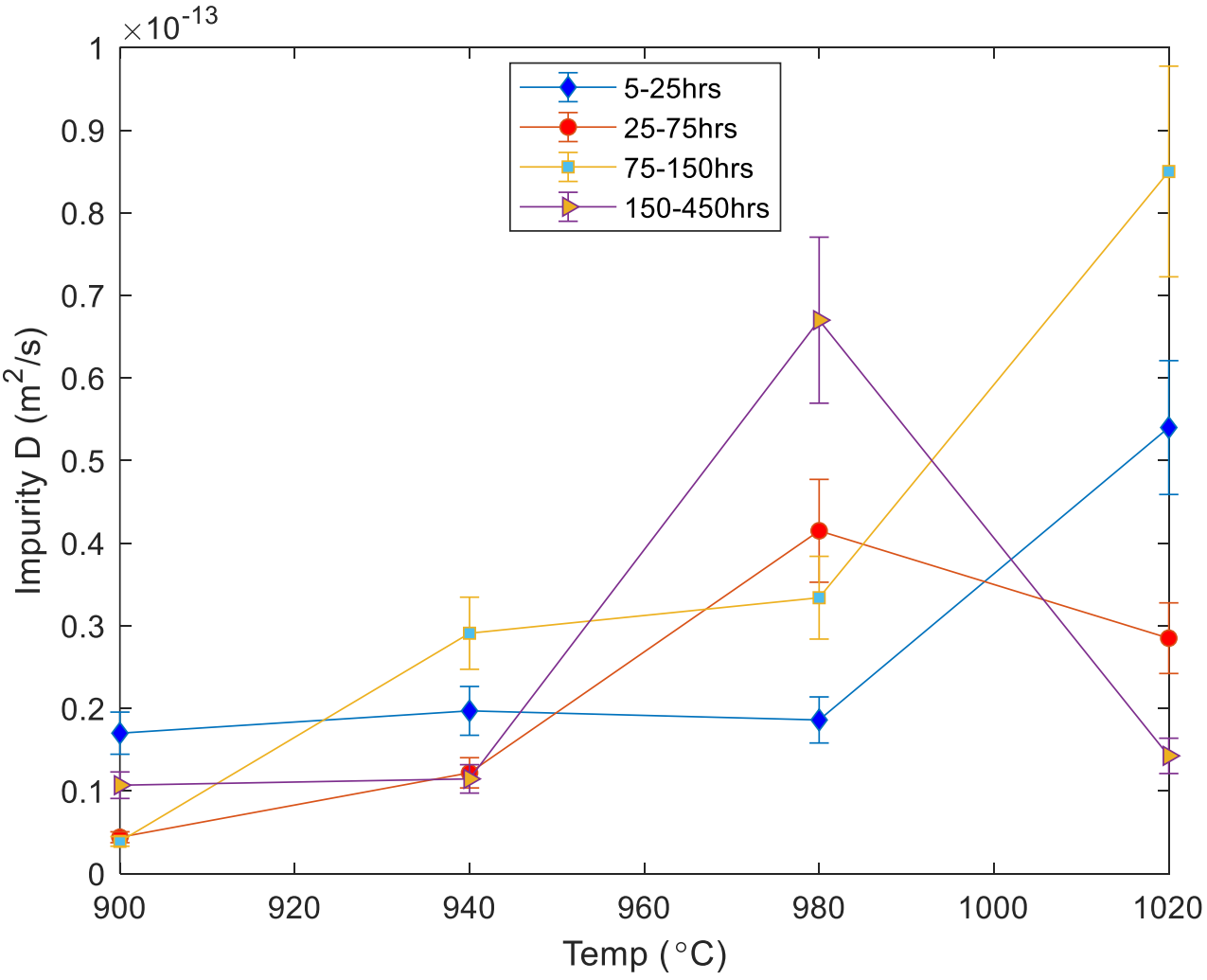

Figure 4.34: Impurity diffusion coefficients vs temperature of Ni solute in Cu solvent for different diffusion times

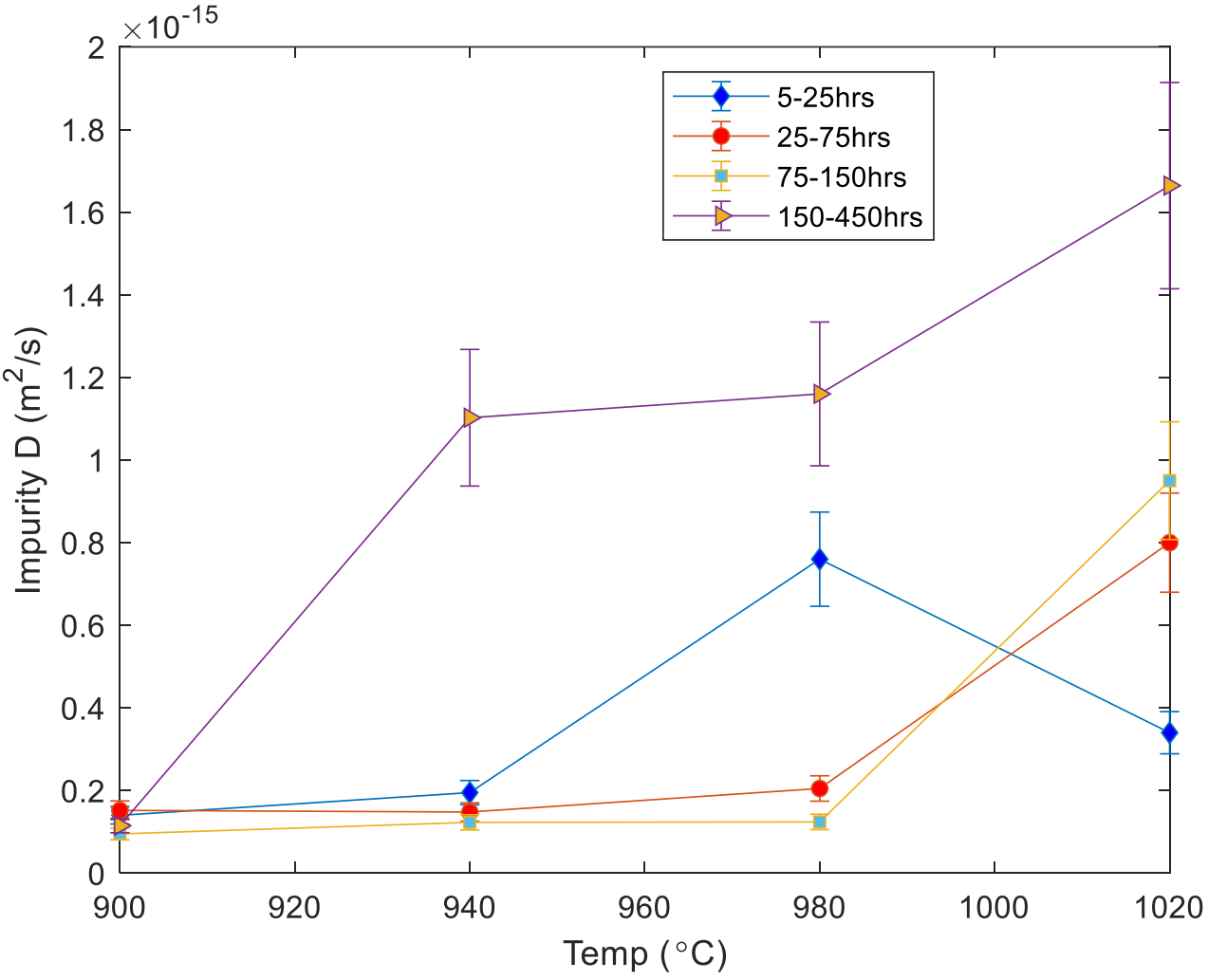

Figure 4.35: Impurity diffusion coefficients vs temperature of Cu solute in Ni solvent after different diffusion times

4.6 Significance of time variation of D(C)s

Here, it is important to acknowledge that researchers have commonly used a general method for determining D(C)s which typically involves a single diffusion time, such as 5 hrs, 25 hrs, or 75 hrs, among others. The prevailing conventional methods used for this purpose are the BM, SF, Wagner, and Hall methods. However, these methods share common limitations. The primary limitation associated with these methods arises from the assumption that there is no initial non-uniform distribution of solute. This implies that they assume a concentration that behaves as a step function in space. This assumption has made it impractical to utilize a general approach to understand how concentration gradients are influenced by pre-existing non-uniform solute distributions within a material and, consequently, how this impacts the diffusion coefficients.

In this research work, a novel method is used which differs from the general approach. This method takes into consideration a non-uniform initial solute distribution, thus disregarding the assumption of a step-function in space. The methodology involves using the FSM to determine the diffusion coefficients in scenarios where concentration gradients exist within a material before diffusion heat treatment takes place, which originate from a non-uniform solute distribution.

Practically, this approach requires two experimental concentration profiles. The initial profile is used to derive the D(C) required to produce the second experimental concentration profile. The significance here lies in the valuable information that is provided on how the concentration gradients in the initial profile influence the D(C) needed to generate the second profile. Additionally, a review of the literature reveals a graphical method that is outlined in Kirkendall et al. [77], which was used to calculate the average constant diffusivity between two concentration profiles.

Nonetheless, it is important to note that the general method, which assumes a step-function in space, has also been utilized to investigate the effect of time. The results of this investigation are presented in Table 4.18 for the impurity diffusion of an Ni solute in Cu solvent and Table 4.19 for the impurity diffusion coefficient of a Cu solute in a Ni solvent at various diffusion times.

Evidently, the impurity diffusion coefficient changes over time, even isothermally. This change is represented as an increase in percentage between different time intervals. Most of these increases exceed 15%, which places them outside the threshold of experimental uncertainty. Consequently, these cases are considered statistically dissimilar, except for a few instances at 900°C and 980°C, where the increase in percentage falls below the threshold of experimental uncertainty.

A similar scenario is depicted in Table 4.20, which shows the calculated average of the interdiffusion concentration coefficients and provides insight into the behavior of D(C)s. As a result, the D(C) undergoes changes over time, even under isothermal conditions.

In light of the concept of DIS, it is reasonable to anticipate variations in D(C) with respect to diffusion time when studying interdiffusion. Empirical studies in the existing literature have indeed provided evidence for the presence of DIS and the resultant variations in D(C)s over time throughout the interdiffusion process. The changes in the solute concentration gradients brought about by diffusion is a contributing factor to the changes in D(C)s over time. This temporal effect can only be ascribed to DIS because DIS would not be apparent without changes of the D(C)s.

Table 4.18: Impurity diffusion coefficient of Ni solute in Cu solvent with diffusion time

Temp(^{0}C)	5 hrs	(% inc.)	25 hrs	(% inc.)	75 hrs	(% inc.)	150 hrs	(% inc.)	450 hrs
900	1.82E-14	3	1.87E-14	200	6.23E-15	57	3.97E-15	163	1.51E-15
940	1.79E-14	29	1.39E-14	56	8.9E-15	16	7.65E-15	2355	3.12E-16
980	4.44E-14	104	2.18E-14	9	2.38E-14	20	1.98E-14	9	1.82E-14
1020	1.15E-13	218	3.62E-14	20	3.01E-14	82	5.49E-14	25	4.4E-14

Table 4.19: Impurity diffusion coefficient of Cu solute in Ni solvent with diffusion time

Temp(^{0}C)	5 hrs	(% inc.)	25 hrs	(% inc.)	75 hrs	(% inc.)	150 hrs	(% inc.)	450 hrs
900	2.8E-15	689	3.55E-16	78	2E-16	120	9.08E-17	136	3.84E-17
940	1.05E-15	182	3.72E-16	42	2.62E-16	42	1.85E-16	3364	6.41E-15
980	1.95E-15	109	9.34E-16	97	4.75E-16	101	2.36E-16	4	2.28E-16
1020	5.6E-15	352	1.24E-15	57	7.9E-16	39	1.1E-15	86	2.05E-15

Table 4.20: Calculated average of interdiffusion concentration coefficients of pure Cu-Ni with diffusion time

Temp(^{0}C)	5 hrs	(% inc.)	25 hrs	(% inc.)	75 hrs	(% inc.)	150 hrs	(% inc.)	450 hrs
900	6.41E-15	149	2.58E-15	44	1.80E-15	44	1.24E-15	3	1.28E-15
940	5.76E-15	53	3.76E-15	24	3.03E-15	9	2.77E-15	19	3.29E-15
980	1.08E-14	19	9.07E-15	35	6.71E-15	10	6.11E-15	32	8.09E-15
1020	4.27E-14	199	1.43E-14	36	1.05E-14	37	1.44E-14	39	1.03E-14

Furthermore, it is commonly assumed in the existing literature that D(C)s obtained by using longer diffusion times remain constant with respect to temperature and can be used to model diffusion at any time and any specific temperature.

However, the findings of the present study challenge this assumption by showing that the time-dependence of the interdiffusion coefficient can introduce errors. These errors arise due to the presence of an initial solute distribution in the material before the diffusion heat treatment takes place. It is important to recognize that a significant factor that impacts the accuracy and reliability of calculated D(C)s from experimental concentration profiles is the existence of an initial solute concentration profile in the material prior to the onset of the diffusion process. Consequently, the presence of a significant initial solute concentration profile at time zero, which precedes the diffusion process, can lead to inaccuracies in the calculation of D(C)s derived from the final experimental solute concentration profile obtained after a lengthy diffusion period.

To validate this concept, the conventional method was applied to calculate D(C) for a long diffusion time of 450 hrs at different temperatures, namely 900°C, 940°C, 980°C, and 1020°C. The calculated D(C) at 450 hrs was then used to simulate the concentration profiles after 5 hrs at these specified temperatures. Subsequently, the simulated concentration profiles at 5 hrs were compared with the actual experimental concentration profiles obtained after 5 hours, and the results are presented in Figure 4.36. Also, the raw data of the 5 profiles taken from each sample were represented using the error bars and compared with the simulated profile at 5 hrs as shown in Figure 4.36.

It is evident that the simulated concentration profiles at 5 hrs, generated by using the D(C) obtained from a longer diffusion time of 450 hrs, exhibit significant disparities when compared to the experimental results. This clear discrepancy confirms that the interdiffusion coefficient changes with time.

Hence, adopting the widely accepted approach of assuming that D(C)s obtained after a longer diffusion time remain constant for any temperature and can be used for simulation at any diffusion time may lead to significant errors.

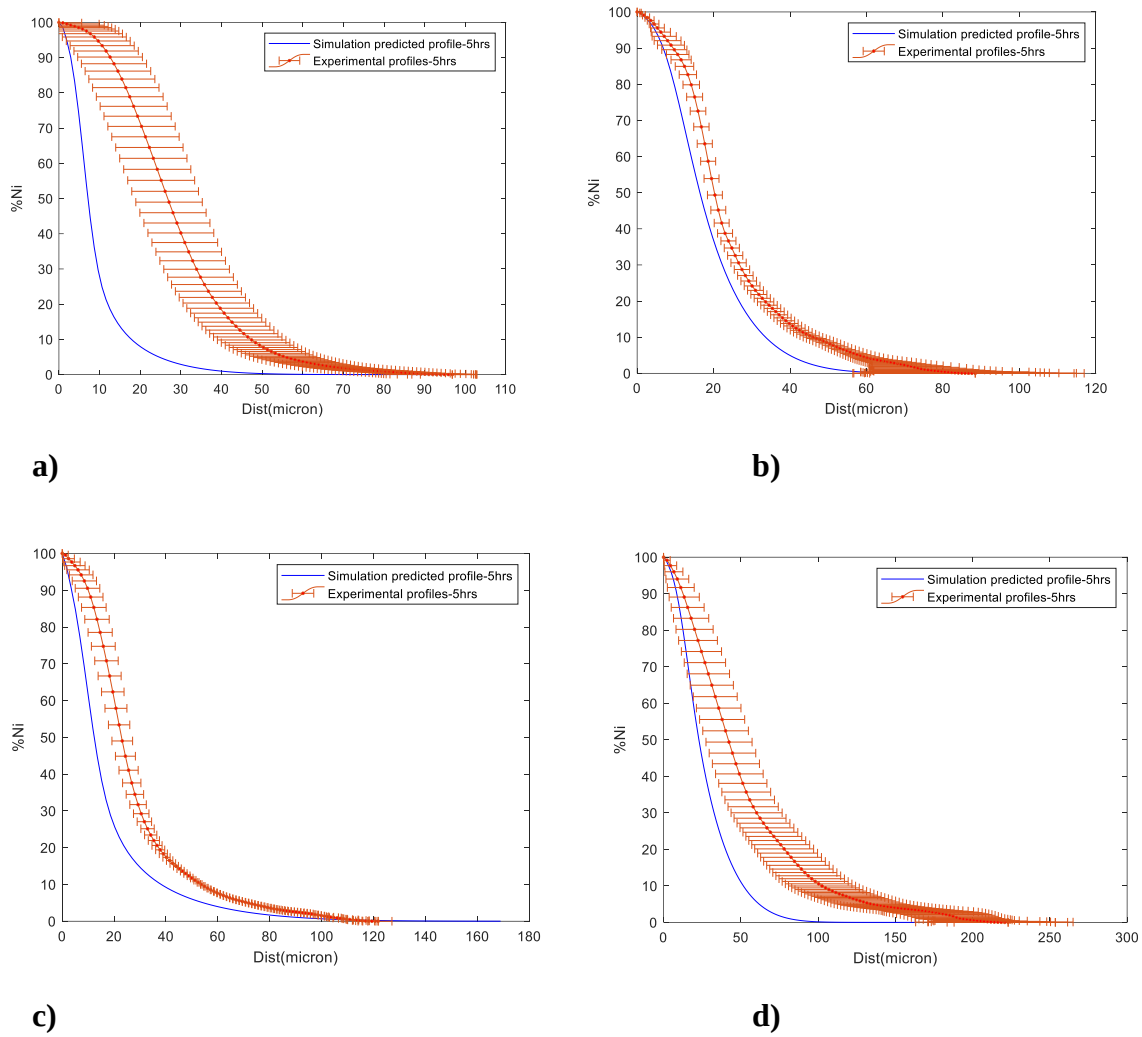

Figure 4.36: Comparison of simulated 5 hr profile obtained with D(C) of 450 hrs and actual experimental concentration profiles at:

a) 900^0 C; b) 940^0 C; c) 980^0 C; and d) 1020^0 C

4.7 Using appropriate D(C) for diffusion analysis

The results of D(C) presented in this work are verified by using the exact D(C) obtained after a specific diffusion time to simulate the concentration profiles after the actual diffusion time. Figures 4.37 (a)-(d) show the experimental concentration profiles at 5 hrs, compared with the simulated profile obtained using D(C) at 5 hrs for various temperatures investigated.

Furthermore, approximately five experimental concentration profiles were acquired from each sample used in this work. These profiles were compared with the simulated profiles at 5 hrs obtained using D(C) at 5 hrs, and the results show that the simulated profile falls within the region of the experimental profiles, as presented in Figure 4.37 (a)-(d).

Therefore, this work has been able to establish that using a single D(C) for all time during diffusion analysis will lead to errors because D(C) indeed changes with time isothermally.

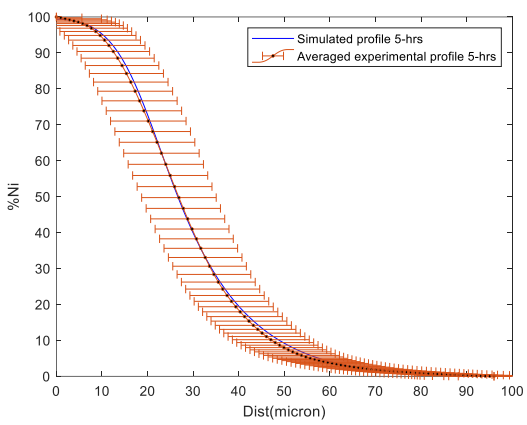

a)

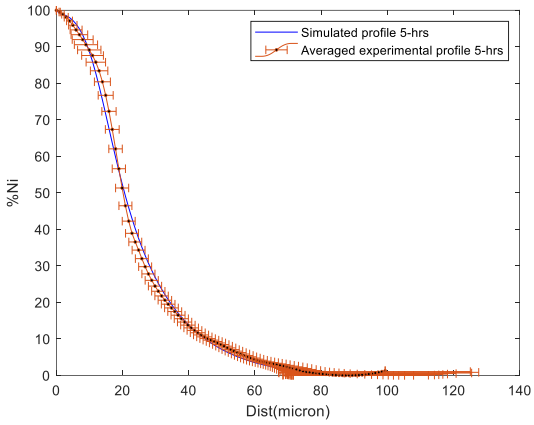

b)

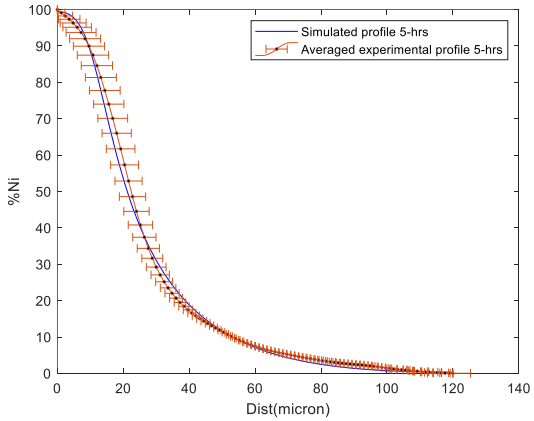

c)

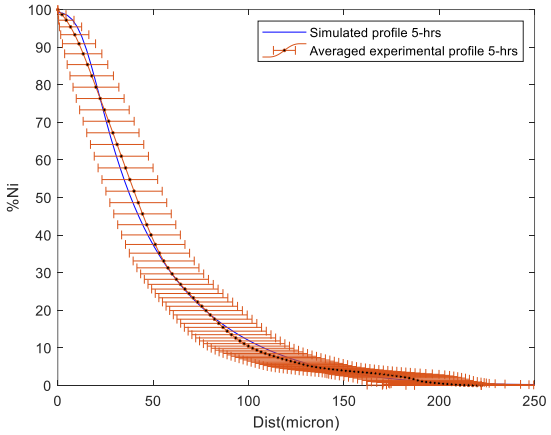

d)

Figure 4.37: Comparison of Simulated 5hrs profile obtained with D(C) of 5hrs and Raw Experimental concentration profiles at 5hrs sample at

a) 900^0 C; b) 940^0 C; c) 980^0 C; d) 1020^0 C

CHAPTER FIVE

5. Summary and Conclusions

The variation of interdiffusion and impurity diffusion coefficients with time has been investigated by using a diffusion couple in a Cu-Ni binary system. High temperatures that range from 900^0C, 940^0C, 980^0C, to 1020^0C are used to anneal the samples at diffusion times of 5 hrs, 25 hrs, 75 hrs, 150 hrs and 450 hrs.

The following conclusions are made based on the results.

(a) Impurity and concentration-dependent interdiffusion coefficients are observed to isothermally change with time at different temperatures investigated.

(b) Anomalous decrease in diffusion coefficient with increase in temperature is observed at certain concentrations and only for certain period of time, which is an indication that the time variation in the diffusion coefficients is attributable to DIS.

(c) In addition, when different solute source concentrations are used, which induce different solute concentration gradients at every concentration, the diffusion coefficients are observed to change. This further supports the fact that the time variation in the diffusion coefficients is attributable to DIS.

(d) Calculated average of the interdiffusion concentration coefficients of pure Cu-Ni at different diffusion time reveals that D(C) actually changes with time.

(e) The generally acknowledged concept in the literature that a single long diffusion time can be used to produce diffusion coefficient at any diffusion time will lead to significant errors in theoretical prediction as demonstrated in this work.

CHAPTER SIX

6.1. Recommendations for future research

For future work, the following items are recommended:

1. Further investigations should be done on ternary and multi-component systems to estimate impurities and concentration-dependent interdiffusion coefficients,
2. Different geometries including 2-dimensional and 3-dimensional geometries should be included where the diffusion interface migrates and surface concentration changes with time, and
3. The newly developed model in this study should be applied to systems with no radioactive isotopes in order to demonstrate its capability to calculate the impurity diffusion coefficients.

REFERENCES

1. Askeland, D., Fulay, P. P., & Wright, W. J. (2011). Atom and ion movements in materials. In The Science and Engineering of Materials (6th ed., pp. 155–195). Cengage Learning.
2. Crank, J. (1975). The Mathematics of Diffusion (2nd ed.). Oxford University Press.
3. Fick, A. (1855). Ueber Diffusion (On Diffusion). Annalen der Physik und Chemie, 94, 59-86.
4. Yueheng Z., Jianpeng Z., Xiaoke W., Chunming D., Lijun Z. (2021). An Effective Approach to Acquire the Impurity Diffusion Coefficients in Binary Alloys with Quantified Uncertainties. Metals, 11, 809. https://doi.org/10.3390/met11050809
5. Illingworth, T. C., Golosnoy, I. O., Gergely, V., & Clyne, T. W. (2005). Numerical modelling of transient liquid phase bonding and other diffusion-controlled phase changes. Journal of Materials Science, 40, 2505–2511.
6. Wang, Z., Fang, L., Cotton, I., & Freer, R. (2015). Ni-Cu interdiffusion and its implication for ageing in Ni-coated Cu conductors. Materials Science and Engineering B: Solid-State Materials and Advanced Technology, 198, 86–94. https://doi.org/10.1016/j.mseb.2015.04.006.
7. Robissoz, R. E. (1976). Interdiffusion in a Bulk Couple of Lead and Lead-50wt% Indium Alloy. Acta Materialia, 24, 609–614.
8. Darken, L. S. (1948). Diffusion, Mobility and their inter-relation through free energy in binary metallic systems. Transactions of the American Institute of Mining and Metallurgical Engineers, 175, 184.
9. Stephenson, G. B. (1988). Deformation During Interdiffusion. Acta Metallurgica, 36(10), 2663–2683. doi: https://doi.org/10.1016/0001-6160(88)90114-9.

10. Larche, F. C., & Cahn, J. W. (1982). The Effect of Self-Stress in Solids. Acta Metallurgica, 30, 1835–1845. doi: 10.1016/0001-6160(82)90023-2.
11. Jain, R. K., & van Overstraeten, R. J. (1974). Calculation of the diffusion-induced stresses in silicon. Physica Status Solidi, 25(1), 125–130. doi: 10.1002/pssa.2210250109.
12. Daruka, I., Szabó, I. A., Beke, D. L., Cserháti, C., Kodentsov, A., & Van Loo, F. J. J. (1996). Diffusion-induced bending of thin sheet couples: Theory and experiments in Ti-Zr system. Acta Materialia, 44(12), 4981–4993. doi: 10.1016/S1359-6454(96)00099-7.
13. Yamane, T., Mori, N., Yoritoshi, M., Yoshinari, M., Mitsue, K., & Takahashi, T. (1988). Effect of High Pressure on Interdiffusion in Cu-Zn Alloys at Temperatures near the Melting Point. Metallurgical Transactions A, 19A, 467–471. doi: 10.1007/BF02649260
14. Girifalco, L. A., & Hubert, G. H. (1958). The Theory of Diffusion in Strained Systems. Ohio. [Online]. Available: https://ntrs.nasa.gov/search.jsp?R=19930085264
15. Donald, S. W., & Gordon, P. W. (1977). Diffusion-Induced Stresses and Plastic Deformation. Metallurgical Transactions A, 8(October), 1977–1531. doi: 10.1007/BF02644856
16. Cowern, N. E. B. (1994). Diffusion in Strained Si (Ge). Physical Review Letters, 72(16), 2585–2588. doi: 10.1103/PhysRevLett.72.2585.
17. Beke, D. L., Szabó, I. A., Erdélyi, Z., & Opposits, G. (2004). Diffusion-induced stresses and their relaxation. Materials Science and Engineering A, 387–389(1-2 SPEC. ISS.), 4–10. doi: 10.1016/j.msea.2004.01.065.
18. Girifalco, L. A., & Grimes, H. H. (1961). Effect of static strains on diffusion. Physical Review, 121(4), 982–991. doi: 10.1103/PhysRev.121.982.
19. Chu, J. L., & Lee, S. (1994). The effect of chemical stresses on diffusion. Journal of Applied Physics, 75(6), 2823–2829. doi: 10.1063/1.356174.

20. Olaye, O., & Ojo, O. A. (2021). Time variation of concentration-dependent interdiffusion coefficient obtained by numerical simulation analysis. Materialia, 16(February 2021), 101056. https://doi.org/10.1016/j.mtla.2021.101056
21. Porter, D. A., Easterling, K. E., & Sherif, M. Y. (2009). Diffusion. In Phase Transformations in Metals and Alloys (3rd ed., pp. 65–114). CRC Press, Taylor & Francis Group.
22. Callister, W. D. Jr. (2001). Diffusion. In Fundamentals of Materials Science and Engineering (5th ed., pp. 126–146). John Wiley & Sons.
23. Balluffi, R. W., Allen, S. M., & Carter, W. C. (2005). Driving Forces and Fluxes for Diffusion. In Kinetics of Materials. John Wiley & Sons, Inc.
24. Daruka, I., Szabó, I. A., Beke, D. L., Cserháti, C., Kodentsov, A., & Van Loo, F. J. J. (1996). Diffusion-induced bending of thin sheet couples: Theory and experiments in Ti-Zr system. Acta Materialia, 44(12), 4981–4993. doi: 10.1016/S1359-6454(96)00099-7.
25. Wu, Y., Duan, G., & Zhao, X. (2015). Effects of magnetic field intensity on carbon diffusion coefficient in pure iron in γ-Fe temperature region. International Journal of Modern Physics B, 29(10-11), 1-8.
26. Zia-Ul-Haq. (1962). Diffusion in Aluminium alloys by activation analysis (Master's thesis). McMaster University.
27. Mehrer, H. (2007). Interdiffusion and Kirkendall Effect. In Diffusion in Solids (p. 165). Springer, Berlin, Heidelberg.
28. Dayananda, M. A., & Sohn, Y. H. (1996). Average effective interdiffusion coefficient and their applications for isothermal multicomponent diffusion couples. Scripta Materialia, 35(6), 683-688.

29. Eversole, W., Peterson, J. D., & Kindsvater, H. (1941). Diffusion Coefficients in Solution. An Improved Method for Calculating D as a Function of Composition. The Journal of Physical Chemistry, 45, 1398-1403.
30. Sauer, F., & Freise, V. (1962). Diffusion in binaren Gemischen mit Volumenanderung. Zeitschrift für Elektrochemie, 66(4), 353–362.
31. F.J.A den Broeder. (1969). A general simplification and improvement of the matano-boltzmann method in the determination of the interdiffusion coefficients in binary systems, Scripta Metallurgica, Volume 3, Issue 5, Pages 321-325, ISSN 0036-9748, https://doi.org/10.1016/0036-9748(69)90296-8.
32. Santra, S., & Paul, A. (2015). Role of the Molar Volume on Estimated Diffusion Coefficients. Metallurgical and Materials Transactions A, 46(9), 3887–3899. doi:10.1007/s11661-015-2988-z.
33. Hall, L. D. (1953). An Analytical Method of Calculating Variable Diffusion Coefficients. Journal of Chemical Physics, 21(1), 87-89. doi:10.1063/1.1698631.
34. Hall, L. D. (1953). An Analytical Method of Calculating Variable Diffusion Coefficients. Journal of Chemical Physics, 21, 87-89.
35. Ahmed, T., Belova, I. V., Evteev, A. V., Levchenko, E. V., & Murch, G. E. (2015). Comparison of the Sauer-Freise and Hall method for obtaining interdiffusion coefficient in Binary alloys. Journal of Phase Equilibria and Diffusion, 36, 366–374.
36. Sarafianos, N. (1986). An Analytical method of calculating variable diffusion coefficients. Journal of Materials Science, 21, 2283-2288.

37. Zhu, L., Chen, Z., Zhong, W. E. I., Wei, C., & Cai, G. (2019). Measurement of Diffusion Coefficients in the bcc Phase of the Ti-Sn and Zr-Sn Binary Systems. Metallurgical and Materials Transactions A, 50(3), 1409–1420. doi: 10.1007/s11661-018-05107-7.
38. Zhong, W., & Zhao, J. (2017). First experimental measurement of calcium diffusion in magnesium using novel liquid-solid diffusion couples and forward-simulation analysis. Scripta Materialia, 127, 92–96. doi: 10.1016/j.scriptamat.2016.09.008.
39. Zhong, W., & Zhao, J. (2017). First Reliable Diffusion Coefficients for Mg-Y and Additional Reliable Diffusion Coefficients for Mg-Sn and Mg-Zn. Metallurgical and Materials Transactions A, 48(12), 5778–5782. doi: 10.1007/s11661-017-4378-1.
40. Zhang, Q., & Zhao, J. (2013). Extracting interdiffusion coefficients from binary diffusion couples using traditional methods and a forward-simulation method. Intermetallics, 34, 132–141. doi: 10.1016/j.intermet.2012.11.012.
41. Zhang, Q., Chen, Z., Zhong, W., & Zhao, J. C. (2017). Accurate and efficient measurement of impurity (dilute) diffusion coefficients without isotope tracer experiments. Scripta Materialia, 128, 32–35. doi: 10.1016/j.scriptamat.2016.09.040.
42. Greta, L., et al. (2018). Diffusion in the Ti-Al-V System. Journal of Phase Equilibria and Diffusion, 39(5), 731–746. doi: 10.1007/s11669-018-0673-9.
43. M.E. C. Jr & Zhao, J. (2019). Phase Equilibria and Diffusion in the Ni-Cr-Pt System at 1200°C. Journal of Phase Equilibria and Diffusion, 40(4), 542–552. doi: 10.1007/s11669-019-00753-9.
44. Chen, Z., Zhang, Q., & Zhao, J. (2019). pydiffusion: A Python Library for Diffusion Simulation and Data Analysis. Journal of Open Research Software, 7(13), 1–7. doi: https://doi.org/10.5334/jors.255.

45. Chen, Z., Liu, Z., & Zhao, J. (2018). Experimental Determination of Impurity and Interdiffusion Coefficients in Seven Ti and Zr Binary Systems Using Diffusion Multiples. Metallurgical and Materials Transactions A, 49(7), 3108–3116. doi: 10.1007/s11661-018-4645-9.
46. Zhu, L., Zhang, Q., Chen, Z., Wei, C., & Cai, G. (2017). Measurement of Interdiffusion and Impurity Diffusion Coefficients in the bcc Phase of the Ti–X (X = Cr, Hf, Mo, Nb, V, Zr) Binary Systems Using Diffusion Multiples. Journal of Materials Science, 52, 3255–3268. doi: 10.1007/s10853-016-0614-0.
47. Prussin, S. (1961). Generation and Distribution of Dislocations by Solute Diffusion. Journal of Applied Physics, 32, 1876-1881.
48. Schwarz, S. M., Kempshall, B. W., & Giannuzzi, L. A. (2003). Effects of Diffusion-Induced Recrystallization on Volume Diffusion in the Copper-Nickel System. Acta Materialia, 51(10), 2765–2776. doi: 10.1016/S1359-6454(03)00082-X.
49. Lin, T., et al. (2020). An Investigation on Diffusion Bonding of Cu/Cu Using Various Grain Sizes of Ni Interlayers at Low Temperature. Materialia (Oxf), 14(May), 100882. doi: 10.1016/j.mtla.2020.100882.
50. Mehrer, H., & Divinski, S. (2009). Diffusion in Metallic Elements and Intermetallics. Defect and Diffusion Forum, 289–292(April 2009), 15–38. doi: 10.4028/www.scientific.net/DDF.289-292.15.
51. Wu, B., Chen, B., Zou, Z., Liao, S., & Deng, W. (2018). Thermal Stability of Ultrafine Grained Pure Copper Prepared by Large Strain Extrusion Machining. Metals (Basel), 8(6), 1–13. doi: 10.3390/met8060381.
52. Cahn, R. W., & Haasen, P. (1996). Physical Metallurgy (4th ed., Vol. 2).

53. Kulik, R., & Soulier, P. (2020). Moving Averages. Springer Series in Operations Research and Financial Engineering, 425–452. doi: 10.1007/978-1-0716-0737-4_15.

54. Olaye, O., & Ojo, O. (2019). Leapfrog / Dufort-Frankel Explicit Scheme for Diffusion-Controlled Moving Interphase Boundary Problems with Variable Diffusion Coefficient and Solute Conservation. Modeling and Simulation in Materials Science and Engineering, 28(1), 1–24.

55. Olaye, O., & Ojo, O. (2020). Change in Concentration-Dependent Diffusion Activation Energy and Frequency Factor with Time: Identified by Numerical Analyses of Experimental Data. Metallurgical and Materials Transactions A, 51(12), 6482–6497.

56. Olaye, O., & Ojo, O. (2021). A New Analytical Method for Computing Concentration-Dependent Interdiffusion Coefficient in Systems with Pre-Existing Solute Concentration Gradient. Journal of Phase Equilibria and Diffusion, vol. 42, no. 2, pp. 303–14, https://doi.org/10.1007/s11669-021-00883-z.

57. Olaye, O., & Ojo, O. A. (2021). Analysis of Concentration Dependent Interdiffusion Coefficient under the Condition of Pre-Existing Non-uniform Solute Distribution. ” Metallurgical and Materials Transactions. A, Physical Metallurgy and Materials Science, vol. 52, no. 7, pp. 2787–94, https://doi.org/10.1007/s11661-021-06268-8.

58. Olaye, O., & Ojo, O. A. (2022). Disparity in the concentration dependence of interdiffusion coefficient under 1D and 2D diffusion interface migration. Results in Physics, 38, 105660. https://doi.org/10.1016/j.rinp.2022.105660.

59. Olaye, O., & Ojo, O. A. (2022). Analysis of Concentration Dependence of Interdiffusion Coefficient under the Condition of a Time-Varying Surface Concentration. Materials Transactions, 63(9), 1217-1223.

60. Reisner, M., Oberkofler, M., Elgeti, S., Balden, M., Hösch, T., Mayer, M., & Silva, T. F. (2019). Interdiffusion and phase formation at iron-tungsten interfaces. Nuclear Materials and Energy, 19, 189-194.
61. Okugawa, M., & Numakura, H. (2015). Discussion of "On the Boltzmann-Matano Analysis of diffusion in a semi-infinite medium." Metallurgical and Materials Transactions A: Physical Metallurgy and Materials Science, 46, 3813-3814.
62. Tian, G. (2023). Time-varying concentration-dependent interdiffusion coefficient in the Cu-Ni system (MSc Thesis). University of Manitoba.
63. Beke, D., Szabo, I., Erdelyi, Z., & Opposits, G. (2004). Materials Science and Engineering, 387, 4-10.
64. Joubert, H. D., Terblans, J. J., & Swart, H. C. (2010). Extracting interdiffusion parameters from Ni/Cu thin films by means of profile reconstruction with the MRI model. Surface and Interface Analysis, 42, 1281-1283.
65. Joubert, H. D., Terblans, J. J., & Swart, H. C. (2009). Comparison of inter-diffusion coefficients for Ni/Cu thin films determined from classical heating analysis and linear temperature ramping analysis by means of profile reconstruction and a numerical solution of Fick's law. Nuclear Instruments and Methods in Physics Research Section B: Beam Interactions with Materials and Atoms, 267, 2575-2578.
66. Ruske, W. (1961). Die Ni-Cu-diffusion in elektrolytisch hergestellten dünnen Nickelschichten. Physica Status Solidi, 1, 85-88.
67. Schwarz, S. M., Kempshall, B. W., & Giannuzzi, L. A. (2003). Effect of diffusion-induced recrystallization on volume diffusion in the Copper-nickel system. Acta Materialia, 51, 2765-2776.

68. Zhao, J., Garay, J., Anseimi-Tamburini, U., & Munir, Z. (2007). Directional electromigration interdiffusion in the Cu-Ni system. Journal of Applied Physics, 102, 1149021-1149027.

69. Fisher, B., & Rudman, P. S. (1961). X-ray diffraction study of interdiffusion in Cu-Ni powder compacts. Journal of Applied Physics, 32, 1604-1611. https://doi.org/10.1063/1.1728404

70. Vandijk, T., & Mittemeijer, E. J. (1977). The effect of interdiffusion on moiré patterns of thin bimetallic films. Thin Solid Films, 41, 173.

71. Johnson, B. C., Bauer, C. L., & Jordan, A. G. (1986). Mechanisms of interdiffusion in copper/nickel thin-film couples. Journal of Applied Physics, 59, 1147.

72. Wang, Z., Fang, L., Cotton, I., & Freer, R. (2015). Ni-Cu interdiffusion and its implication for aging in Ni-coated Cu conductors. Materials Science and Engineering B, 198, 86-94.

73. Ikushima, A. (1959). Diffusion of Nickel in Single Crystals of Copper. Journal of the Physical Society of Japan, 14, 1636.

74. Correa da Silva, L. C., & Mehl, R. F. (1951). Interface and Marker Movements in Diffusion in Solid Solutions of Metals. Journal of Metals, 3, 155-173. https://doi.org/10.1007/BF03397292

75. Anand, M. S., Murarka, S. P., & Agarwala, R. P. (1965). Diffusion of copper in Nickel and Aluminum. Journal of Applied Physics, 36, 3860.

76. Helfmeier, H., & Feller-Kniepmeier, M. (1970). Diffusion of Copper in Nickel Single Crystals. Journal of Applied Physics, 41, 3202. https://doi.org/10.1063/1.1659400

77. Kirkendall, E., Thomassen, L., & Uethegrove, C. (1939). Rates of Diffusion of Copper and Zinc in Alpha Brass. Transactions of the American Institute of Mining and Metallurgical Engineers, 133(967), 186-203.

78. Gasparin, S., Berger, J., Dutykh, D., & Mendes, N. (2018). Stable explicit schemes for simulation of nonlinear moisture transfer in porous materials. Journal of Building Performance Simulation, 11(2), 129-144. doi: 10.1080/19401493.2017.1298669
79. Afolabi, O. C., Sada, H., Olaye, O., & Ojo, O. A. (2022). Calculation and use of variable diffusivity for the analysis of transient liquid phase bonding behavior. Metallurgical and Materials Transactions A, The Minerals, Metals & Materials Society and ASM International. https://doi.org/10.1007/s11661-022-06755-6.
80. I. Gregor, D. Patra, Statistical Analysis of Diffusion Coefficient Determination, J. Of Fluoresc. 2005;15, 415–422, doi: 10.1007/s10895-005-2633-0.
81. C.D. Le , Measurement of Diffusion Coefficients of Binary Liquid Systems By The Moire Pattern Method, McMaster University (Thesis), 1968 .